

Evaluation of Portable Data Collector Potential

September 30, 2002

**Prepared for
NASA Ames Research Center
Moffett Field, California**

**Prepared by
Eric H. Bolz**

**Science Applications International Corporation
Arlington, Virginia**

Work Performed Under Contract No. NAS2-98002

**Task Order 68
Sub-task 3**

Evaluation of Portable Data Collector Potential

Introduction

In September of 1995 a series of tests were conducted utilizing operational air carrier aircraft in an attempt to determine the potential usefulness that a portable data collector could have in aiding Center-TRACON Automation System (CTAS) performance assessment. The data collector packages consisted of a Global Positioning System (GPS) receiver with portable antenna, a data collection computer attached to the receiver, and a trained observer situated on the flight deck whose primary function was to manually log several parameters from aircraft instruments. Furthermore, ground-tracking radar data from the Federal Aviation Administration's (FAA's) Air Route Traffic Control Center (ARTCC) was acquired for each of the flights conducted. The plan was to determine the potential utility of the resulting data for evaluating CTAS arrival time prediction algorithms.

The three data sets (GPS, radar and observer) have been analyzed and merged into time-correlated data sets for purposes of this analysis. The details of this process are discussed later. In analyzing and comparing the characteristics of these data sets, problems and weaknesses have been identified with each. These are then examined and recommendations for improving performance in subsequent tests are made. The analysis of the resulting raw data is presented in tabular and graphic form in Appendix A.

Data Reduction Process

Figure 1 depicts a CTAS Trajectory/Radar data file. The horizontal and vertical coordinates assumed by the CTAS modeling process comprise the first two sets of data. As is readily apparent, this data is created in significant detail, including modeling the turn maneuvers as segments of an arc. The third set of data is the radar tracking data. This data has been converted to a local X-Y coordinate frame, the results of which are shown along with the (Mode C transponder) altitude and real time. The 'Real_Time' column is in seconds referenced to the base time-of-day stated in the title of the data file (and included in the title of the figure). Also presented are two columns showing the flight progress in terms of path distance along the horizontal trajectory, and cross-track distance relative to that path. (The provision of the CTAS horizontal and vertical trajectory data, conversion of radar to X-Y coordinates, and calculation of flight progress was performed by a post-flight analysis program and is not a normal part of the ARTCC radar data recovery process.)

Due to the scan rate of the ARTCC radar, data updates are available at approximately 12-second intervals. The slow scan rate is one of the fundamental problems in applying exacting wind detection and arrival time prediction calculations involving the radar data. The other two problems identified are the filter lag inherent in the radar data tracking algorithm, and problems identifying and correlating the time corresponding to each data point presented. These problems are explored later.

Figure 1. Example CTAS/Radar data file (UA_1154_9_13) Start Time 09:25:11

Horizontal Trajectory data

ET#	Path_dist (nmi)	Tru_Cours (deg)	X-coord (nmi)	Y-coord (nmi)	Del_dist (nmi)	Radius (nmi)	Turn (deg)	X-center (nmi)	Y-center (nmi)
10	82.297	74.08	351.625	421.000	0.0000	0.0000	0	0.000	0.000
9	80.179	74.08	353.662	421.581	2.1180	0.0000	0	0.000	0.000
8	79.920	75.48	353.911	421.649	0.2586	10.5399	1	356.553	411.445
7	25.891	75.48	406.215	435.190	54.0286	0.0000	0	0.000	0.000
6	25.025	80.48	407.060	435.370	0.8657	9.9211	5	408.702	425.586
6	24.160	85.48	407.919	435.476	1.7314	9.9211	10	408.702	425.586
6	23.372	90.03	408.708	435.507	2.5191	9.9211	15	408.702	425.586
5	16.667	90.03	415.413	435.503	6.7056	0.0000	0	0.000	0.000
4	15.899	95.03	416.179	435.470	0.7682	8.8034	5	415.408	426.700
4	15.131	100.03	416.940	435.369	1.5364	8.8034	10	415.408	426.700
4	14.362	105.03	417.690	435.203	2.3046	8.8034	15	415.408	426.700
4	13.594	110.03	418.422	434.971	3.0727	8.8034	20	415.408	426.700
4	12.826	115.03	419.131	434.677	3.8409	8.8034	25	415.408	426.700
4	12.058	120.03	419.812	434.322	4.6091	8.8034	30	415.408	426.700
4	11.290	125.03	420.460	433.910	5.3773	8.8034	35	415.408	426.700
4	10.522	130.03	421.069	433.442	6.1455	8.8034	40	415.408	426.700
4	9.753	135.03	421.635	432.923	6.9137	8.8034	45	415.408	426.700
4	9.611	135.95	421.736	432.821	7.0554	8.8034	46	415.408	426.700
3	5.458	135.95	424.623	429.836	4.1530	0.0000	0	0.000	0.000
2	5.458	135.58	424.623	429.836	0.0000	0.0000	0	424.623	429.836
1	0.000	135.58	428.443	425.937	5.4583	0.0000	0	0.000	0.000

Vertical Trajectory data

Time (sec)	Path_dist (nmi)	G_alt (ft)	Mach	Vtr (kts)	Vcal (kts)	InFPA (deg)	ENGC	Thrust (lbs)	Wf (lb/hr)	Fuel (lbs)	DAItdt (ft/m)	Vgnd (kt)	Tcour (deg)	WSpd (kt)	WDir (deg)	Temp (degR)	Pres (lb/ft2)
0	82.3	30381	0.817	491.6	317.8	0.00	0	0	0	0	0	508	74.1	19	281	428.8	657.3
18	79.8	30381	0.817	491.6	317.8	0.00	0	0	0	0	0	509	75.5	19	280	428.8	657.3
314	37.6	30381	0.817	491.7	317.8	0.00	0	0	0	0	0	513	75.5	22	273	428.8	657.1
320	36.8	30032	0.817	492.4	320.1	-4.19	-1	315	0	0	-3802	513	75.5	22	271	430.1	667.1
328	35.6	29654	0.812	489.6	320.0	-2.99	-1	294	0	0	-2691	510	75.5	22	272	431.6	678.2
388	27.3	26978	0.772	471.5	320.0	-3.09	-1	82	0	0	-2663	487	75.5	18	279	442.1	760.6
417	23.4	25692	0.754	463.1	320.0	-3.14	-1	-18	0	0	-2659	479	89.6	16	283	447.3	803.0
456	18.3	23946	0.730	452.1	320.0	-3.30	-1	-130	0	0	-2720	466	90.0	15	288	454.4	863.4
485	14.6	22635	0.713	444.1	320.0	-3.34	-1	-202	0	0	-2707	458	103.5	14	291	459.8	911.0
514	10.9	21318	0.696	436.1	320.0	-3.45	-1	-272	0	0	-2745	450	127.2	14	294	465.1	961.0
543	7.4	19988	0.680	428.3	320.0	-3.54	-1	-337	0	0	-2760	441	136.0	14	296	470.5	1013.7
551	6.4	19988	0.660	415.8	310.2	0.00	-1	-253	0	0	0	429	136.0	13	298	470.5	1013.7
580	3.1	19988	0.596	375.5	278.9	0.00	-1	12	0	0	0	388	135.6	13	297	470.5	1013.7
610	0	19988	0.536	338.0	250.0	0.00	-1	155	0	0	0	351	135.6	13	297	470.5	1013.8

X	Y	Alt	Vgnd	Heading	dAItdt	Real_time	Time	Path_dist	Cross_track_dist
351.625	421.000	29000	508	74	-100	7238.34	0.00	82.297	0.000
353.125	421.312	29000	505	77	0	7250.34	12.00	80.769	-0.111
354.750	421.688	29000	503	77	0	7262.34	24.00	79.097	-0.173
356.562	422.000	29000	500	79	0	7274.34	36.00	77.265	-0.325
358.188	422.438	29000	498	76	0	7286.34	48.00	75.581	-0.308
359.688	422.688	29000	496	79	0	7298.55	60.21	74.066	-0.442
361.312	423.125	29000	495	76	0	7310.35	72.01	72.385	-0.426
363.000	423.500	29000	494	77	0	7322.35	84.01	70.657	-0.486
364.562	423.938	29000	493	75	0	7334.35	96.01	69.035	-0.454
366.250	424.562	29000	492	71	0	7346.35	108.01	67.244	-0.272
367.875	425.125	29000	492	71	0	7358.36	120.02	65.530	-0.135
369.438	425.688	29000	492	70	0	7370.36	132.02	63.876	0.019
371.000	426.312	29000	492	69	0	7382.36	144.02	62.207	0.231
372.625	426.875	29000	492	70	0	7394.56	156.22	60.493	0.369
374.250	427.438	29000	492	71	0	7406.36	168.02	58.779	0.507
375.812	427.938	29000	493	72	0	7418.37	180.03	57.141	0.599
377.625	428.500	29000	494	72	0	7430.37	192.03	55.245	0.689
379.125	429.125	29000	495	69	0	7442.37	204.03	53.636	0.918
380.875	429.625	29000	496	73	0	7454.37	216.03	51.817	0.964
382.438	430.188	29000	498	71	0	7466.37	228.03	50.163	1.117
384.000	430.562	29000	498	75	0	7478.38	240.04	48.557	1.087
385.562	431.125	29000	499	72	0	7490.58	252.24	46.904	1.241
387.312	431.625	29000	500	73	0	7502.58	264.24	45.084	1.286
389.000	432.250	29000	501	71	0	7514.38	276.04	43.293	1.468
390.688	432.875	29000	502	70	0	7526.38	288.04	41.503	1.650
392.250	433.500	29000	504	69	0	7538.39	300.05	39.834	1.864
393.750	434.125	29000	504	68	0	7550.39	312.05	38.225	2.093
395.438	434.625	28700	505	72	-300	7562.39	324.05	36.466	2.154
397.062	435.188	28300	505	71	-700	7574.39	336.05	34.752	2.292
398.750	435.812	27800	506	70	-1200	7586.39	348.05	32.962	2.473
400.375	436.250	27300	506	73	-1700	7598.39	360.05	31.279	2.490
402.000	436.750	26900	507	73	-2100	7610.40	372.06	29.580	2.567
403.500	437.125	26400	507	75	-2300	7622.40	384.06	28.034	2.554
405.188	437.250	25800	506	83	-2500	7634.40	396.06	26.369	2.252
406.875	437.125	25100	505	91	-2700	7646.40	408.06	24.934	1.762
408.375	436.938	24500	503	95	-2800	7658.40	420.06	23.662	1.436
410.062	436.688	24000	501	97	-2900	7670.41	432.07	22.019	1.182
411.750	436.438	23600	499	98	-2800	7682.41	444.07	20.331	0.933
414.125	436.188	22900	496	97	-2900	7694.41	456.07	17.955	0.684
415.688	436.000	22500	493	97	-2600	7706.41	468.07	16.405	0.501
417.188	435.688	22100	490	100	-2400	7718.41	480.07	14.948	0.359
417.812	435.438	21500	486	108	-2500	7730.42	492.08	14.306	0.259
419.062	434.938	20800	482	111	-2800	7742.22	503.88	12.994	0.209
421.000	433.500	19600	477	122	-3300	7754.42	516.08	10.611	0.001
422.250	432.875	19300	473	118	-3200	7766.22	527.88	9.292	0.407
423.500	432.000	19100	469	123	-3000	7778.42	540.08	7.794	0.697
423.812	431.375	19000	465	137	-2500	7790.22	551.88	7.128	0.487
424.875	430.438	19100	460	133	-1700	7802.43	564.09	5.716	0.600
426.438	429.125	19000	456	131	-600	7814.23	575.89	3.680	0.799
427.375	428.312	19000	451	131	-300	7826.43	588.09	2.444	0.899
428.562	427.500	19000	446	126	-100	7838.23	599.89	1.033	1.179
429.269	426.746	19000	442	132	-25	7847.43	609.09	0.000	1.156

Figure 2. Recorded GPS Output Data File (UA_1154_9_13)

```

%10:28:59,1084.69,,, $GPGGA,172836,4029.975,N,10558.711,W,1,04,3.0,8556.8,M,19.5,M, $GPVTG,067.0,T,
056.0,M,452.7,N,838.4,K
%10:29:03,1088.53,,, $GPGGA,172840,4030.162,N,10558.130,W,1,04,3.0,8501.2,M,19.5,M, $GPVTG,067.1,T,
056.1,M,451.2,N,835.6,K
%10:29:06,1091.28,,, $GPGGA,172843,4030.323,N,10557.711,W,1,03,2.7,8502.2,M,19.,M, $GPVTG,063.4,T,0
52.4,M,458.8,N,849.8,K
%10:29:09,1094.8,,, $GPGGA,172846,4030.434,N,10557.302,W,1,04,3.0,8426.4,M,19.5,M, $GPVTG,067.1,T,0
56.0,M,450.0,N,833.4,K
%10:29:14,1099.96,,, $GPGGA,172852,4030.723,N,10556.407,W,1,04,3.0,8329.0,M,19.6,M, $GPVTG,067.0,T,
056.0,M,446.2,N,826.3,K
%10:29:17,1102.70,,, $GPGGA,172854,4030.890,N,10555.984,W,1,03,2.7,8330.0,M,19.6,M, $GPVTG,062.5,T,
051.5,M,455.5,N,843.6,K
%10:29:20,1105.45,,, $GPGGA,172857,4030.987,N,10555.596,W,1,04,3.0,8237.7,M,19.6,M, $GPVTG,066.8,T,
055.8,M,445.5,N,825.0,K
%10:29:22,1107.92,,, $GPGGA,172900,4031.116,N,10555.200,W,1,04,3.0,8193.2,M,19.6,M, $GPVTG,066.7,T,
055.6,M,44.5,N,25.1,
%10:29:30,1115.83,,, $GPGGA,17207,4031.488,N,10554.041,W,1,04,3.0,8070.5,M,19.6,M, $GPVTG,067.8,T,0
56.8,M,444.0,N,822.2,K
%10:29:34,1119.78,,, $GPGGA,172911,4031.655,N,10553.461,W,1,04,3.0,8013.3,M,19.6,M, $GPVTG,069.8,T,
058.8,M,443.7,N,821.7,K
%10:29:37,1122.53,,, $GPGGA,172914,4031.765,N,10553.039,W,1,04,3.0,7972.6,M,19.6,M, $GPVTG,071.5,T,
060.5,M,441.6,N,817.8,K
%10:29:40,1125.22,,, $GPGGA,172917,4031.862,N,10552.639,W,1,04,3.0,7937.4,M,19.6,M, $GPVTG,072.4,T,
061.4,M,440.0,N,814.9,K
%10:29:44,1129.29,,, $GPGGA,172921,4031.998,N,10552.012,W,1,04,3.0,7891.7,M,19.6,M, $GPVTG,074.5,T,
063.5,M,438.4,N,811.9,K
%10:29:50,1135.38,,, $GPGGA,172927,4032.170,N,10551.071,W,1,04,3.0,7834.5,M,19.7,M, $GPVTG,077.6,T,
066.6,M,432.5,N,801.0,K

```

Figure 2 presents an example partial set of GPS data recovered from the test. In each line of data, the first several columns are of primary importance. The first item is time-of-day in hh:mm:ss. It is apparent that, while the data rate is higher than the 12-second interval of the radar data, it is variable and unpredictable, running from as little as 2 seconds to as high as 8 seconds in the small example depicted. A second, and more serious, problem encountered is apparent from a closer examination of the data within each record. (Each record consists of two lines in the table shown.) The problem is that characters are dropped on a seemingly random basis, which distorts (sometimes radically) the information and sometimes renders it unreadable. For example, in the third line (10:29:06) a value on the right end just before the letter 'M' should be '19.5', but the '5' has been dropped. In the eighth line (10:29:22), near the end of the continuation line, the value '44.5' should be '444.5', the value '25.1' should be '825.1', and a letter 'K' should appear at the very end. In the next line (10:29:30), the value '17207' should be '172907'. In fact, this particular field is also a GPS time representation, and is keyed to the time tags on the observer data (discussed below). The values immediately to the right are, in order, latitude, (north), longitude, (west), an unknown field, the number of satellites in view, the GPS GDOP (geometric dilution of precision) figure and then the geometric altitude in meters.

The consequences of this data collection problem are more apparent if the original data files from which the Figure 2 data was extracted are viewed in their raw form (see Figure 3). Comparing this raw file to the processed file reveals that three entire records were skipped during reduction because sense could not be easily made of the lines of data. The record at 10:29:12 is missing two commas in the sequence 'T056.0M'. The record at 10:29:25 is missing two commas in the sequence '\$GPVTG066.T'. The next record is missing 22 characters in the sequence ',N'.

Figure 3. Recorded GPS Output Data File (UA_1154_9_13) in Raw Form

```
%10:28:59, 1084.69, , , $GPGGA,172836,4029.975,N,10558.711,W,1,04,3.0,8556.8,M,19.5,M,
$GPVTG,067.0,T,056.0,M,452.7,N,838.4,K
%10:29:03, 1088.53, , , $GPGGA,172840,4030.162,N,10558.130,W,1,04,3.0,8501.2,M,19.5,M,
$GPVTG,067.1,T,056.1,M,451.2,N,835.6,K
%10:29:06, 1091.28, , , $GPGGA,172843,4030.323,N,10557.711,W,1,03,2.7,8502.2,M,19. ,M,
$GPVTG,063.4,T,052.4,M,458.8,N,849.8,K
%10:29:09, 1094.8, , , $GPGGA,172846,4030.434,N,10557.302,W,1,04,3.0,8426.4,M,19.5,M,
$GPVTG,067.1,T,056.0,M,450.0,N,833.4,K
%10:29:12, 1097.37, , , $GPGGA,172849,4030.594, ,10556.805,W,1, ,3.08371. ,M,196,M,
TG,06.1,T056.0M,4470,N,27.8,
%10:29:14, 1099.96, , , $GPGGA,172852,4030.723,N,10556.407,W,1,04,3.0,8329.0,M,19.6,M,
$GPVTG,067.0,T,056.0,M,446.2,N,826.3,K
%10:29:17, 1102.70, , , $GPGGA,172854,4030.890,N,10555.984,W,1,03,2.7,8330.0,M,19.6,M,
$GPVTG,062.5,T,051.5,M,455.5,N,843.6,K
%10:29:20, 1105.45, , , $GPGGA,172857,4030.987,N,10555.596,W,1,04,3.0,8237.7,M,19.6,M,
$GPVTG,066.8,T,055.8,M,445.5,N,825.0,K
%10:29:22, 1107.92, , , $GPGGA,172900,4031.116,N,10555.200,W,1,04,3.0,8193.2,M,19.6,M,
$GPVTG,066.7,T,055.6,M,44.5,N,25.1,
%10:29:25, 1110.78, , , $GPGGA,172902,4031.246,N,10554.805,W,1,04,3.0,8152.0,M,19.6,M,
$GPVTG066.T,05.9,M,44.4, .1,K
%10:29:28, 1113.25, , , N,10554.424,W,1,04,3.0,8112.5,M,19.6,M,
067.1,T,056.0,M,444.0,N,822.2,K
%10:29:30, 1115.83, , , $GPGGA,17207,4031.488,N,10554.041,W,1,04,3.0,8070.5,M,19.6,M,
$GPVTG,067.8,T,056.8,M,444.0,N,822.2,K
%10:29:34, 1119.78, , , $GPGGA,172911,4031.655,N,10553.461,W,1,04,3.0,8013.3,M,19.6,M,
$GPVTG,069.8,T,058.8,M,443.7,N,821.7,K
%10:29:37, 1122.53, , , $GPGGA,172914,4031.765,N,10553.039,W,1,04,3.0,7972.6,M,19.6,M,
$GPVTG,071.5,T,060.5,M,441.6,N,817.8,K
%10:29:40, 1125.22, , , $GPGGA,172917,4031.862,N,10552.639,W,1,04,3.0,7937.4,M,19.6,M,
$GPVTG,072.4,T,061.4,M,440.0,N,814.9,K
%10:29:44, 1129.29, , , $GPGGA,172921,4031.998,N,10552.012,W,1,04,3.0,7891.7,M,19.6,M,
$GPVTG,074.5,T,063.5,M,438.4,N,811.9,K
```

It is suspected that the dropped characters are an artifice of the data collection computer (and it's software), not the GPS receiver. Extreme care must be exercised in designing for the data collection of serial data streams such as that emanating from the GPS receiver. Interrupt-driven, or DMA channel, techniques must be used in order to guarantee collection of such data with integrity. Otherwise, when the CPU is busy with other tasks, such as formatting a data record and writing to disk, data overruns will occur, resulting in dropped characters as observed herein.

In order to make sense of this data for the present analysis purposes, a two-step procedure was employed. First, the initial processing step of Figures 2 and 3 were performed, resulting in records which were consistent at least to the point where the same number of parameters (separated by commas) were present in each line. Then a second step was performed. A program was developed which converted the GPS latitude/longitude data to X-Y coordinates consistent with the coordinates of the radar data. To do this, the equations from the C-language source program listings provided in the EGADS folder, and the local Denver stereographic projection coordinates in the MAP2 file, were employed. At the same time, each of the raw GPS parameters of interest was tracked in a loop to identify "outliers" which resulted from dropped or distorted characters. Where these outliers were found, the entire data record was dropped. The end result was a consistent, accurate set of data, although it was of course somewhat more sparse than the original data output by the receiver.

The final computational step in data processing was to merge the three data sources (radar, GPS, and observer) into one time-correlated data set, and to derive values for GPS ground speed and track angle at that time. To achieve a consistent time basis, the time references that were used to tag the radar data and the GPS information were examined. GPS of course provides its own highly accurate (potentially) time standard, which is a part of the data output stream that was acquired by the data acquisition computer. GPS time, however, differs by a known amount (several seconds) from UTC. The radar data files are annotated with local time; however, it is not known exactly how accurate that this time standard is in comparison to UTC. Furthermore, the output from the radar data-tracking algorithm is the data that is time-stamped. This may lag the raw radar return information by several seconds.

Furthermore, there is another apparent discrepancy between the time-stamp assigned by the data collection computer (which applies to the GPS data and observer data) and radar time. To assess the validity of the time stamp, the converted GPS X-Y data and the radar X-Y data were matched up manually. The time offset was noted. The value of that offset ranged from -120 seconds to +180 seconds, and seemed to group around multiples of 60 seconds. While the source of this even-minute clustering is not known, it is suspected that it is the result of errors in time initialization either of the data collection computer or in the annotation of the radar data. Regardless of cause, and because of the other sources of time uncertainty mentioned, and because assessment of the radar data (while of interest) was not the primary objective of this analysis, the offsets derived in the manual match-up process were used as the basis of the data merge.

In the merge process, the GPS data was interpolated to determine probable GPS information at each of the radar data points. The GPS data was averaged over a seven-point interval (roughly 20 seconds) in order to match the radar data point and to derive ground speed and track angle information. An important distinction should be made here in comparing the GPS with the radar data. The GPS data was available in raw form on a historical basis. The radar data available to us was the output of the tracking algorithm employed in real time in the ARTCC computer. Raw radar return data was not available for this analysis. A real-time tracking algorithm necessarily introduces lags in the resulting information. The processed GPS data outputs, being based on a historical data file using averaging over a time interval around the desired point in time, results in no such lag and exhibits a high degree of accuracy. The resulting differences, particularly in ground speed and track angle, are quite apparent, as will be addressed later.

A primary objective of this analysis is to determine the degree to which accurate, timely winds-aloft information can be derived. It is not possible to determine winds aloft from either the radar data or the GPS raw lat-lon output alone. Two sources of wind information do exist, but both are dependent on the ability of the observer to accurately notate information in real time. In some cases the observer annotated wind magnitude and direction as derived by the FMS and available directly from the FMS system outputs. In other cases, due to the absence of direct wind magnitude and direction data, the quantities altitude, OAT (outside air temperature), IAS (indicated air speed) and heading data were recorded. In some cases, all of the above were collected. In those cases where IAS, altitude and OAT information are available, TAS (true air speed) was calculated by the analysis program during the data merge process. In cases where OAT was not recorded, TAS was derived assuming an ISA atmosphere. In some cases, actual

TAS readings were recorded, avoiding the need for OAT, IAS and altitude. Based on TAS and heading (and local magnetic variation), airspeed velocity was compared to GPS velocity to derive winds. The outputs presented here contain (where applicable) both the airspeed-derived winds and the observer recorded (FMS) winds.

The process of automatically grouping observer data (since IAS, altitude, OAT and heading are all needed) in order to derive winds was found to be rather problematic. Sometimes, three of the items were available within a reasonable period of time, but not the fourth. This process could certainly be improved in the future. For example, the OAT data could be pre-processed to obtain a temperature profile that could be interpolated to match points where the other three items are available. Also, there are other good sources of altitude information that can be used to fill in the gaps in altitude data. Also, a degree of crosschecking of the manual data could be performed in order to correct or throw out misleading readings. The results that are presented here are based simply on logical groupings of the raw data.

Data Analysis and Tabular Results

After the merge was complete, the output was converted to Excel for presentation and plotting. The results are presented in Appendix A. Data is presented in tabular form, and graphically as a series of four plots. The tabular output is presented in three sections. Refer, for example, to table A.8 in the appendix. On the left, the GPS data is presented: latitude, longitude, altitude, X, Y, ground speed, track angle, # satellites in view and GDOP. The middle section presents the radar data: (transponder) altitude, X, Y, ground speed and track angle. The right-hand set of columns present the manually observed data, along with results calculated from that data. Observed data include altitude, OAT, IAS, heading, and (where collected) observed wind bearing and wind magnitude. Comments were also occasionally recorded. The next column is TAS, whether it was calculated or observed (observed values, where available, were used preferentially in the calculation of winds). The final two columns are the calculated values for wind bearing and magnitude. These are presented where possible regardless of whether observed wind information was recorded.

Four data plots are presented for each case. Refer, for example, to figure A.8 in the Appendix. The first plot (upper left corner) is simply an X-Y plot including both the radar and GPS data. In most cases, these curves directly overlap each other (there are some exceptions). The second plot (upper right) presents altitude information. The radar (dots) and GPS (squares) altitudes are presented, and where recorded, the observed data is shown as small triangles. The altitude plot was chosen to be the place to plot GPS GDOP, since anomalies in GPS altitude often correlated with occurrences of high GDOP. GDOP is scaled on the right-hand axis. The third plot (lower left) presents bearings and other angular data. The radar track angle (dots) and the GPS-derived track angle (squares) are shown. The observer-recorded heading is shown as triangles (note that heading is magnetic, while the other angles are true). Where available, observer-recorded wind bearing is shown as 'x' symbols. Calculated (based on other observer data and the GPS data) wind bearings are shown as 'crossed-x' symbols. The final plot (lower right) presents velocities. The radar ground speed (dots) and GPS-derived ground speed (squares) are depicted. Where available, calculated or directly observed values for TAS are presented as triangles. Observed wind speed ('x') and calculated wind speed ('crossed-x') are shown.

A casual examination of the tabular data quickly reveals cases where considerable effort was exerted by the observer to record needed data throughout the flight case (such as table A.6) as opposed to cases where relatively little was collected (see table A.11). Note that it may not be fair to judge the efforts of case 11, since apparently other problems prevented collection of the other requisite data, resulting in a very short case where only the lower portion of the descent is presented.

To get a closer look at problems such as sparse data, and to get a picture of the character of the observer data collected, the summary chart in table 1 was prepared. Two cases where only abbreviated data was available are cases 11 and 15. In case 11, only the latter portion of the descent is available due to an abrupt, significant GPS time and altitude shift (accompanied by a large drop in GDOP) that occurred midway through the descent. In case 15, only the very early portion of the flight, still at cruise altitude, was available because the GPS data set terminated early. An example of a poorly conducted task of observation is case 20. In this case, altitude and OAT were collected, not heading. TAS was collected but mislabeled; the actual data was IAS, not TAS. Since heading was not recorded, winds aloft could not be calculated. Data collection procedures in most of the other cases were quite good, however.

The data collection parameters recorded fall into a few basic groups. First are the cases where altitude, IAS and heading (with and without OAT) were collected (cases 1-5, 11, 12, 13, 15, 21-25 and 30). In these cases, TAS could be calculated from the IAS information, and winds aloft could be calculated from the TAS, heading and GPS velocity data. Supplementing these cases were those where TAS was directly observed (cases 6, 7, 9, 10, 14, 20 and 31). The calculation of winds aloft in this analysis used TAS if available, ignoring IAS data in those cases. This produced one anomalous analysis in case 9 where the recording of TAS was present, but rather sparse. More wind data could have been calculated had the TAS been ignored and the IAS data utilized in that case.

In one case (27) direct observations of wind bearing and magnitude data from the FMS were recorded, but insufficient altitude/IAS/heading data were noted to perform independent wind calculations (the heading data was quite sparse). In the remaining cases where FMS wind data were observed (8, 16-19, 26, 28 and 29), sufficient altitude, heading and IAS or TAS data was collected to achieve very valid comparisons of the air-derived, real-time wind estimates to the post-flight calculation results. The resulting plots for these last cases are perhaps the most interesting.

Table 1. Observer Data Collection Characteristics

Figure	Case	Alt	IA	OA	Hd	W_Brng/M	TA	Calc Winds
		S	T	g	ag		S	
A.1	ASH_7491_9_14	Y	Y	Y	Y			
A.2	ASH_7491_9_15	Y	Y	Y	Y			
A.3	ASH_7491_9_19	Y	Y	Y	Y			
A.4	ASH_7725_9_13	Y	Y	Y	Y			
A.5	ASH_7725_9_14	Y	Y	Y	Y			
A.6	UA_132_9_19	Y	Y		Y		Y	
A.7	UA_132_9_26	Y			Y		Y	
A.8	UA_286_9_21	Y	Y		Y	Y		
A.9	UA_296_9_20	Y	Y		Y		Y	Sparse TAS
A.10	UA_296_9_22	Y			Y		Y	
A.11	UA_470_9_27	Y	Y	Y				Sparse data
A.12	UA_470_9_28	Y	Y	Y	Y			
A.13	UA_470_9_29	Y	Y	Y	Y			
A.14	UA_724_9_13	Y			Y		Y	
A.15	UA_724_9_28	Y	Y	Y	Y			Sparse data
A.16	UA_746_9_26	Y			Y	Y	Y	
A.17	UA_746_9_27	Y			Y	Y	Y	
A.18	UA_746_9_29	Y	Y		Y	Y	Y	
A.19	UA_760_9_21	Y			Y	Y	Y	
A.20	UA_796_9_21	Y		Y			Y	N-no heading
A.21	UA_796_9_29	Y	Y	Y	Y			
A.22	UA_1103_9_12	Y	Y	Y	Y			
A.23	UA_1154_9_13	Y	Y		Y			
A.24	UA_1154_9_15	Y	Y		Y			
A.25	UA_1154_9_25	Y	Y	Y	Y			
A.26	UA_1180_9_20	Y			Y	Y	Y	
A.27	UA_1180_9_21	Y	Y		Y	Y		N (heading sparse)
A.28	UA_1618_9_13	Y			Y	Y	Y	
A.29	UA_1618_9_15	Y	Y		Y	Y		

A.30	UA_1790_9_1	Y	Y	Y	
	9				
A.31	UA_1790_9_2	Y		Y	Y
	7				

Graphic Results

In the majority of the cases, the radar and GPS X-Y data overlaid so closely at the scale presented that they are virtually indistinguishable. There is one very notable exception (case 6) and four cases where a minor departure is depicted (4, 14, 22 and 23). In case 6 the points depart by several miles. Looking ahead to the Altitude plot where GDOP is shown, it can be seen that GDOP starts at a high value (>4.0) and gets higher as the flight progresses. As shown in the accompanying table, only 3 satellites are in view throughout the flight. The conclusion is that the GPS data is in this case relatively useless; therefore, any conclusions regarding wind estimates are suspect. In case 4, 22 and 23 the GDOP values remain quite nominal. In case 14 GDOP is quite high through most of the flight.

The altitude plots also tell a story relative to GDOP. In a few cases, the GPS was unable to estimate altitude, or terminated that estimation at some point, or interrupted altitude updates for brief periods of time due to lack of confidence (within the GPS receiver) in the data available to it. For example in case 6, which was addressed above, the GPS altitude never deviated from its estimate near 39000 ft. In case 14, the GPS froze altitude data after reaching 24000 ft. In most of the cases, the GPS data tracked the radar (mode-C transponder) data quite well. For example, in case 8, where GDOP is low, the altitude plots track closely. There is a significant difference between the two values for altitude at any point due to the fact that the GPS number is a geometric altitude above the GPS datum, while the radar number is the flight level reported by the transponder (uncorrected, of course). The observer data seems to track well also, although it should, logically, track the radar plot more closely since it is also a flight level value. The next case (9) is an example where this is true.

There are a number of cases where the sensitivity of the GPS receiver's estimate of altitude to GDOP is quite apparent. For example, in case 4 at roughly 10:40:30 the GDOP figure spikes briefly, accompanied by a dip in the GPS altitude figure. Later, at roughly 10:45 GDOP jumps up, accompanied by a temporary 'level off' in GPS altitude even though the radar track demonstrates a relatively constant descent. In case 9 at roughly 10:01:30 the GDOP figure is unsteady, along with a commensurate fluctuation in GPS altitude, even though the aircraft is at level cruise. In case 12 unsteadiness in the GDOP figure at 13:02 is accompanied by an upward 'bulge' in the GPS altitude plot while the aircraft is at level cruise. Case 17 demonstrates a situation where the two altitude values track very closely during a rather unsteady descent. However, late in the descent, at roughly 13:01, GDOP increases and the GPS ceases updating altitude altogether.

The last two plots for each case should be discussed together, since they represent two aspects of the velocity vector, bearing and magnitude. Two basic quantities are depicted: aircraft velocity, and wind velocity. Looking at the 'Bearings and Winds' plot for case 3, it can be seen that the radar tracker estimate for aircraft track angle, and the post-flight derived value for GPS track

angle closely agree. Similarly, the ‘Speeds and Winds’ plot shows relatively close agreement for aircraft ground speed, although the smoothing and lag of the radar tracker algorithm is quite apparent relative to the noisier, but more accurate, GPS estimate. There are several observer-recorded heading points shown on the ‘Bearings’ plot that agree closely with the track angle also. However, this will not be generally true because, first of all, heading is influenced by winds, and, second, heading is magnetic while the track angle measures are true bearings. The local magnetic variation is 11° east. On the corresponding ‘Speeds’ plot the ‘observer’ TAS points, which were calculated from the observed IAS, altitude and OAT values, are in the neighborhood of the ground speed curves, differing by winds.

These plots also depict wind bearings and magnitudes. Where the observer noted FMS winds, they are plotted along with the observed-data (post flight) derived winds. In this case only the derived winds are available. It should be mentioned at this point that the estimation of wind speed and bearing from the data that we have available is potentially tenuous. The fact that calculated wind is the (relatively small) vector difference between two large vector quantities means that small errors in the original quantities lead to large errors in the result. However, the estimation of winds is critical to the objective of assessing CTAS arrival time prediction impacts. Errors in the GPS-based estimate of velocity, errors in the notation of the observed data, and errors in time correlation of the two can all be amplified in the wind estimation process. The GDOP measure is therefore of significant interest, as is a manual review of the observer data prior to performing the calculation. Such a review was not conducted here, and there are examples where the wind estimates fluctuate considerably. However, the varying time interval required for collecting the four necessary parameters (altitude, OAT, IAS and heading) is an error source. It is significant that we have cases where both the FMS-derived wind estimates and observer data-derived estimates exist to serve as a cross check.

There are several examples where the two wind measurement techniques are shown to correlate closely. For example, in case 8 both wind bearing measures hover around a value of 285°, while the wind magnitudes track so closely that they almost overlay each other. This is certainly a validation of the observation technique that was used. This case, however, involves a straight aircraft course. Case 27 involves a turn initiated at 13:12. The source data for calculating winds is sparse in this case, so it is difficult to draw firm conclusions. However, prior to the turn, the derived wind bearing and speed values track the FMS values well, while during the turn they are significantly different. The bearing values differ by 70 to 90 degrees, while the magnitudes differ by roughly 100 knots. Unfortunately, this is the only comparative case we have where observer TAS must be calculated from altitude, IAS and OAT, and that also involves turning maneuvers. The only other such case is 29, which again involves a straight course (and closely agreeing values for FMS winds and derived winds similar to case 8).

There are some cases where TAS must be calculated where self-consistency of the resulting wind estimation can be used as the basis for evaluating this method during a turning maneuver. For example, in case 12 a significant turn starts at 13:10:30. With the exception of one “wild” point at 13:11:01, the wind bearings remain relatively constant, and speed is steadily (and consistently) diminishing. The ‘wild’ point relates directly to the time-correlation issue mentioned earlier. The wind was calculated based on a stale heading value of 90° although the actual heading had changed (at the point in time where the calculation was made) to 120°. Improved processing

algorithms could probably avoid many such situations. A similar result occurs in case 13. Here, stale measurement data results in three 'wild' points starting at 13:14:18. The first two result in erroneous wind bearings, and the third results in an erroneous speed value. The data then settles back to its original consistency.

There are several cases that involved turning maneuvers where TAS was observed directly (avoiding the calculation of TAS from IAS). In some of these cases FMS wind data was also recorded, enabling a direct comparison to be made. Case 16 is interesting because there are 'wild' data points during the straight portion of the route as well as during the turn. The wind magnitude calculation remains relatively smooth (and in agreement with the FMS data) during the time period from 13:00:00 to 13:01:59, but two erroneous wind bearing values occur. The first is a shift of 140° at 13:00:47 and a shift of 100° in the other direction at 13:01:47. The underlying data (TAS, heading) appear smoothly changing, indicating that the cause is rather subtle. Indeed, through that period of time the heading numbers and GPS track bearings are almost perfectly constant. The cause is related to the fact that TAS (during the descent) is rapidly diminishing, and thus it is the staleness of the TAS information that is causing the problem during the straight segment. The turn starts at 13:03:11. From that point, the remaining calculations disagree sharply from the FMS winds. This is due primarily to staleness in the heading data.

Case 17, which involves a similar route, is very similar to case 16 except that there are no wild data points prior to the initiation of the turn. Once the turn point is reached, some wild points crop up. Case 18 also involves the same route, but with considerably different results. In this case the calculated wind information is basically in error throughout the descent. This seems to arise for several reasons. The initial part of the descent (from 12:54:00 until roughly 12:56:00) is conducted at a high descent rate (3800 ft/min) in comparison to the other two flights (2400 ft/min typical). This aggravates the data latency problem involving the TAS information. The FMS detected consistently high winds (averaging 60 knots) that were almost entirely in the cross-track direction. This by all rights should have resulted in a significant deviation of observed heading from track angle (crab angle). However, during the descent the heading was a constant 95° (magnetic, equals 106° true), while the GPS track angle remained at 108° . Inevitably, the result of the calculation would be a small wind magnitude (it averaged about 20 knots throughout that period). Obviously, when the wind is in the cross track direction, calculation of its magnitude and direction are extremely sensitive to errors in measuring or reading heading.

Case 19 involves flight along a route similar to cases 16 through 18. In this case the wind detected by the FMS is almost a perfect tailwind, and the results of the wind calculation agree reasonably well in both bearing and magnitude. During the turn portion, an erroneous bearing value is determined, most likely due to a stale value for heading. Case 26 is similar (also involving a tailwind). There is good agreement between the FMS and calculated wind data, even during the turning maneuver.

Findings and Recommendations

Flaws in the methods used for acquiring and processing this data have been found in all three aspects of test instrumentation: the technical, procedural and data analysis aspects. These have had serious consequences, but virtually all are amenable to corrective action.

Technical Aspects

The two primary technical problems found lie in the functioning of the GPS system and the data collection system. The GPS was found to experience significant periods where high GDOP resulted in erroneous and inconsistent results. This is partially due to the nature of the temporary antenna installation that was used, and so may be unavoidable in future tests. This is not necessarily a major obstacle. GPS coverage analysis can be used (considering the geographic region of interest, the aircraft headings involved and date and time of flight) to minimize this problem by avoiding flights at times when poor satellite coverage is anticipated. Another factor that will result in improved performance in future tests is the fact that the GPS Selective Availability function, where random errors were intentionally introduced in the unsecure channel, has been discontinued, and resulting GPS performance is greatly improved.

The software design of the data collection computer needs to be improved to avoid data overrun errors (and resulting loss of characters). This is really not difficult to do if an interrupt-driven data channel design approach is used. It is of course possible to utilize the data in the form in which it was collected; the consequence is that some data records are lost, and there is always a chance that an erroneous data character is mistakenly interpreted as valid. Methods to minimize the number of keystrokes required of the observer in recording the data observations should be looked into as well. The more easily the data can be entered, the more often data points can be taken, reducing the possibility and severity of the latency (or staleness) problems that were experienced.

Procedural Aspects

Two major procedural issues were uncovered in this analysis. The first regards time correlation between the radar data and the airborne data, and the second regards the procedures used for collection of manual observations. In flight testing, time correlation between disparate data sources is a perennial problem. In theory, GPS time can be related directly to Universal Coordinated Time (UTC). GPS time differs by a fixed number of seconds based on the number of leap seconds that have occurred since January 1, 1970. This information is available on the Internet from the United States Naval Observatory. The time value contained in this data was examined for several cases, and very little sense could be made of it. Differences (between GPS time and local time) on the order of ten minutes or so were commonly found. Furthermore, shifts of multiple seconds were observed at points where GDOP shifts. The solution to this problem hopefully lies in the use of a more modern GPS receiver that provides a reliable time value. It was not possible to judge the quality of the time stamp on the radar data. Two sources of error are likely. First, it is not known how closely the ARTCC clock is calibrated to UTC. Even if it is not, UTC-slaved clocks can be utilized by a ground observer to calibrate the radar time stamp. The other issue regards latency of any given radar point relative to its time stamp.

The time stamp probably relates to the time of filter processing output (the time that a radar display would be updated) rather than the specific instant corresponding to the radar hit on the target. In an ideal world, both the tracker output (and its time stamp) and the raw range/bearing/altitude hit information, with its time stamp, would be available (they would not need to be provided in a single database; they could be merged later). This would allow evaluation of the tracker algorithm as it influences the CTAS arrival time prediction process.

The second procedural issue regards the manual collection of airborne data by the observer. The first issue regards the parameters collected. It is quite apparent from the graphical results that the FMS wind estimates are more accurate and reliable than the post-flight estimates that are based on observed parameters. They are also not very sensitive to latency problems; a wind reading that is merged a few seconds late is still an accurate reading. However, the result of calculations based on non-simultaneous readings of heading, TAS, etc. can be wildly inaccurate. Furthermore, the calculation of winds based on manually noted heading information is fraught with difficulty. Particularly in crosswind situations, for example, a one-degree error in heading information can have a sizeable impact on the resulting wind estimate.

Where FMS winds are not available, the manual reading of altitude, OAT, IAS (and/or TAS) and heading can, within limits, result in good information. It was not obvious from the results examined here that the direct availability of TAS information proves superior to deriving TAS from IAS, altitude and OAT. However, eliminating the need to record all three of those parameters greatly reduces the manual workload level, meaning that data can be recorded more often during critical phases of flight (particularly during turning maneuvers). Of that list of parameters, altitude is least important since both radar and GPS altitude are available. In the absence of radar altitude, a few scattered altimeter readings could be used within the data reduction program to model the altitude profile accurately based on the GPS information. Likewise, OAT does not usually change radically. Relatively sparse OAT data could be used to define a temperature profile during the descent. The time-critical items are airspeed (whether IAS or TAS) and heading. These must be recorded often, and each pair should be recorded in quick succession (particularly during turns).

Data Analysis Aspects

Steps could be implemented to improve the quality of the wind information derivable from such data (indeed, even from a reanalysis of the present data). For example, the basic approach used here was to average and interpolate and merge the GPS data at each radar time point, and then to let the observed data slip into the nearest appropriate time slot. This resulted in output data records every twelve seconds (roughly). A considerable improvement would result if the altitude and OAT data were used to establish profiles of altitude versus time and OAT versus time, such that an appropriate value for altitude and OAT could be synthesized at the point in time when each IAS reading was taken. The IAS/TAS and heading information should then be processed relative to the GPS averaging/interpolation process to derive winds at the instant that each heading observation was taken. In other words, the GPS data should first be merged with the observer data. Only after this is accomplished should the radar data be merged in as well. Wind estimates derived from the merged data set should exhibit little or no latency since they will be matched in time to the GPS information.

Appendix A

Tabular and Graphic Results for the Portable Data Collector Tests

Table A.1 Tabular Results for Case ASH_7491_9_14

ASH_7491_9_14	GPS DATA					RADAR DATA					OBSERVER DATA													
TOD	GPS_LAT	GPS_LON	GPS_ALT	GPS_X	GPS_Y	GPS_GS	GPS_TRK	G_SATS	GDOP	R_ALT	R_X	R_Y	R_GS	R_TRK	OBS_ALT	OBS_OAT	OBS_IAS	OBS_HDG	OBS_WBRG	OBS_WMAG	OBS_CMT	C/O_TAS	CALC_WBRG	CALC_WMAG
9:50:18	41.01786	105.6247	24154	420.05	466.29	281	163	4	2.3	23000	419.94	466.56	284	163										
9:50:30	41.00234	105.6185	24161	420.34	465.36	287	163	4	2.3	23000	420.38	465.38	284	161										
9:50:42	40.98709	105.6126	24180	420.62	464.45	291	163	4	2.3	23000	420.69	464.50	284	160										
9:50:54	40.97213	105.6068	24176	420.89	463.55	281	163	4	2.3	23000	420.56	463.94	284	174										
9:51:06	40.95709	105.6008	24184	421.17	462.65	293	162	4	2.3	23000	420.88	462.94	286	166										
9:51:18	40.94207	105.5947	24161	421.46	461.75	286	162	4	2.3	23000	421.56	461.75	287	155										
9:51:30	40.92660	105.5883	23995	421.76	460.83	281	162	4	2.3	22900	421.88	460.81	288	160										
9:51:42	40.91153	105.5821	23751	422.05	459.93	284	161	4	2.3	22700	422.19	459.88	289	161										
9:51:54	40.89647	105.5755	23471	422.36	459.03	279	161	4	2.3	22400	422.38	459.06	290	165										
9:52:06	40.88100	105.5688	23189	422.68	458.11	296	161	4	2.3	22200	422.50	458.50	291	167										
9:52:18	40.86556	105.5619	22926	423.00	457.18	295	161	4	2.3	22000	422.88	457.69	292	159	220	-9	210					287		
9:52:30	40.84997	105.5550	22669	423.32	456.25	296	160	4	2.3	21500	423.38	456.31	293	160										
9:52:42	40.83455	105.5481	22419	423.65	455.33	297	159	4	2.3	21300	423.63	455.25	293	165				157						
9:52:54	40.81936	105.5412	22192	423.97	454.42	293	153	4	2.3	21100	423.88	454.38	293	164										
9:53:06	40.80505	105.5321	21984	424.39	453.57	290	151	4	2.3	20900	424.31	454.00	293	150										
9:53:18	40.79066	105.5221	21789	424.86	452.71	291	151	4	2.3	20700	424.88	453.19	292	147	210									
9:53:30	40.77670	105.5122	21617	425.32	451.88	276	151	4	2.3	20300	425.44	451.94	292	153										
9:53:42	40.76284	105.5021	21472	425.79	451.05	267	150	4	2.3	20200	425.81	451.00	291	157										
9:53:54	40.74937	105.4920	21334	426.26	450.25	278	149	4	2.3	20100	426.38	450.25	290	147										
9:54:06	40.73640	105.4820	21169	426.72	449.48	272	149	4	2.3	19900	426.63	449.88	289	147										
9:54:18	40.72355	105.4720	20981	427.19	448.71	268	149	4	2.3	19800	426.94	449.06	289	155										
9:54:30	40.71089	105.4621	20778	427.65	447.96	272	148	4	2.3	19400	427.75	447.94	287	147	200									
9:54:42	40.69812	105.4520	20512	428.12	447.20	276	148	4	2.3	19200	428.19	447.19	286	149										
9:54:54	40.68496	105.4418	20234	428.59	446.42	276	146	4	2.3	19000	428.63	446.38	284	151										
9:55:06	40.67205	105.4310	19971	429.10	445.65	275	145	4	2.3	18800	429.00	445.94	283	143										
9:55:18	40.65907	105.4197	19713	429.62	444.87	274	144	4	2.3	18600	429.38	445.19	281	150	190									
9:55:30	40.64625	105.4081	19467	430.16	444.11	275	144	4	2.3	18400	430.00	444.50	280	141										
9:55:54	40.62138	105.3849	19039	431.24	442.63	280	142	4	2.3	17900	431.25	442.63	277	146										
9:56:06	40.60911	105.3726	18812	431.81	441.91	279	141	4	2.3	17800	431.81	441.88	276	144										
9:56:18	40.59700	105.3602	18613	432.39	441.18	270	140	4	2.3	17900	432.25	441.50	276	135	180									
9:56:30	40.58527	105.3478	18427	432.96	440.49	264	139	4	2.9	17800	432.69	440.69	276	147										
9:56:42	40.57341	105.3349	18207	433.56	439.79	274	139	4	2.3	17500	433.50	439.69	276	143										
9:56:54	40.56216	105.3222	17983	434.15	439.12	276	138	4	1.7	17400	434.25	439.06	276	134										
9:57:06	40.55047	105.3091	17802	434.76	438.43	269	137	4	1.7	17200	434.81	438.38	276	139										
9:57:18	40.53892	105.2956	17537	435.38	437.74	282	138	4	1.7	17000	435.19	438.00	276	136	170									
9:57:30	40.52752	105.2822	17289	436.00	437.07	286	138	4	1.7	16900	435.69	437.25	276	143										
9:57:42	40.51577	105.2686	17043	436.64	436.37	289	138	4	1.7	16400	436.63	436.19	277	140										
9:57:54	40.50390	105.2548	16794	437.28	435.67	296	137	4	1.7	16200	437.38	435.56	277	133										

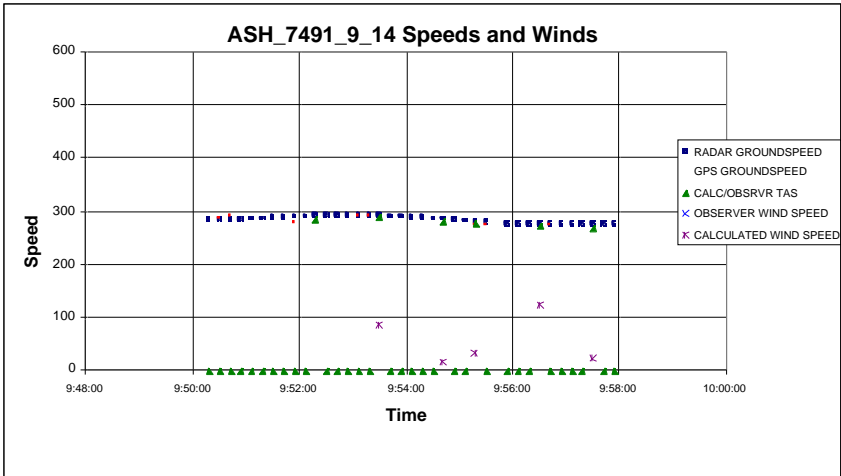
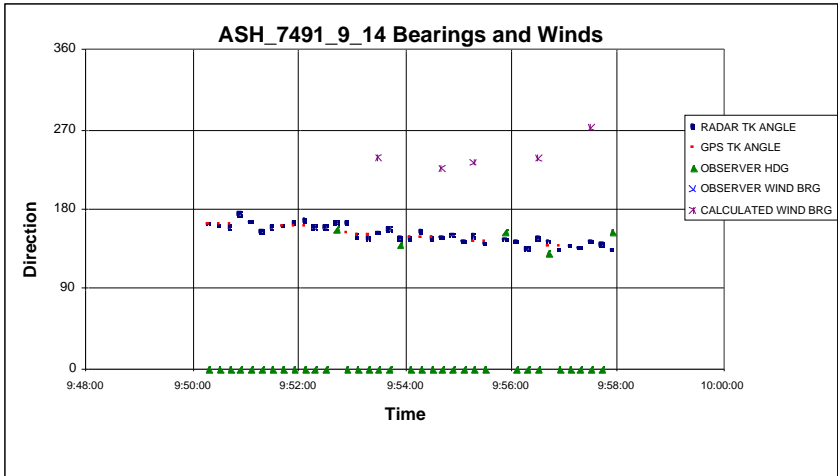
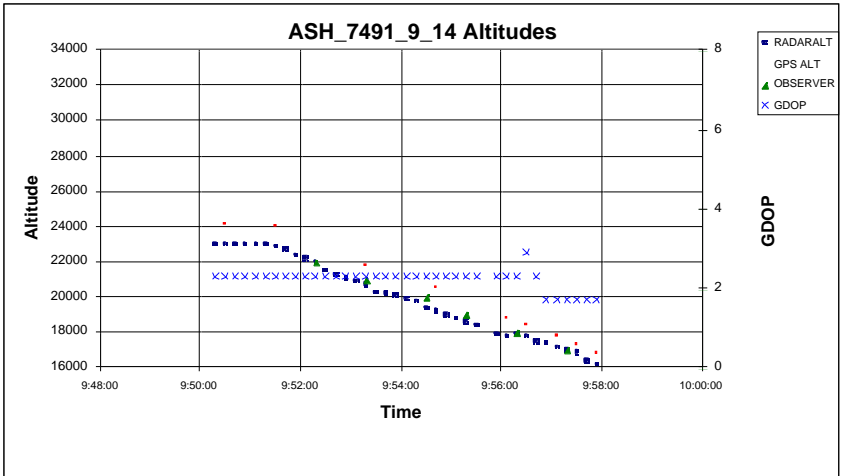
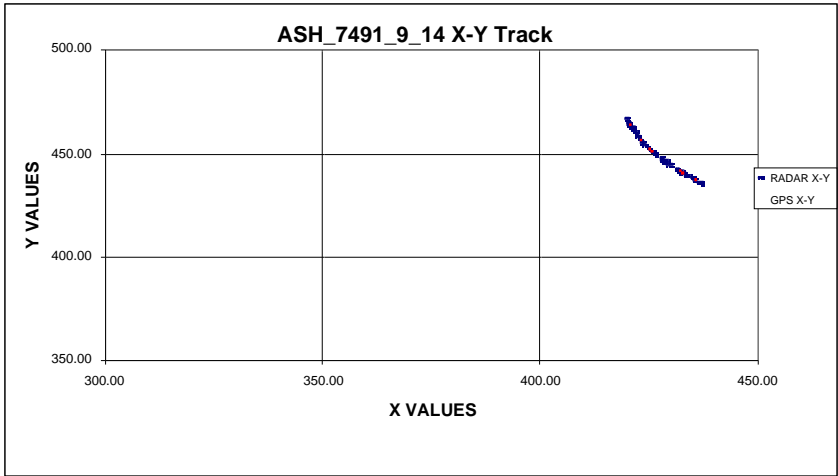


Figure A.1 Graphic Results for Case ASH_7491_9_14

Table A.1 Tabular Results for Case ASH_7491_9_15

ASH_7491_9_15	<--		GPS		DATA				--> <--		RADAR		DATA		--> <--		OBSERVER		DATA				-->			
TOD	GPS_LAT	GPS_LON	GPS_ALT	GPS_X	GPS_Y	GPS_GS	GPS_TRK	G_SATS	GDOP	R_ALT	R_X	R_Y	R_GS	R_TRK	OBS_ALT	OBS_OAT	OBS_IAS	OBS_HDG	OBS_WBRG	OBS_WMAG	OBS_CMT	C/O_TAS	CALC_WBRG	CALC_WMAG		
9:34:39	41.04437	105.6431	23640	419.20	467.87	320	160	4	2.1	23000	419.56	467.63	306	154												
9:34:51	41.02819	105.6356	23665	419.55	466.90	306	160	4	2.1	23000	419.88	466.63	306	160												
9:35:03	41.01194	105.6281	23696	419.90	465.93	314	160	4	2.1	23000	419.88	466.06	306	174												
9:35:15	40.99538	105.6204	23729	420.26	464.94	316	160	4	2.2	23000	420.50	465.19	307	160												
9:35:27	40.97922	105.6129	23760	420.61	463.97	322	160	4	2.2	23000	421.13	463.69	307	158												
9:35:39	40.96282	105.6052	23808	420.97	462.99	306	159	4	2.2	23000	421.31	462.63	308	166												
9:35:51	40.94703	105.5971	23878	421.35	462.05	322	154	4	2.2	23000	421.25	461.56	308	178												
9:36:03	40.93143	105.5869	23931	421.82	461.12	315	150	4	2.2	23000	422.00	461.38	308	164												
9:36:15	40.91603	105.5755	23838	422.35	460.20	305	150	4	2.2	22900	422.31	460.50	307	162												
9:36:27	40.90155	105.5648	23668	422.85	459.34	290	150	4	2.2	22600	423.19	459.13	307	152												
9:36:39	40.88742	105.5542	23503	423.33	458.50	294	150	4	2.2	22400	423.56	458.13	306	157												
9:36:51	40.87350	105.5439	23352	423.82	457.67	276	150	4	2.2	22200	424.00	457.31	306	153												
9:37:03	40.86055	105.5342	23218	424.26	456.89	276	150	4	2.2	22000	424.31	457.06	305	139												
9:37:15	40.84649	105.5237	23059	424.75	456.06	284	150	4	2.3	21900	424.81	456.13	304	148	220			190				265				
9:37:27	40.83305	105.5137	22910	425.22	455.26	282	150	4	2.3	21500	425.56	455.00	303	147							1200					
9:37:39	40.81980	105.5038	22785	425.67	454.47	277	150	4	2.3	21400	425.94	454.19	301	153												
9:37:51	40.80684	105.4941	22637	426.12	453.70	273	150	4	2.3	21200	426.44	453.50	299	147												
9:38:03	40.79316	105.4840	22386	426.59	452.88	268	150	4	2.3	21000	426.69	452.50	297	160												
9:38:15	40.78001	105.4741	22203	427.05	452.10	274	150	4	2.3	20800	427.00	452.13	295	146	210			190								
9:38:27	40.76651	105.4641	22002	427.52	451.29	275	150	4	2.3	20700	427.44	451.31	293	150							1200	256	355			21
9:38:39	40.75302	105.4542	21794	427.98	450.49	277	150	4	2.3	20300	428.25	450.25	291	145												
9:38:51	40.73964	105.4442	21584	428.44	449.69	284	148	4	2.3	20100	428.75	449.31	289	150												
9:39:03	40.72650	105.4336	21369	428.94	448.91	283	146	4	2.4	20000	429.19	448.56	287	150	200											
9:39:15	40.71366	105.4223	21160	429.46	448.14	281	145	4	2.4	19800	429.50	448.19	286	143								254	298			30
9:39:27	40.70092	105.4108	20972	430.00	447.39	281	144	4	2.4	19700	429.94	447.56	285	144												
9:39:39	40.68809	105.3990	20770	430.54	446.62	274	144	4	2.4	19200	430.69	446.25	284	149												
9:39:51	40.67553	105.3875	20583	431.08	445.88	274	144	4	2.4	19100	431.31	445.56	283	141												
9:40:03	40.66320	105.3762	20400	431.60	445.14	284	144	4	2.4	18900	431.75	444.75	282	148												
9:40:15	40.65091	105.3649	20212	432.13	444.42	269	144	4	2.4	18700	432.13	444.44	282	135	190			190								
9:40:27	40.63847	105.3533	20007	432.67	443.67	268	144	4	2.4	18500	432.56	443.69	281	145								1100	251	333		17
9:40:39	40.62566	105.3413	19787	433.23	442.91	268	144	4	2.5	18100	433.31	442.56	280	146												
9:40:51	40.61338	105.3298	19544	433.76	442.18	266	144	4	2.5	17800	433.88	441.94	279	140												
9:41:03	40.60134	105.3186	19283	434.28	441.47	257	144	4	2.5	17700	434.50	441.19	278	140												
9:41:15	40.58976	105.3078	18999	434.79	440.78	257	144	4	2.5	17500	435.00	440.44	277	144												
9:41:27	40.57801	105.2968	18698	435.30	440.08	251	144	4	2.5	17200	435.19	440.19	276	144												
9:41:39	40.56641	105.2860	18383	435.80	439.39	243	144	4	2.5	16900	435.69	439.44	274	145								1600				
9:41:51	40.55550	105.2758	18116	436.27	438.75	243	143	4	2.5	16500	436.44	438.44	272	144								252	126			9
9:42:03	40.54459	105.2653	17947	436.76	438.10	240	143	4	2.6	16400	436.94	437.81	270	142												
9:42:15	40.53400	105.2551	17789	437.24	437.47	244	143	4	2.6	16300	437.50	437.13	269	141								1300				
9:42:27	40.52327	105.2447	17620	437.72	436.84	238	142	4	2.6	16200	437.63	436.88	266	141												
9:42:39	40.51242	105.2340	17440	438.22	436.19	236	142	4	2.6	16100	438.19	436.25	264	142												
9:42:51	40.50209	105.2237	17307	438.70	435.58	247	142	4	2.6	16004	438.91	435.29	262	143												

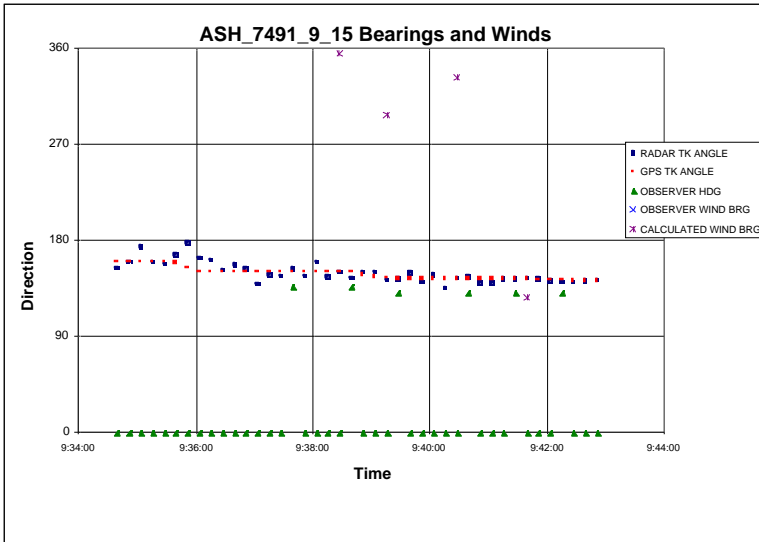
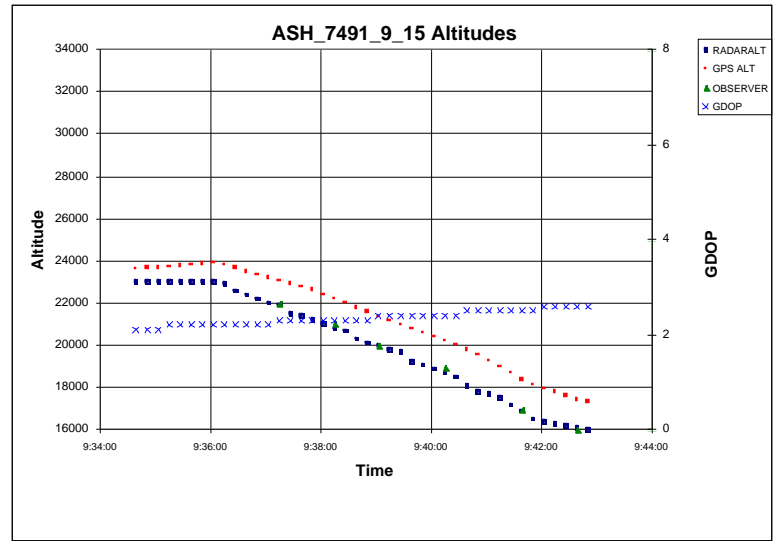
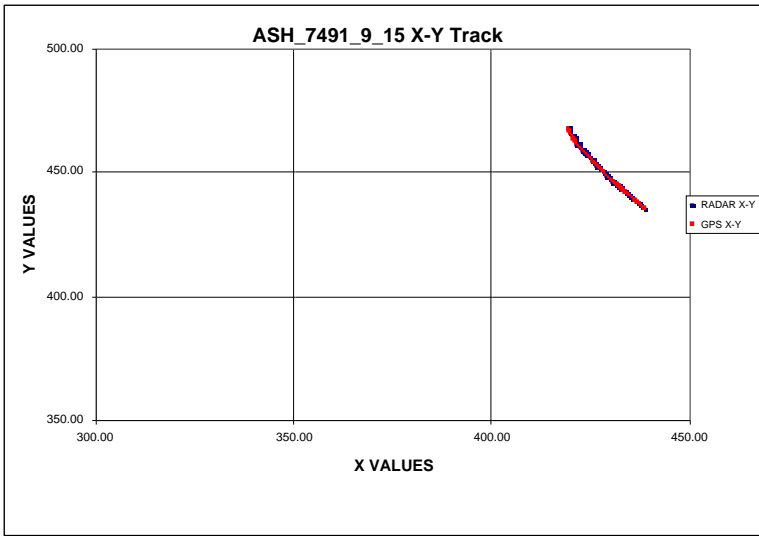


Figure A.2 Graphic Results for Case ASH_7491_9_15

Table A.3 Tabular Results for Case ASH_7491_9_19

ASH_7491_9_19	GPS DATA										RADAR DATA				OBSERVER DATA										
TOD	GPS_LAT	GPS_LON	GPS_ALT	GPS_X	GPS_Y	GPS_GS	GPS_TRK	G_SATS	GDOP	R_ALT	R_X	R_Y	R_GS	R_TRK	OBS_ALT	OBS_OAT	OBS_IAS	OBS_HDG	OBS_WBRG	OBS_WMAG	OBS_CMT	C/O_TAS	CALC_WBRG	CALC_WMAG	
9:33:54	41.02023	105.6295	23979	419.84	466.43	322	162	4	2.3	23000	419.81	466.81	312	166											
9:34:06	41.00378	105.6225	23967	420.16	465.44	307	161	4	2.3	23000	420.19	465.75	311	162											
9:34:18	40.98747	105.6155	23952	420.49	464.47	317	160	4	2.3	23000	420.44	464.69	311	165											
9:34:30	40.97095	105.6080	23963	420.84	463.48	315	159	4	2.3	23000	420.75	463.69	312	163											
9:34:42	40.95415	105.5999	23942	421.22	462.48	309	160	4	2.3	23000	420.88	463.19	312	165											
9:34:54	40.93794	105.5923	23891	421.57	461.51	320	161	4	2.3	23000	421.25	462.31	312	159	230										
9:35:06	40.92102	105.5847	23702	421.93	460.50	328	161	4	2.3	22900	421.63	460.69	313	165											
9:35:18	40.90362	105.5769	23490	422.29	459.46	336	160	4	2.3	22700	422.19	459.81	314	152											
9:35:30	40.88569	105.5689	23265	422.67	458.39	340	160	4	2.3	22500	422.56	458.88	315	156											
9:35:42	40.86826	105.5607	23056	423.05	457.35	345	158	4	2.3	22300	422.81	458.19	316	159	220										
9:35:54	40.85097	105.5517	22858	423.47	456.31	326	154	4	2.3	22100	423.06	457.19	316	164											
9:36:06	40.83434	105.5416	22668	423.94	455.32	324	150	4	2.3	21700	423.75	455.63	318	159											
9:36:18	40.81817	105.5302	22426	424.47	454.36	305	145	4	2.3	21500	424.44	454.63	319	149											
9:36:30	40.80373	105.5174	22168	425.06	453.50	313	144	4	2.3	21300	424.75	453.69	321	158											
9:36:42	40.79004	105.5046	21914	425.66	452.68	308	143	4	2.3	21100	425.31	452.88	322	149											
9:36:54	40.77634	105.4914	21670	426.27	451.87	310	143	3	2.0	21000	425.75	452.50	323	136											
9:37:06	40.76262	105.4780	21456	426.89	451.05	303	143	4	2.3	20700	426.31	451.56	324	145											
9:37:18	40.74891	105.4646	21246	427.51	450.24	298	142	4	2.3	20400	427.25	450.44	324	142											
9:37:30	40.73553	105.4513	21032	428.12	449.44	304	142	4	2.3	20200	427.94	449.63	324	140											
9:37:42	40.72208	105.4379	20768	428.75	448.64	307	142	4	2.3	20000	428.56	448.75	324	143											
9:37:54	40.70864	105.4245	20530	429.37	447.84	302	142	4	2.3	19900	428.81	448.44	323	142											
9:38:06	40.69492	105.4109	20303	430.00	447.03	298	142	4	2.3	19700	429.50	447.69	321	139											
9:38:18	40.68166	105.3978	20080	430.60	446.24	298	143	4	2.3	19300	430.38	446.38	319	144											
9:38:30	40.66830	105.3847	19869	431.21	445.45	296	143	3	2.0	19100	430.94	445.63	317	143											
9:38:42	40.65510	105.3719	19661	431.80	444.66	285	144	3	2.0	18900	431.69	444.88	315	138											
9:38:54	40.64139	105.3593	19541	432.39	443.85	286	145	4	2.7	18600	432.00	444.56	312	136											
9:39:06	40.62804	105.3472	19324	432.95	443.06	291	145	4	2.7	18500	432.56	443.69	310	144											
9:39:18	40.61530	105.3357	19162	433.49	442.30	286	144	4	2.7	18100	433.31	442.56	308	146											
9:39:30	40.60227	105.3237	18913	434.05	441.52	284	143	4	2.7	17900	433.94	441.81	306	142											
9:39:42	40.58889	105.3106	18681	434.65	440.73	297	142	3	2.3	18000	434.44	441.00	303	146											
9:39:54	40.57579	105.2976	18495	435.26	439.95	299	142	4	2.7	17800	435.00	440.19	301	146											
9:40:06	40.56293	105.2848	18352	435.86	439.19	288	141	3	2.3	17600	435.38	439.88	299	135											
9:40:18	40.55068	105.2721	17930	436.45	438.46	297	141	3	2.3	17500	435.88	439.06	297	144											
9:40:30	40.53744	105.2585	17719	437.08	437.68	296	141	3	2.3	17200	437.00	438.00	296	137											
9:40:42	40.52500	105.2458	17528	437.67	436.94	296	141	3	2.3	16900	437.56	437.13	294	144											
9:40:54	40.51182	105.2324	17422	438.30	436.15	279	140	3	2.3	16700	438.06	436.38	293	146											
9:41:06	40.49936	105.2197	17028	438.88	435.42	277	140	3	2.3	16500	438.44	436.13	292	132											
9:41:17	40.48818	105.2083	16424	439.42	434.75	275	140	3	2.3	16316	439.01	435.38	291	138											

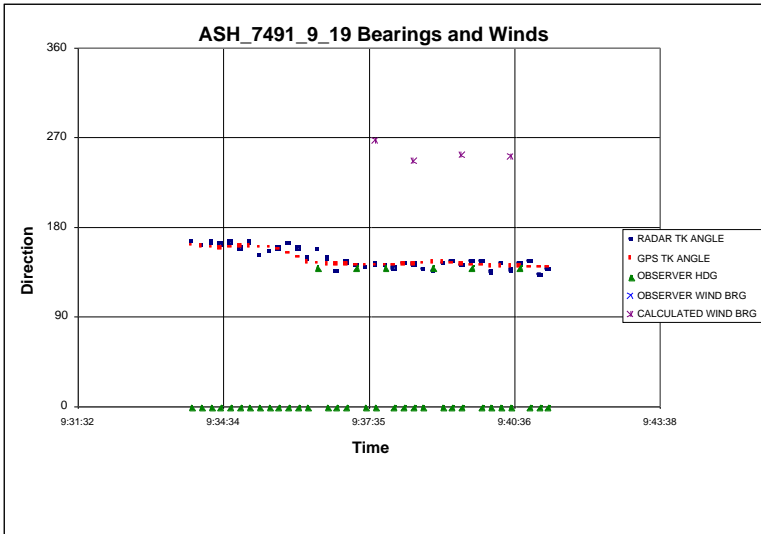
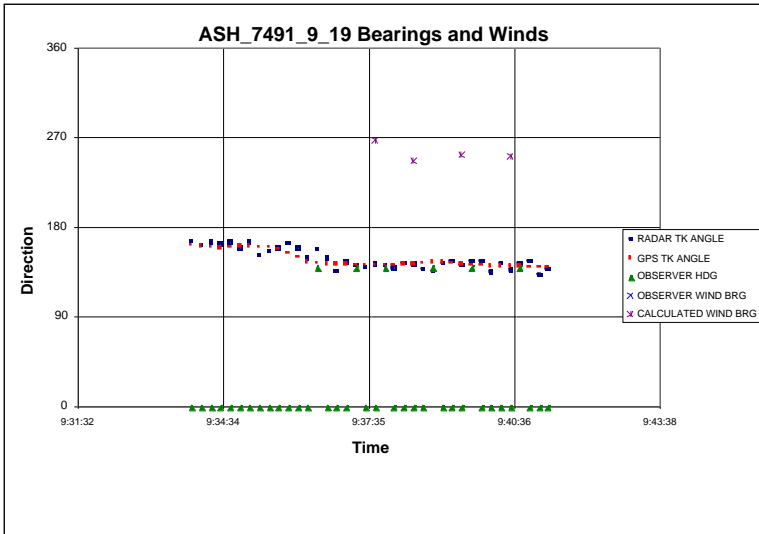
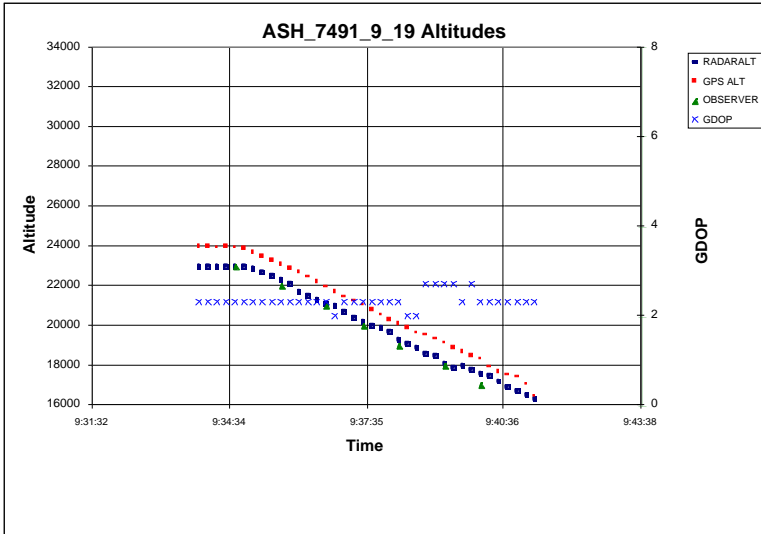
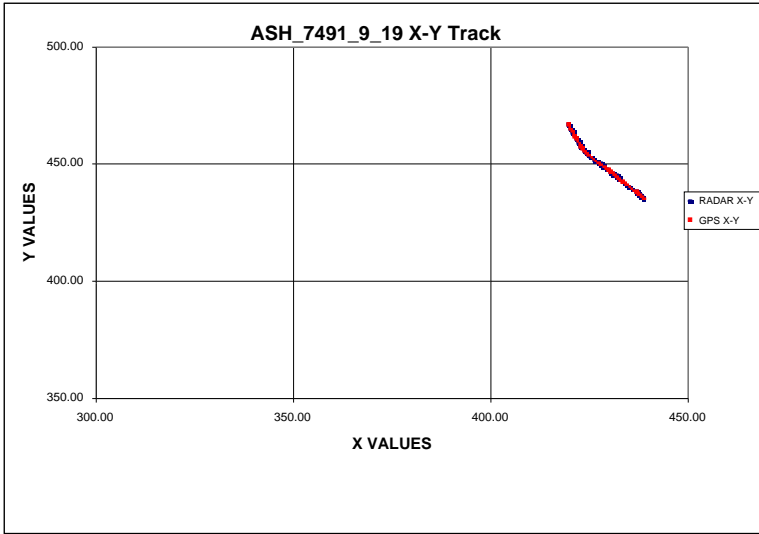


Figure A.3 Graphic Results for Case ASH_7491_9_19

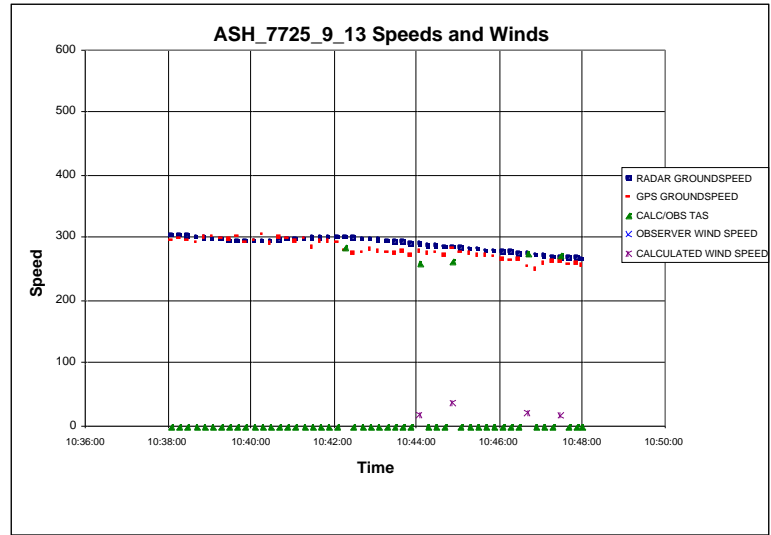
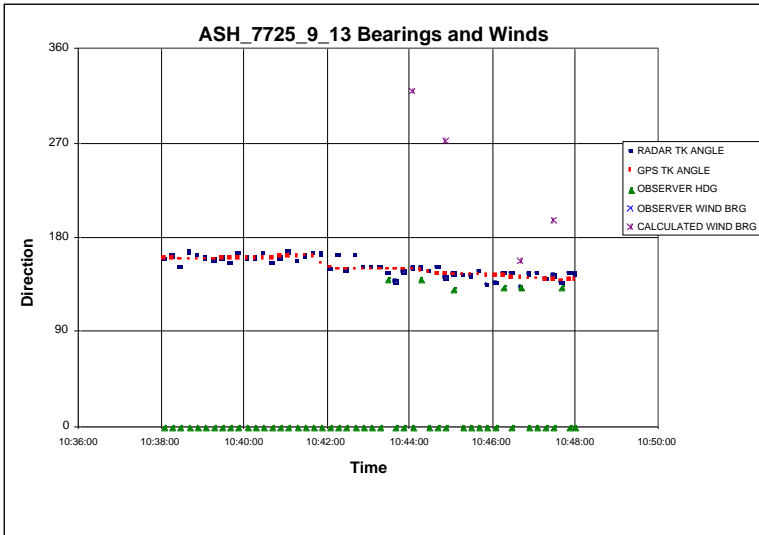
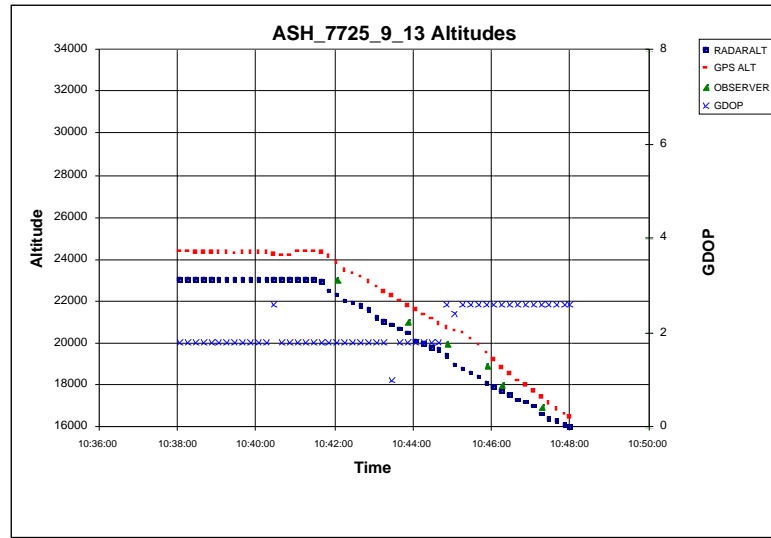
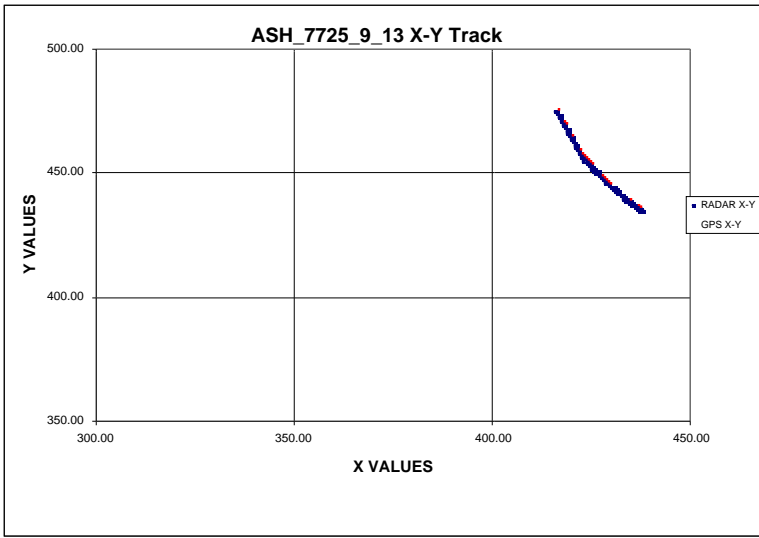


Figure A.4 Graphic Results for Case ASH_7725_9_13

Table A.5 Tabular Results for Case ASH_7725_9_14

ASH_7725_9_14	GPS DATA						RADAR DATA				OBSERVER DATA				OBSERVER DATA									
TOD	GPS_LAT	GPS_LON	GPS_ALT	GPS_X	GPS_Y	GPS_GS	GPS_TRK	G_SATS	GDOP	R_ALT	R_X	R_Y	R_GS	R_TRK	OBS_ALT	OBS_OAT	OBS_IAS	OBS_HDG	OBS_WBRG	OBS_WMAG	OBS_CMT	C/O_TAS	CALC_WBRG	CALC_WMAG
10:31:14	41.10185	105.8347	26082	410.48	471.24	271	142	4	1.8	25000	410.69	471.25	288	132	250	-14	192	134			wx qs from atc	273	227	16
10:31:25	41.08980	105.8223	26119	411.05	470.52	288	142	4	1.8	25000	410.94	470.56	289	146										
10:31:38	41.07738	105.8095	26146	411.63	469.78	279	141	4	1.8	25000	411.75	469.69	289	140										
10:31:50	41.06528	105.7969	26163	412.21	469.06	279	141	4	1.8	25000	412.19	469.06	289	143							desc by 9 mile			
10:32:02	41.05303	105.7838	26177	412.81	468.33	269	141	4	1.8	25000	412.44	468.75	288	142										
10:32:13	41.04113	105.7713	26221	413.38	467.62	278	141	4	1.8	25000	414.13	467.13	290	136										
10:32:25	41.02944	105.7589	26225	413.95	466.92	277	140	4	2.2	25000	413.94	466.94	290	136										
10:32:38	41.01753	105.7461	26188	414.54	466.22	289	141	4	1.8	25000	414.56	466.19	290	149										
10:32:50	41.00532	105.7330	26088	415.14	465.49	290	140	4	1.8	25000	415.31	465.69	291	135										
10:33:02	40.99318	105.7200	25969	415.74	464.77	291	140	4	1.8	24900	415.81	464.81	292	146							ramm 160 230			
10:33:14	40.98083	105.7067	25809	416.35	464.03	304	139	4	1.8	24500	416.56	463.75	291	145							alt 3031.			
10:33:26	40.96777	105.6926	25538	417.00	463.25	306	139	4	1.8	24300	417.25	462.94	291	141										
10:33:38	40.95512	105.6788	25262	417.63	462.50	314	138	4	1.8	24100	417.94	462.13	292	140							dme 80			
10:33:50	40.94162	105.6639	24977	418.31	461.70	313	136	4	1.8	23900	418.56	461.38	294	140	245									
10:34:02	40.92912	105.6484	24746	419.02	460.96	313	136	4	1.8	23700	419.00	461.00	296	133										
10:34:14	40.91636	105.6325	24515	419.76	460.20	307	136	4	1.8	23500	419.69	460.38	296	133										
10:35:02	40.86711	105.5698	23589	422.64	457.27	320	137	4	1.8	22600	422.63	457.31	296	135										
10:35:14	40.85447	105.5541	23378	423.36	456.52	318	139	4	1.8	22400	423.50	456.56	298	132	234	-10	220	127			76/307 gs	306	301	14
10:35:26	40.84134	105.5389	23165	424.06	455.74	315	140	4	1.8	22000	424.44	455.56	300	135							72 308 dvv			
10:35:38	40.82793	105.5246	22932	424.72	454.94	317	140	4	1.8	21900	425.00	454.69	302	144	225	-9	230				1000fpm	316	46	12
10:35:50	40.81453	105.5103	22701	425.38	454.15	308	141	4	1.8	21700	425.69	453.88	304	141										
10:36:02	40.80111	105.4961	22461	426.04	453.35	312	141	4	1.8	21500	425.88	453.38	306	154	220						69 309 knot dvv			
10:36:14	40.78728	105.4819	22199	426.70	452.53	309	142	4	1.8	21300	426.63	452.56	308	142										
10:36:26	40.77365	105.4680	21925	427.34	451.72	316	142	4	1.8	20900	427.69	451.31	310	140										
10:36:38	40.75969	105.4538	21645	428.00	450.89	314	142	4	1.8	20700	428.13	450.50	311	148										
10:36:50	40.74563	105.4397	21358	428.65	450.05	305	144	4	1.7	20400	428.81	449.69	313	142										
10:37:02	40.73164	105.4267	21066	429.25	449.22	302	145	4	1.7	20200	429.50	449.00	314	137										
10:37:14	40.71789	105.4142	20815	429.83	448.40	299	145	4	1.9	19900	429.81	448.56	314	142										
10:37:26	40.70429	105.4021	20588	430.39	447.60	305	145	4	1.8	19700	430.38	447.63	313	147	202						there was a confusion			
10:37:38	40.69046	105.3897	20319	430.97	446.77	307	145	4	1.7	19300	431.25	446.44	313	145							60 309			
10:37:50	40.67650	105.3772	20030	431.55	445.94	303	145	4	1.7	19000	431.94	445.63	312	141	195						1500fpm			
10:38:02	40.66264	105.3648	19732	432.13	445.12	309	144	4	1.9	18800	432.38	444.69	311	151										
10:38:14	40.64863	105.3521	19462	432.71	444.28	317	144	4	1.8	18500	432.81	444.31	310	137										
10:38:26	40.63442	105.3392	19047	433.32	443.44	317	144	4	1.8	18200	433.25	443.44	309	148										
10:38:38	40.61995	105.3261	18637	433.92	442.58	319	145	4	1.7	17800	434.19	442.19	308	145	185									
10:38:50	40.60549	105.3133	18241	434.52	441.72	312	146	4	1.7	17500	434.88	441.38	307	141										
10:39:02	40.59099	105.3007	17885	435.11	440.86	305	146	4	1.7	17200	435.44	440.44	306	147	177									
10:39:14	40.57676	105.2885	17507	435.68	440.02	310	146	4	1.7	16900	435.75	440.00	306	145										
10:39:26	40.56209	105.2760	17162	436.26	439.14	310	146	4	1.9	16700	436.38	439.19	306	143										
10:39:38	40.54770	105.2634	16808	436.85	438.29	309	145	4	1.9	16400	436.69	438.31	306	155										
10:39:50	40.53329	105.2508	16570	437.44	437.43	319	145	4	1.8	16000	437.63	437.06	306	147	161									
10:40:02	40.51887	105.2380	16335	438.04	436.58	314	145	4	1.8	15800	438.19	436.19	306	147										
10:40:14	40.50433	105.2251	16152	438.64	435.71	310	144	4	2.5	15600	438.81	435.38	306	144										
10:40:16	40.50109	105.2221	16128	438.78	435.52	308	145	4	2.5	15577	438.90	435.28	306	143							47.7 311 dvv	305	293	5

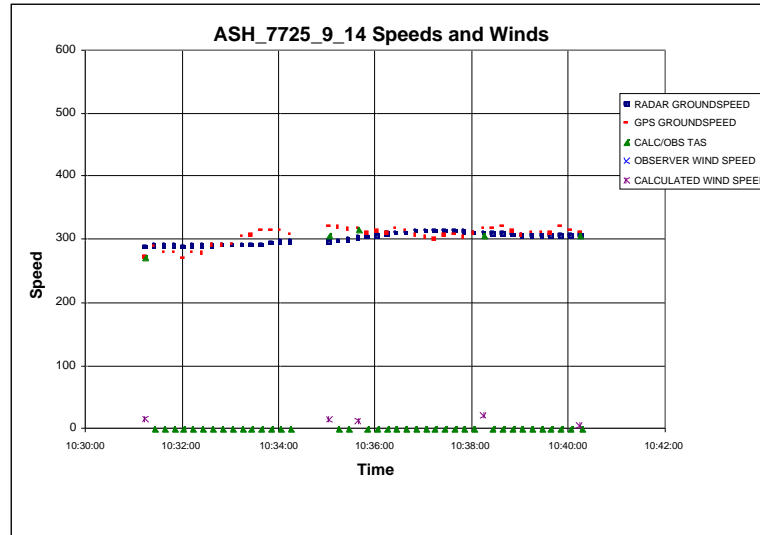
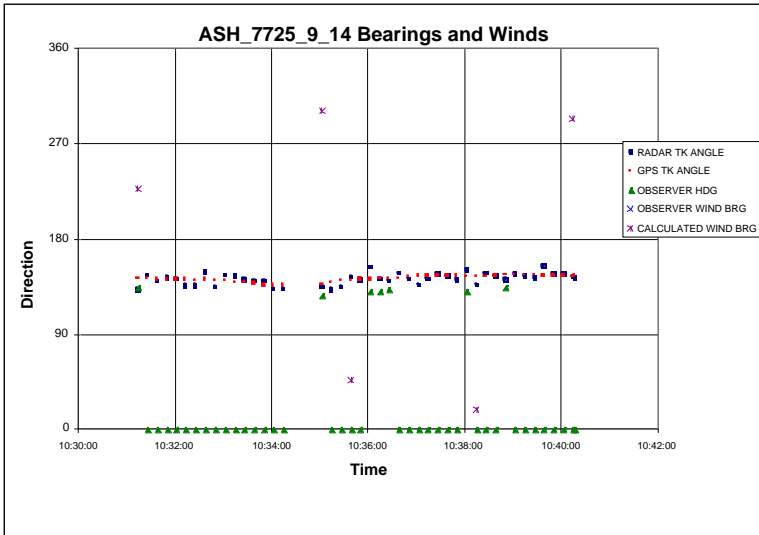
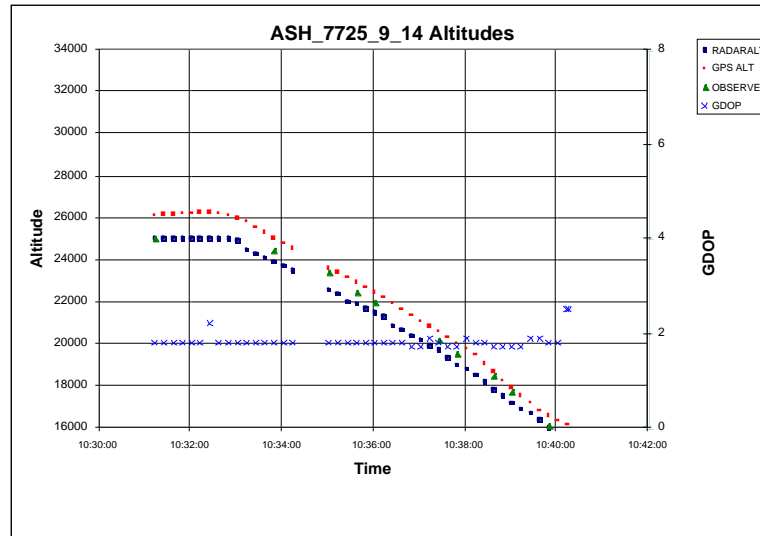
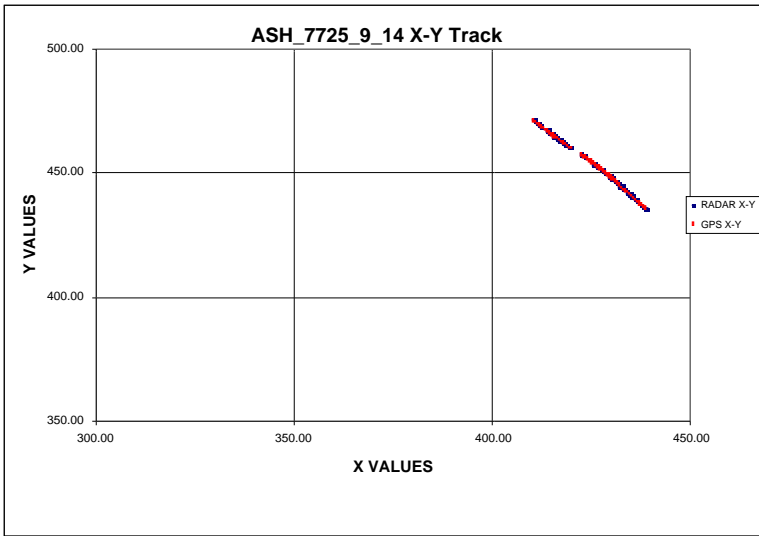


Figure A.5 Graphic Results for Case ASH_7715_9_14

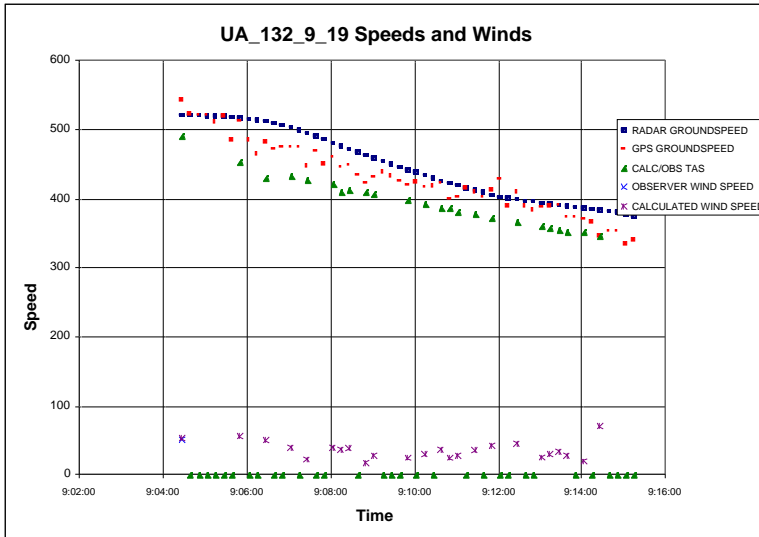
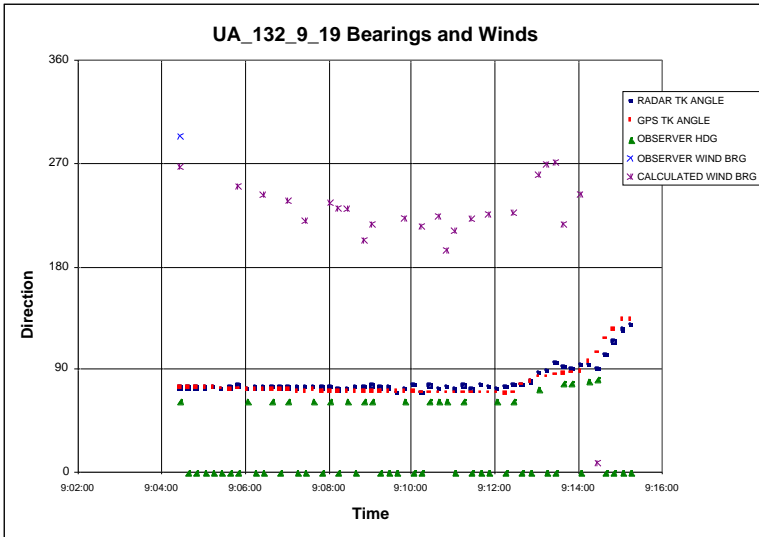
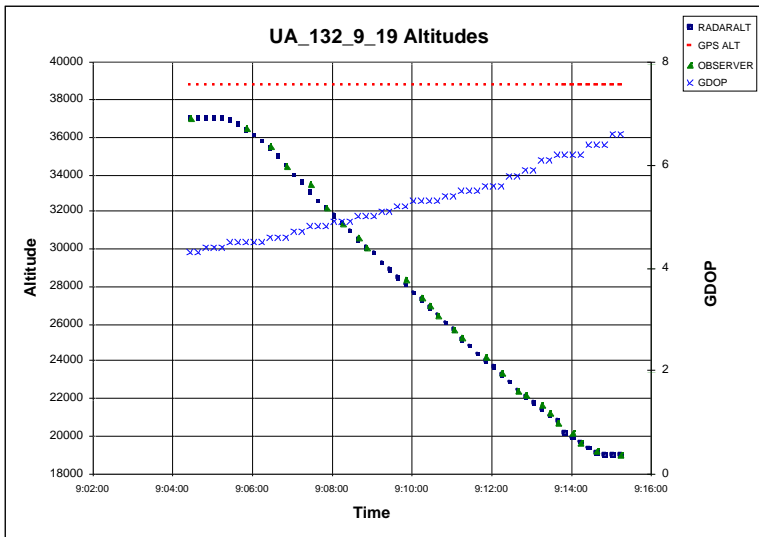
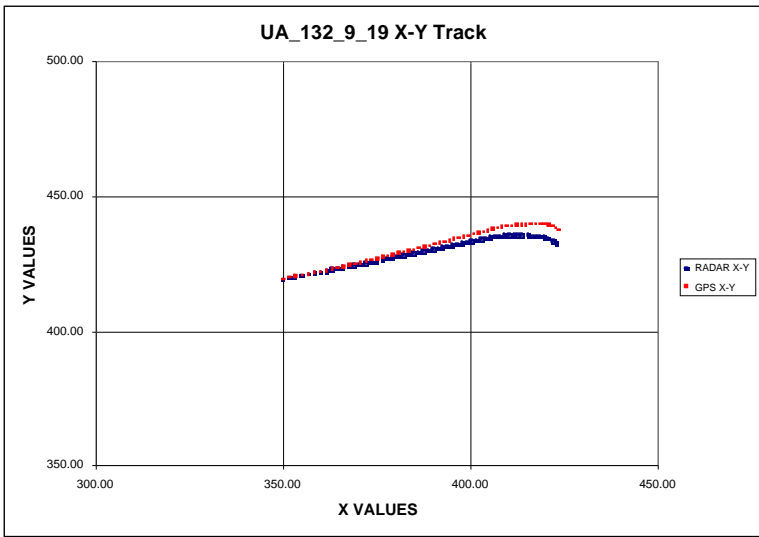


Figure A.6 Graphic Results for Case UA_132_9_19

Table A.7 Tabular Results for Case ua_132_9_26

UA_132_9_26	GPS			GPS DATA			GPS DATA			RADAR DATA			OBSERVER DATA			OBSERVER DATA								
TOD	GPS_LAT	GPS_LON	GPS_ALT	GPS_X	GPS_Y	GPS_GS	GPS_TRK	G_SATS	GDOP	R_ALT	R_X	R_Y	R_GS	R_TRK	OBS_ALT	OBS_OAT	OBS_IAS	OBS_HDG	OBS_WBRG	OBS_WMAG	OBS_CMT	C/O_TAS	CALC_WBRG	CALC_WMAG
9:44:22	40.23127	107.2333	33546	346.58	419.09	491	76	4	2.5	33000	346.44	419.00	502	76	330		63		gwt 319200		473	295	23	
9:44:34	40.23819	107.1987	33546	348.17	419.49	495	76	4	2.5	33000	348.00	419.38	501	76								479	299	21
9:44:46	40.24516	107.1639	33547	349.78	419.90	501	76	4	2.5	33000	349.69	419.81	501	76										
9:44:58	40.25192	107.1292	33542	351.37	420.29	504	77	4	2.5	33000	351.25	420.31	500	73	330		64					478	310	47
9:45:10	40.25920	107.0950	33530	352.95	420.66	506	79	4	2.5	33000	352.88	420.63	500	77										
9:45:22	40.26348	107.0584	33527	354.63	420.96	509	82	4	2.5	33000	354.44	420.88	499	80										
9:45:34	40.26733	107.0236	33537	356.23	421.18	477	84	4	2.5	33000	356.13	421.19	498	80	330									
9:45:46	40.27021	106.9877	33552	357.88	421.34	493	87	4	2.5	33000	357.56	421.31	497	83								473	340	104
9:45:58	40.27182	106.9512	33565	359.56	421.43	499	88	4	2.5	33000	359.31	421.44	496	85										
9:46:10	40.27262	106.9149	33577	361.22	421.47	497	90	4	2.5	33000	360.94	421.38	494	90						ctas cif				
9:46:22	40.27279	106.8789	33605	362.98	421.47	486	90	4	2.5	33000	362.69	421.50	493	87										
9:46:34	40.27299	106.8430	33649	364.53	421.48	503	89	4	2.5	33000	364.31	421.44	491	91										
9:46:46	40.27347	106.8062	33701	366.22	421.50	508	89	4	2.5	33000	366.00	421.44	490	90	330									
9:46:58	40.27413	106.7700	33745	367.88	421.53	495	88	4	2.4	33100	367.69	421.50	488	89								479	343	112
9:47:10	40.27511	106.7339	33765	369.54	421.58	497	88	4	2.4	33100	369.31	421.50	487	90										
9:47:22	40.27637	106.6971	33780	371.23	421.66	487	87	4	2.4	33000	371.06	421.63	486	87										
9:47:34	40.27778	106.6603	33792	372.92	421.74	505	87	4	2.4	33000	372.75	421.75	486	86	330									
9:47:46	40.27936	106.6229	33799	374.64	421.83	455	86	4	2.4	33000	374.44	421.88	486	86								481	66	27
9:47:58	40.28100	106.5877	33800	376.25	421.93	507	87	4	2.4	33000	376.19	421.88	487	89										
9:48:10	40.28267	106.5505	33798	377.96	422.02	503	87	4	2.4	33000	377.81	422.06	488	85										
9:48:22	40.28427	106.5145	33628	379.61	422.11	488	87	4	2.4	32800	379.50	422.13	489	87										
9:48:34	40.28588	106.4776	33231	381.31	422.21	512	87	4	2.4	32500	381.13	422.19	491	88										
9:48:46	40.28741	106.4412	32582	382.98	422.31	517	87	4	2.4	31800	382.75	422.31	492	86	320									
9:48:58	40.28892	106.4048	31894	384.66	422.40	504	87	4	2.4	31200	384.50	422.44	493	86										
9:49:10	40.29033	106.3686	31029	386.31	422.48	519	87	4	2.4	30300	386.19	422.44	494	89	310							484	293	39
9:49:22	40.29175	106.3315	30052	388.02	422.57	519	87	4	2.4	29400	387.75	422.50	495	88	300									
9:49:58	40.29605	106.2202	27320	393.13	422.84	498	87	4	2.3	26700	392.88	422.81	495	87	270							502	10	16
9:50:10	40.29751	106.1829	26541	394.84	422.93	505	87	4	2.3	26000	394.63	422.94	496	86	260									
9:50:22	40.29893	106.1465	25822	396.51	423.02	503	87	4	2.3	25300	396.25	423.06	497	86								498	339	16
9:50:34	40.30032	106.1106	25121	398.16	423.11	487	87	4	2.3	24600	397.94	423.06	497	89	250							495	22	18
9:50:46	40.30169	106.0750	24507	399.79	423.20	492	87	4	2.0	24000	399.63	423.25	497	85	240									
9:50:58	40.30303	106.0394	24069	401.42	423.29	458	87	4	2.3	23600	401.19	423.31	497	87								491	61	36
9:51:10	40.30434	106.0055	23499	402.98	423.37	471	87	4	2.3	23100	402.81	423.31	497	89	230									
9:51:22	40.30571	105.9708	22801	404.57	423.46	474	87	4	2.3	22400	404.50	423.38	497	88								473	352	13
9:51:34	40.30706	105.9371	22019	406.12	423.55	474	87	4	2.3	21600	405.94	423.50	496	86	220							465	325	17
9:51:46	40.30839	105.9022	21443	407.72	423.64	480	87	4	2.3	20900	407.44	423.63	495	85	210									
9:51:58	40.30975	105.8668	20841	409.35	423.74	489	87	4	2.3	20500	409.25	423.69	494	87								471	308	24
9:52:10	40.31096	105.8324	20646	410.93	423.82	473	87	4	2.3	20300	410.75	423.88	493	84										
9:52:22	40.31222	105.7981	20371	412.50	423.91	466	86	4	2.3	20000	412.81	424.06	491	85	200									
9:52:34	40.31360	105.7646	19948	414.03	424.00	474	86	4	2.3	19300	414.88	424.00	490	90								452	294	25
9:52:46	40.31492	105.7311	19546	415.57	424.09	474	87	4	2.3	19000	416.44	424.19	488	85										
9:52:58	40.31614	105.6983	19342	417.08	424.18	442	87	4	2.2	19000	417.94	424.25	486	87										
9:53:10	40.31721	105.6663	19352	418.55	424.26	424	87	4	2.2	18900	418.63	424.25	483	89								440	41	21
9:53:22	40.31828	105.6346	19370	420.00	424.33	428	87	4	2.2	19000	420.19	424.38	481	87								432	11	13
9:53:34	40.31942	105.6034	19382	421.44	424.42	423	86	4	2.2	19000	422.25	424.56	477	85								415	313	11
9:53:46	40.32061	105.5742	19388	422.77	424.50	389	86	4	2.2	19000	423.50	424.56	473	89										
9:53:58	40.32184	105.5463	19395	424.05	424.59	357	88	4	2.2	19000	424.88	424.63	469	88	190									
9:54:10	40.32256	105.5193	19408	425.29	424.64	356	93	4	2.2	19000	426.13	424.63	463	89								377	21	55
9:54:22	40.32208	105.4930	19423	426.50	424.63	343	101	4	2.2	19000	426.56	424.63	456	90								353	9	99
9:54:34	40.31863	105.4687	19434	427.61	424.43	331	111	4	2.2	19000	427.81	424.50	448	94										
9:54:46	40.31197	105.4469	19483	428.62	424.05	323	112	4	2.2	19100	429.19	423.75	437	108										
9:54:47	40.31127	105.4451	19485	428.70	424.01	325	111	4	2.2	19100	429.29	423.72	436	108										

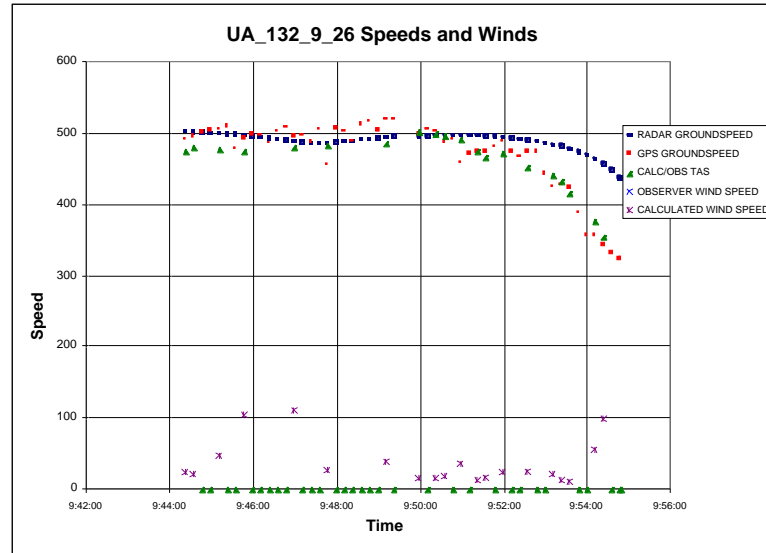
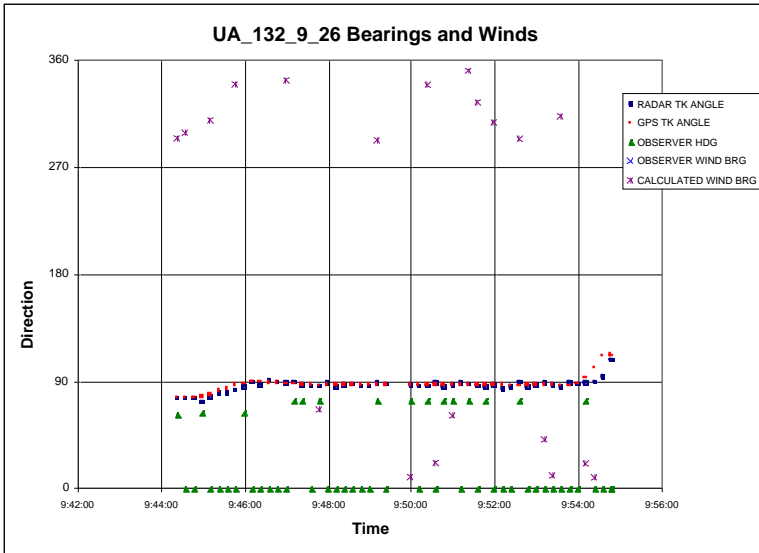
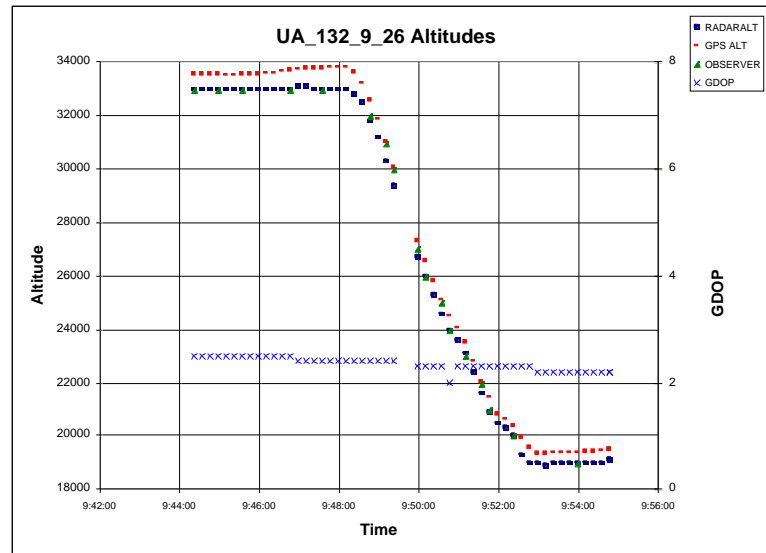
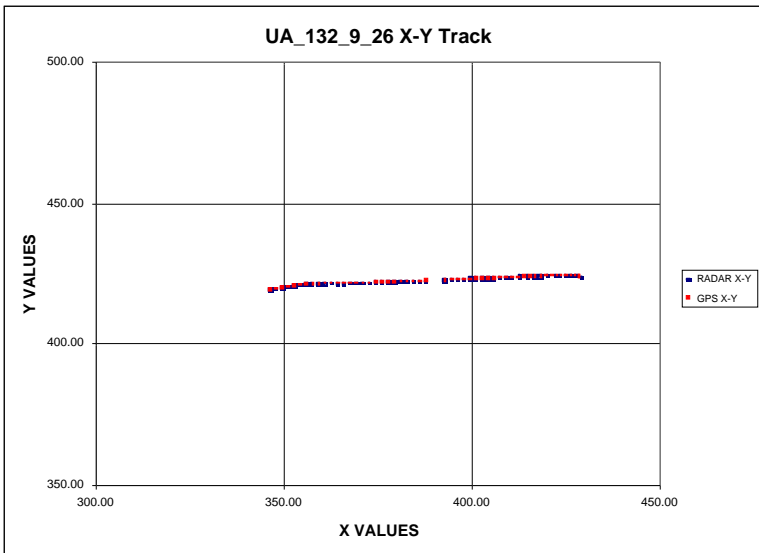


Figure A.7 Graphic Results for Case UA_132_9_26

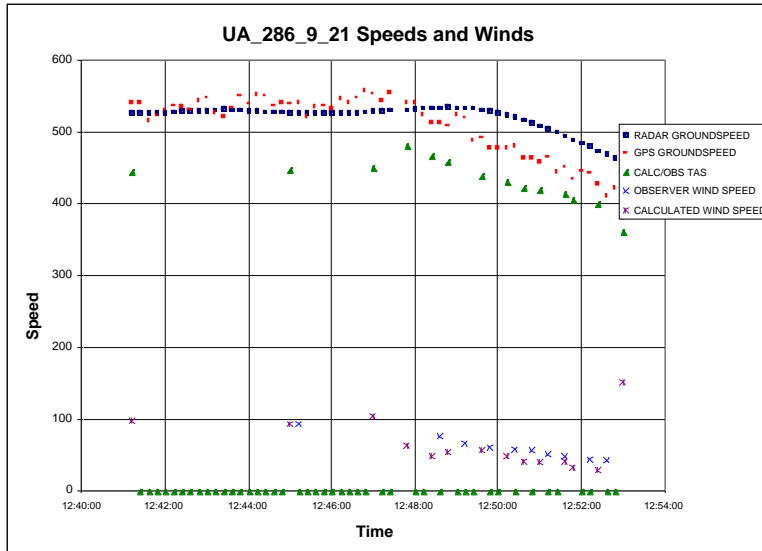
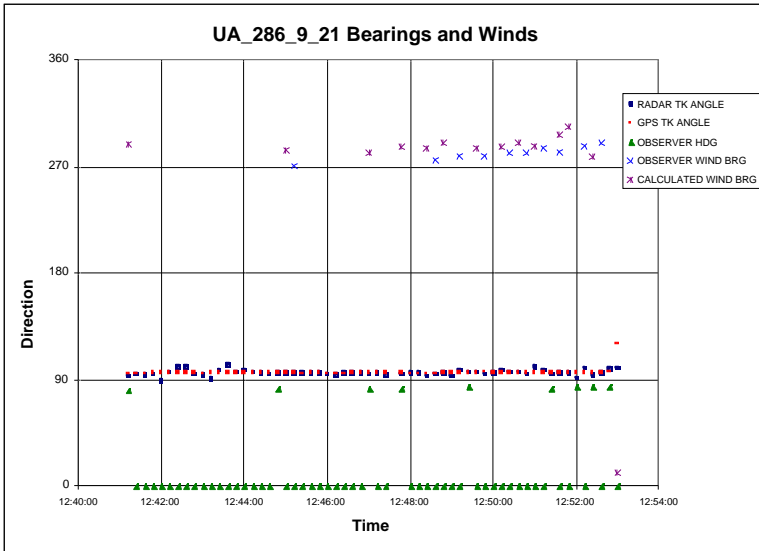
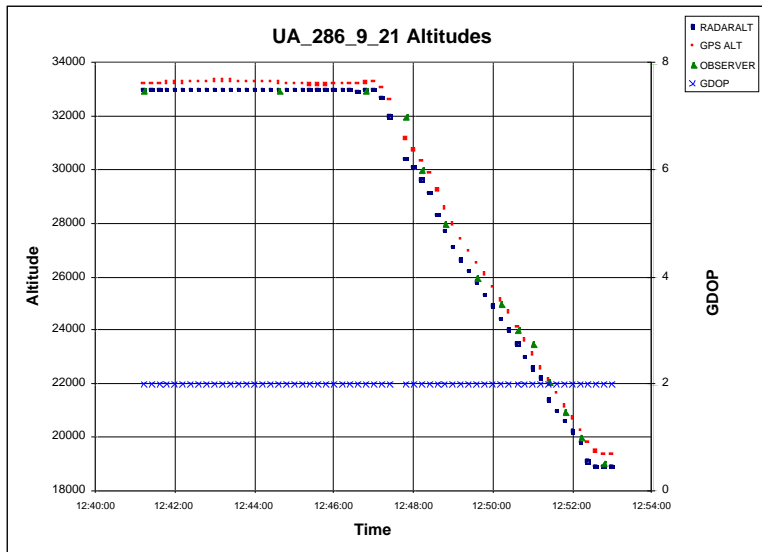
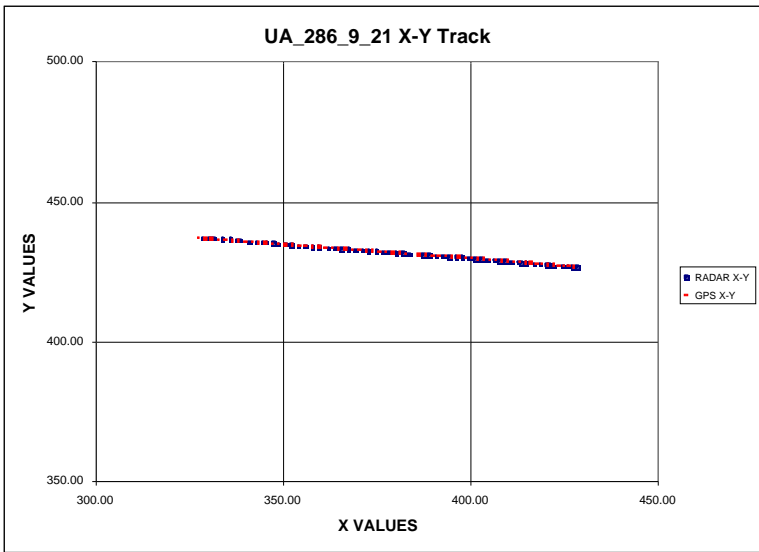


Figure A.8 Graphic Results for Case UA_286_9_21

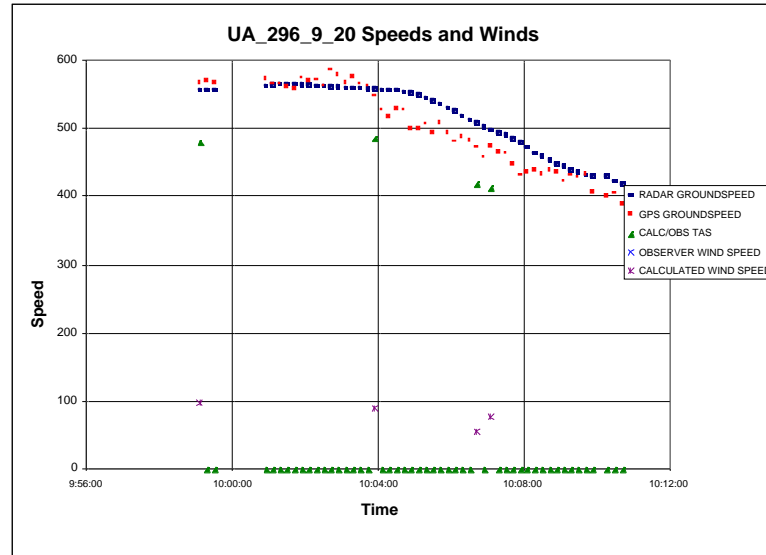
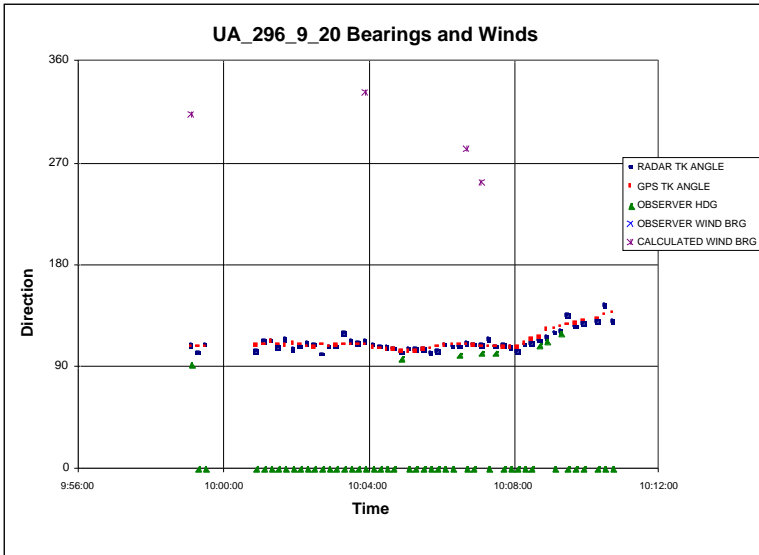
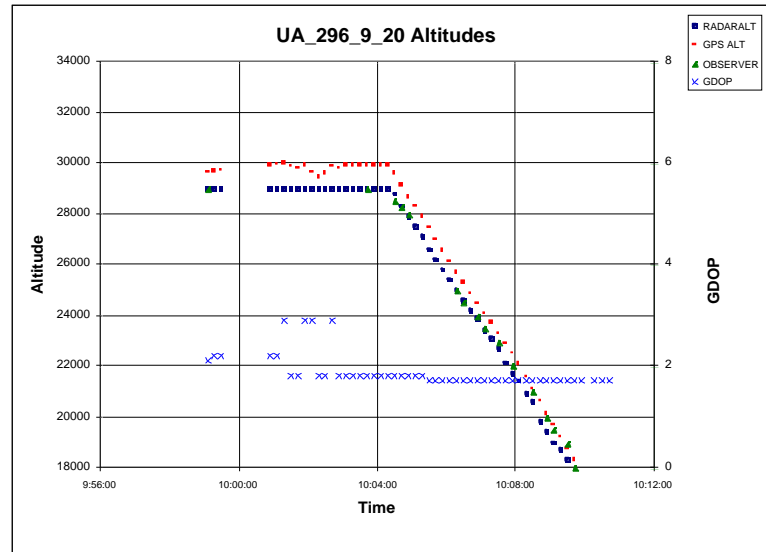
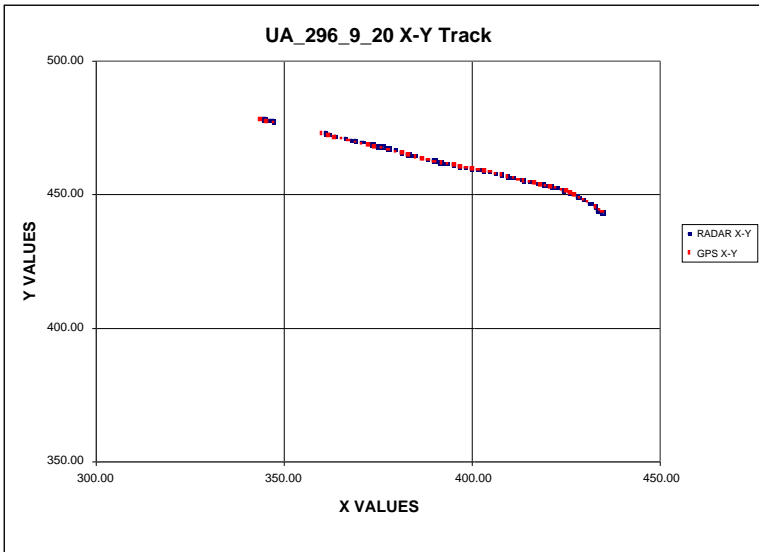


Figure A.9 Graphic Results for Case UA_296_9_20

Table A.10 (continued)

10:15:16	40.92869	106.1393	28284	396.70	460.79	486	110	4	1.7	28000	396.13	461.00	478	106					94	
10:15:28	40.91906	106.1046	27570	398.28	460.21	495	110	4	1.7	27400	397.63	460.44	482	109	270			474	351	48
10:15:40	40.90958	106.0708	26789	399.82	459.65	528	110	4	1.8	26600	399.31	459.88	486	109				468	321	72
10:15:52	40.89975	106.0355	26052	401.43	459.07	506	109	4	1.8	25800	400.81	459.25	491	111	260					
10:16:04	40.89007	106.0001	25540	403.05	458.50	500	109	4	1.8	25200	402.38	458.81	492	107	250			469	335	47
10:16:16	40.88120	105.9669	25041	404.56	457.97	500	108	4	1.8	24700	404.38	458.00	495	111				457	321	51
10:16:28	40.87235	105.9327	24476	406.12	457.45	486	108	4	1.8	24100	405.75	457.56	498	109	240					
10:16:40	40.86369	105.8988	23910	407.66	456.94	462	108	4	1.8	23600	407.00	457.13	499	109						
10:16:52	40.85546	105.8662	23304	409.15	456.46	483	108	4	1.8	23000	408.56	456.56	501	110	230			444	318	45
10:17:04	40.84671	105.8315	22851	410.74	455.95	482	108	4	1.8	22300	410.06	456.19	499	106	220					
10:17:16	40.83859	105.7992	22088	412.21	455.47	486	108	4	1.8	21300	412.88	455.19	500	108				442	315	49
10:17:28	40.83012	105.7656	21545	413.74	454.97	478	108	4	1.8	20800	414.19	454.69	501	110	210					
10:17:40	40.82189	105.7330	21040	415.23	454.49	460	108	4	1.8	20400	415.06	454.50	502	105				434	329	34
10:17:52	40.81357	105.7004	20592	416.72	454.00	474	109	4	1.8	20000	416.50	454.00	504	108						
10:18:04	40.80452	105.6666	20146	418.27	453.48	473	109	4	1.8	19200	418.69	453.25	501	109				427	320	54
10:18:16	40.79647	105.6364	19642	419.64	453.01	465	109	4	1.8	18700	420.25	452.81	497	107						
10:18:28	40.78781	105.6034	19088	421.15	452.50	456	108	4	1.8	18300	421.69	452.25	493	110	190					
10:18:40	40.77971	105.5722	18590	422.58	452.03	451	109	4	1.8	17900	422.44	452.00	486	109				419	316	36
10:18:52	40.77183	105.5403	18064	424.04	451.57	431	119	4	1.8	17600	423.63	451.44	481	113	180			417	13	86
10:19:04	40.76023	105.5113	17749	425.37	450.89	431	121	4	1.9	17200	425.00	451.00	475	109						
10:19:16	40.74642	105.4868	17561	426.50	450.07	430	134	4	1.9	17000	426.81	449.69	467	121						
10:19:28	40.72913	105.4649	17531	427.51	449.05	436	140	4	2.3	17000	427.88	448.56	459	132	170			401	309	35
10:19:40	40.71023	105.4448	17403	428.44	447.93	439	141	4	2.3	17000	428.75	447.56	451	137						
10:19:52	40.69194	105.4253	17342	429.34	446.84	435	140	4	2.3	17000	429.25	446.88	444	142						
10:20:04	40.67200	105.4038	17370	430.33	445.66	443	140	4	2.3	17000	430.19	445.88	439	138				407	304	37
10:20:16	40.65372	105.3839	17367	431.26	444.57	454	139	4	2.0	17000	431.56	444.13	435	141				406	304	49
10:20:28	40.63497	105.3634	17405	432.21	443.46	420	140	4	2.3	17000	432.44	443.06	432	141				130	319	290
10:20:40	40.61674	105.3435	17429	433.13	442.38	439	141	4	2.3	16900	433.63	441.94	431	136	170					
10:20:52	40.59758	105.3233	17352	434.07	441.24	409	141	4	2.3	16900	433.94	441.44	431	144				410	178	0
10:21:04	40.57870	105.3037	17126	434.98	440.12	412	141	4	2.3	16900	434.81	440.25	431	144						
10:21:16	40.56168	105.2864	16667	435.79	439.11	402	141	4	2.1	16100	436.19	438.69	432	140						
10:21:28	40.54379	105.2680	16577	436.64	438.05	405	141	4	2.1	16200	436.88	437.75	431	143						
10:21:40	40.52658	105.2502	16784	437.47	437.03	388	141	4	2.1	16400	437.81	436.63	429	141						
10:21:52	40.50917	105.2321	17051	438.31	436.00	385	141	4	2.1	16700	438.56	435.56	426	144						
10:21:56	40.50273	105.2255	17112	438.62	435.62	382	141	4	2.1	16773	438.63	435.36	424	148						

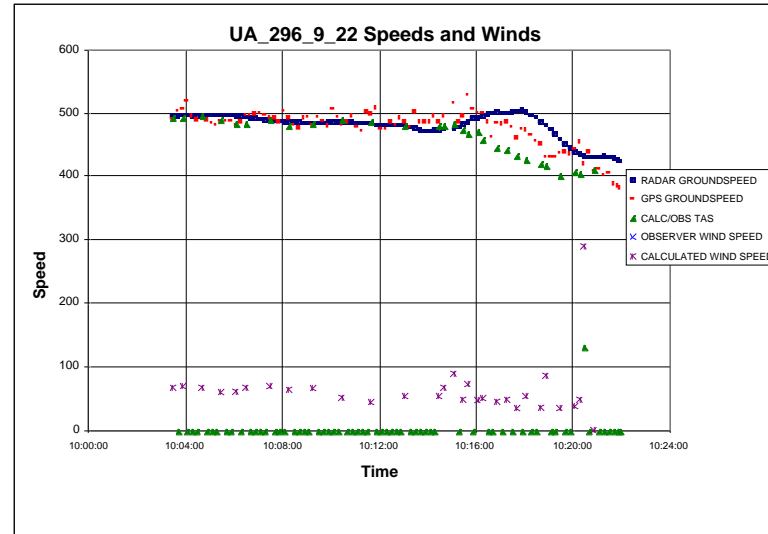
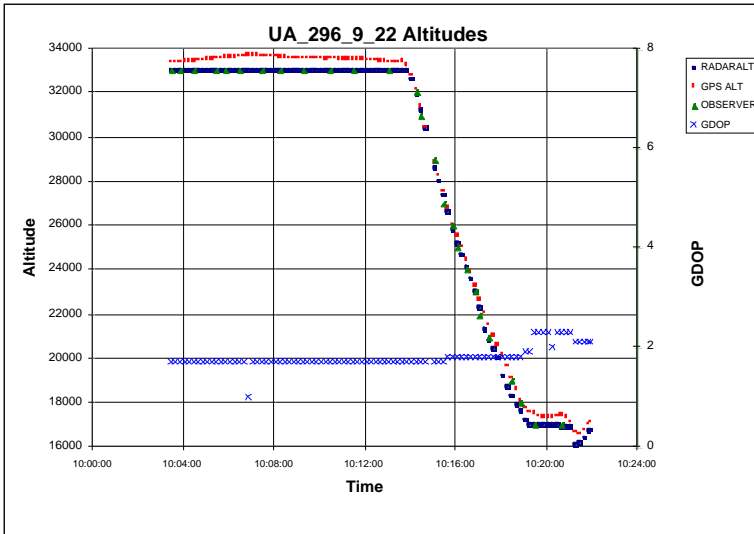
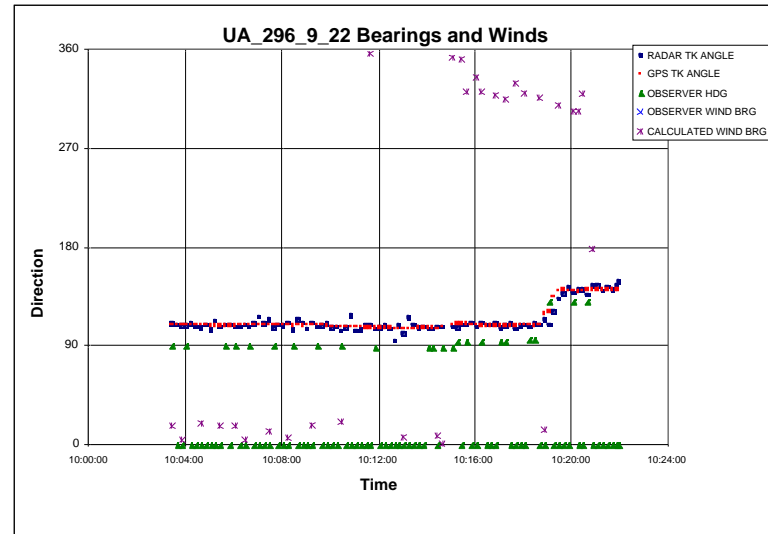
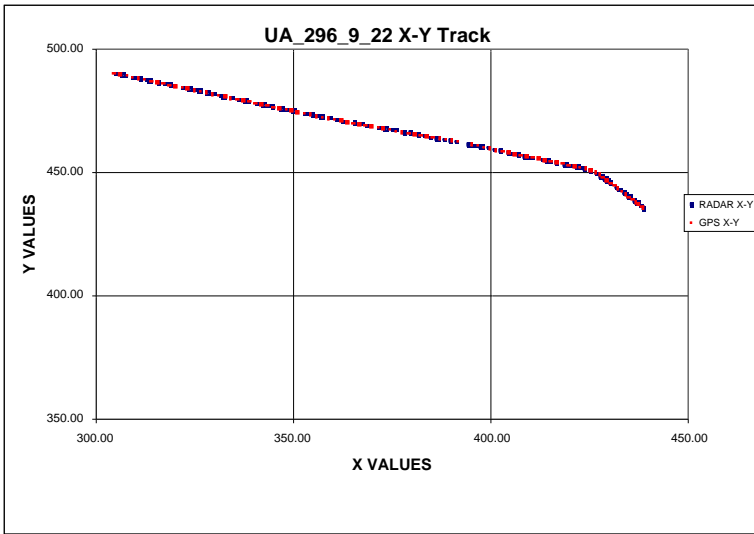


Figure A.10 Graphic Results for Case UA_296_9_22

Table A.11 Tabular Results for Case UA_470_9_27

UA_470_9_27	<--	GPS DATA						RADAR DATA				OBSERVER DATA				C/O_TAS			--->					
TOD	GPS_LAT	GPS_LON	GPS_ALT	GPS_X	GPS_Y	GPS_GS	GPS_TRK	G_SATS	GDOP	R_ALT	R_X	R_Y	R_GS	R_TRK	OBS_ALT	OBS_OAT	OBS_IAS	OBS_HDG	OBS_WBRG	OBS_WMAG	OBS_CMT	C/O_TAS	CALC_WBRG	CALC_WMAG
13:13:23	40.52523	105.9864	25103	403.79	436.62	458	88	4	1.9	24500	403.38	436.63	473	81	250	-8	280	60						
13:13:34	40.52594	105.9554	24648	405.21	436.67	447	88	4	1.9	24000	404.94	436.63	468	87										
13:13:46	40.52692	105.9217	24178	406.74	436.74	439	89	4	1.9	23500	406.31	436.75	463	86	240			80						
13:13:58	40.52703	105.8899	23653	408.20	436.76	443	89	4	1.9	23000	408.13	436.63	459	91										
13:14:10	40.52763	105.8568	23185	409.71	436.80	432	89	4	1.8	22500	409.25	436.81	455	84	230			280						
13:14:22	40.52789	105.8239	22751	411.22	436.83	439	89	4	1.8	22100	410.88	436.88	451	87										
13:14:34	40.52797	105.7934	22345	412.62	436.84	435	89	4	1.8	21600	412.63	436.75	449	92	220	-1					385	257	51	
13:14:46	40.52802	105.7627	21892	414.02	436.86	423	90	4	1.8	21300	414.25	437.06	449	83										
13:14:58	40.52786	105.7309	21395	415.47	436.86	433	91	4	1.8	20900	415.56	436.88	449	94	210									
13:15:10	40.52771	105.6984	20862	416.96	436.87	427	96	4	1.8	20400	416.38	436.94	451	88										
13:15:22	40.52486	105.6667	20482	418.42	436.71	433	103	4	1.8	20000	417.75	436.94	451	89	200									
13:15:34	40.51929	105.6370	20007	419.77	436.39	397	110	4	1.8	19300	419.63	436.31	447	103										
13:15:46	40.51079	105.6093	19610	421.05	435.89	397	125	4	2.4	18900	421.06	436.06	443	101										
13:15:58	40.49811	105.5856	19774	422.14	435.14	396	131	4	2.4	18900	422.19	435.25	436	115										
13:16:10	40.48345	105.5642	19892	423.13	434.27	398	133	4	2.4	19000	422.56	434.69	427	129										
13:16:22	40.46774	105.5423	19912	424.14	433.34	384	133	4	2.4	19000	423.63	433.94	419	126										
13:16:34	40.45308	105.5224	19905	425.06	432.47	399	133	4	4.6	19000	424.94	432.50	409	134	190									
13:16:46	40.43799	105.5015	19936	426.03	431.57	365	130	4	2.4	18900	426.00	431.63	399	131										
13:16:58	40.42455	105.4811	19941	426.97	430.78	360	130	4	2.4	19000	426.88	430.94	393	129										
13:17:10	40.41140	105.4611	19928	427.90	430.00	342	129	4	2.4	19000	427.94	430.25	387	125		270								
13:17:23	40.39862	105.4406	19952	428.85	429.24	350	129	4	2.4	19000	428.31	429.75	384	138										
13:17:34	40.38700	105.4220	19971	429.71	428.56	341	129	4	2.4	19000	429.25	428.94	381	133										
13:17:45	40.37666	105.4056	20004	430.47	427.95	324	129	4	2.4	19000	430.47	428.16	377	127										

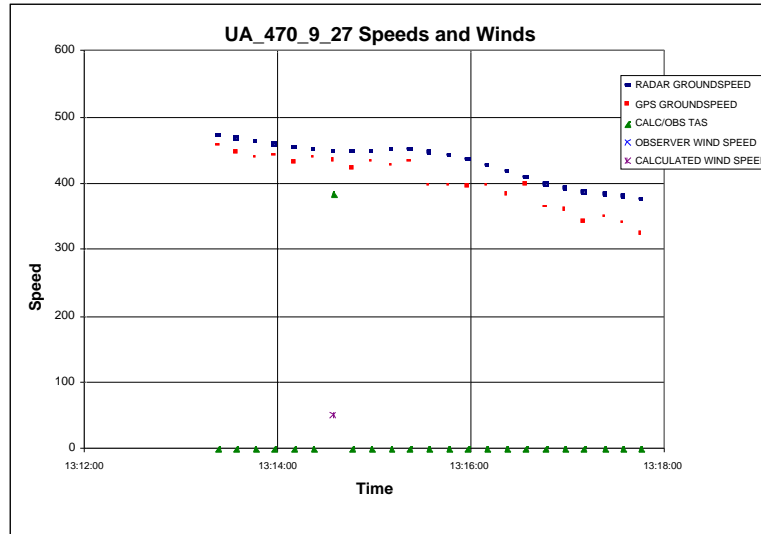
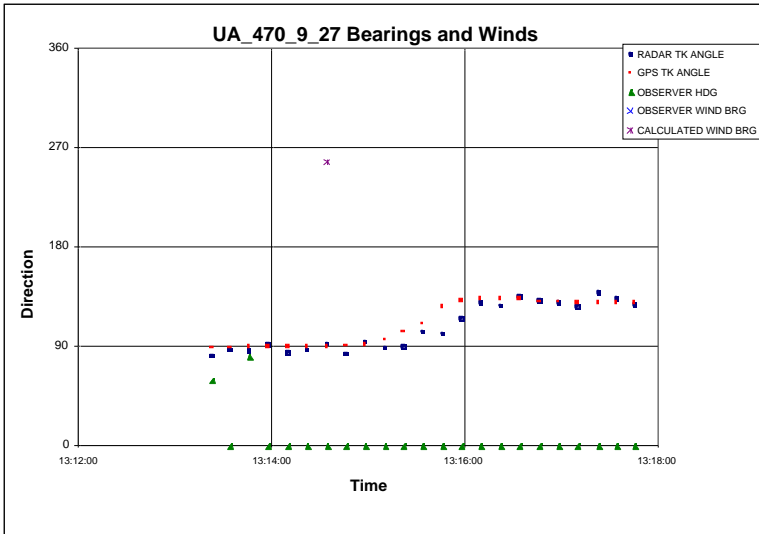
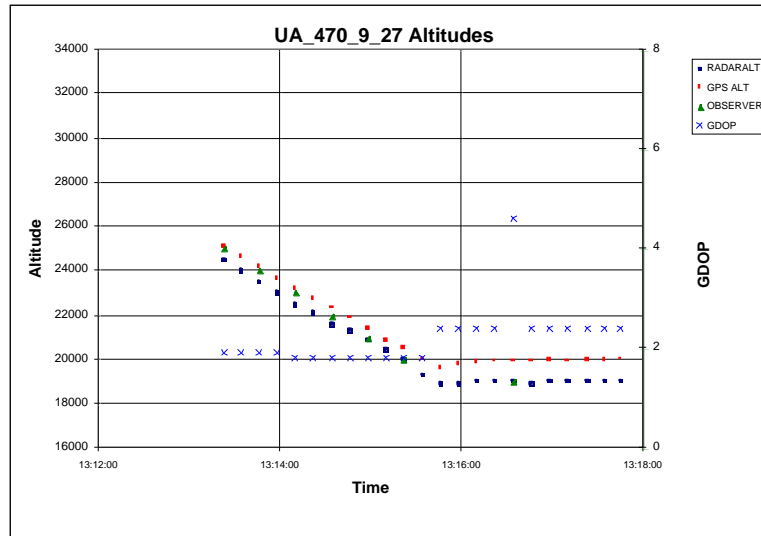
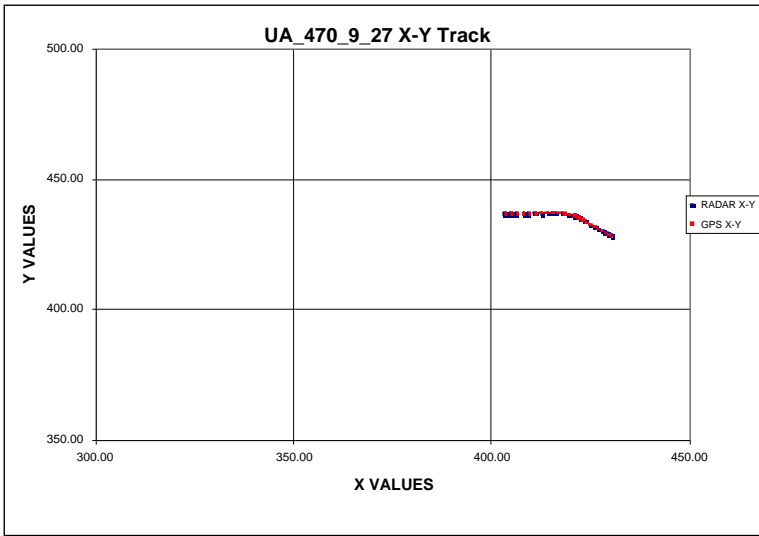


Figure A.11 Graphic Results for Case UA_470_9_27

Table A.12 (continued)

13:09:38	40.54295	105.8330	26556	410.80	437.73	439	85	4	1.9	25500	410.94	437.81	481	85	-4	275		400	206	88
13:09:50	40.54478	105.8010	26274	412.26	437.85	434	85	4	1.9	25300	412.69	437.81	479	88			85			
13:10:02	40.54691	105.7683	25953	413.76	437.99	416	84	4	1.9	24800	414.75	438.13	477	84						
13:10:14	40.54914	105.7369	25594	415.19	438.13	412	85	4	1.9	24500	416.13	438.13	474	88		250	275			
13:10:25	40.55070	105.7082	25342	416.50	438.24	412	87	4	1.9	24300	417.63	438.38	470	83	-4			394	198	63
13:10:38	40.55046	105.6782	24892	417.87	438.24	399	100	4	2.4	23900	418.38	438.19	466	97			90			
13:10:50	40.54521	105.6504	24207	419.15	437.93	405	119	4	4.8	23400	419.63	437.88	463	102	237					
13:11:01	40.53492	105.6252	23621	420.31	437.33	395	125	4	4.7	22400	421.19	436.63	456	116	-1	275		389	20	160
13:11:14	40.52195	105.6001	23159	421.46	436.56	395	128	4	4.7	22200	422.31	436.00	449	118	226	275	120			
13:11:26	40.50874	105.5784	22903	422.46	435.78	391	128	4	2.0	22000	423.25	435.25	441	125	1		120	384	238	20
13:11:38	40.49503	105.5562	22604	423.49	434.97	377	133	4	4.7	21600	424.31	434.44	433	127	220	275	120			
13:11:50	40.48067	105.5368	22226	424.38	434.12	366	137	4	2.4	21300	424.75	433.94	424	135	15		130	391	188	38
13:12:02	40.46581	105.5182	21797	425.25	433.24	370	137	4	4.6	21000	425.50	433.06	415	138	210					
13:12:14	40.44982	105.4988	21363	426.14	432.29	372	137	4	4.6	20200	426.75	431.56	406	140	2	270		369	235	23
13:12:26	40.43524	105.4816	20826	426.94	431.42	372	137	4	2.4	19800	427.69	430.75	397	134	200		135			
13:12:38	40.42007	105.4633	20369	427.79	430.52	366	140	4	4.6	19500	428.50	429.88	389	136		270				
13:12:50	40.40424	105.4460	20027	428.60	429.58	348	141	4	4.5	19200	428.81	429.31	382	146	2			363	206	31
13:13:02	40.38879	105.4302	19773	429.33	428.66	348	142	4	4.5	19100	429.44	428.50	377	144			130			
13:13:08	40.38069	105.4222	19725	429.70	428.18	340	142	4	4.5	19048	430.06	427.75	375	142	190					

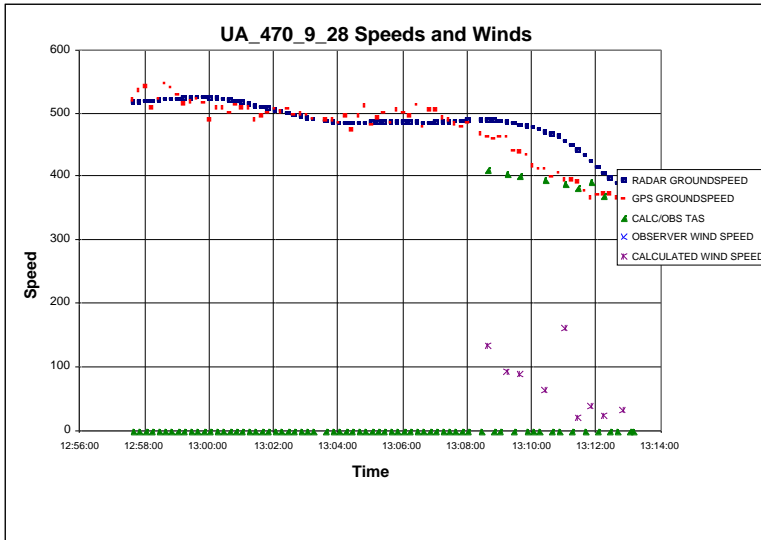
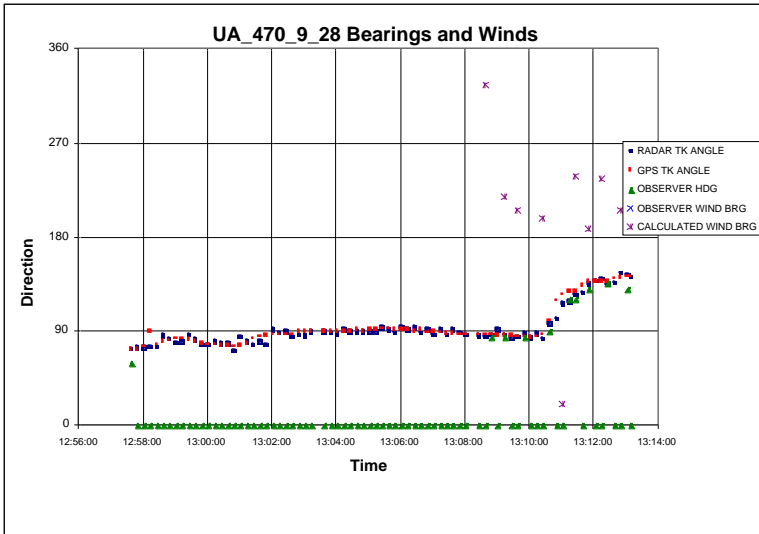
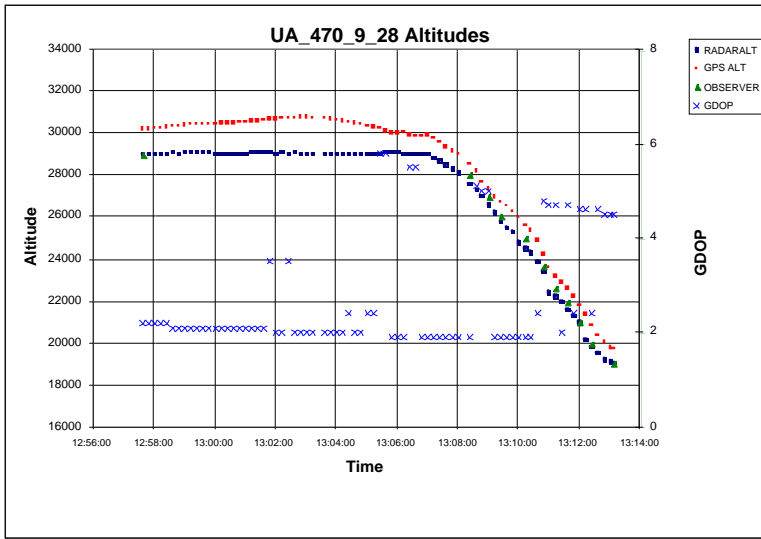
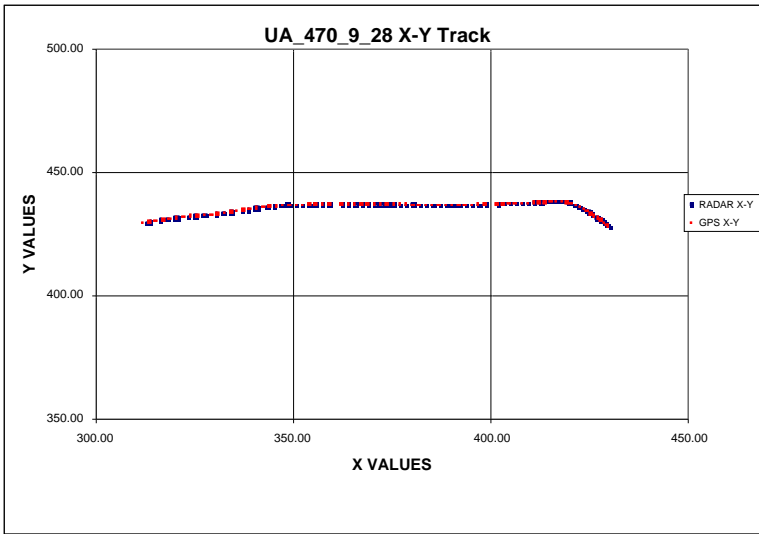


Figure A.12 Graphic Results for Case UA_470_9_28

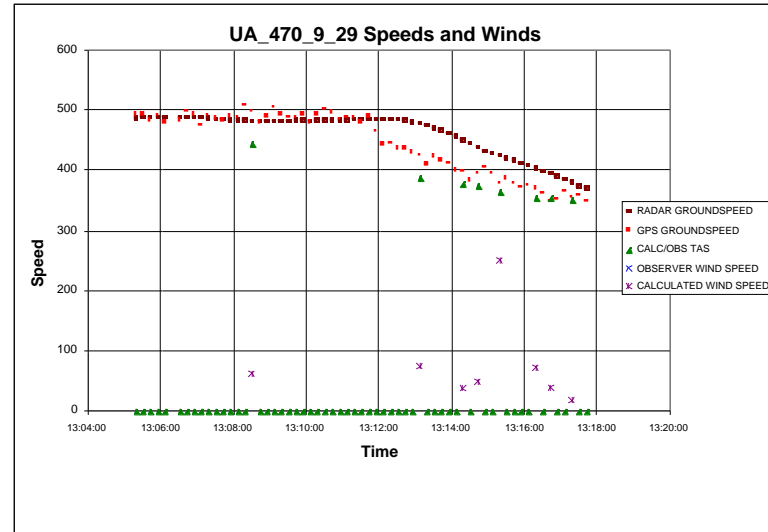
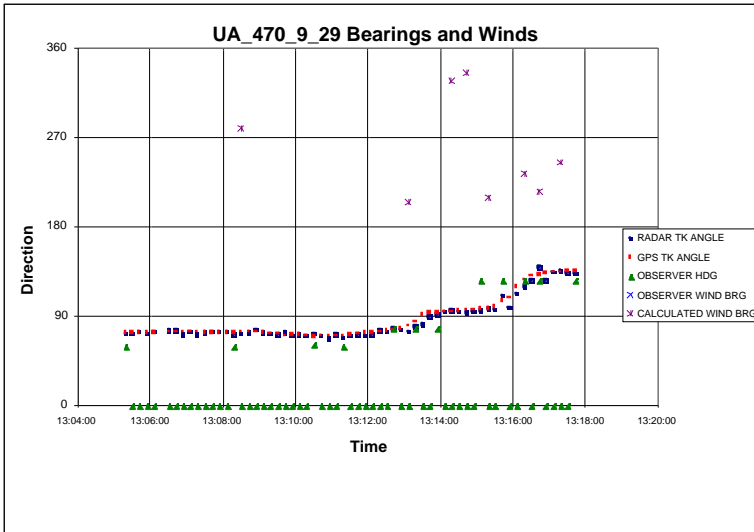
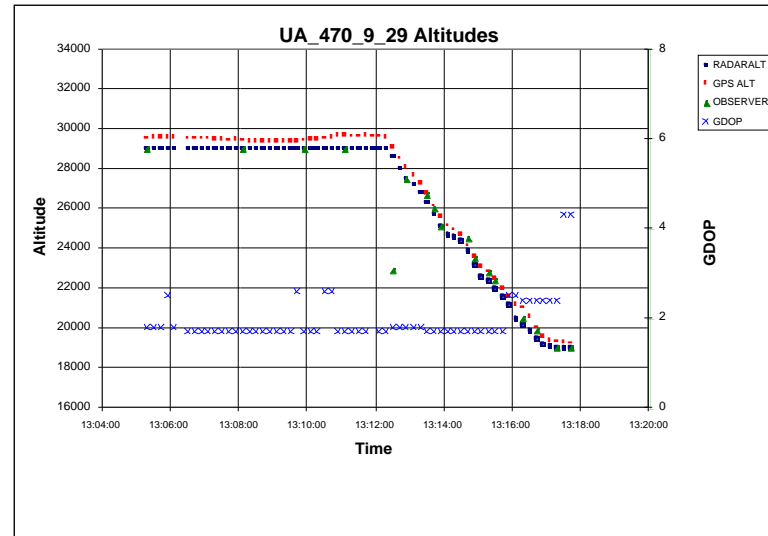
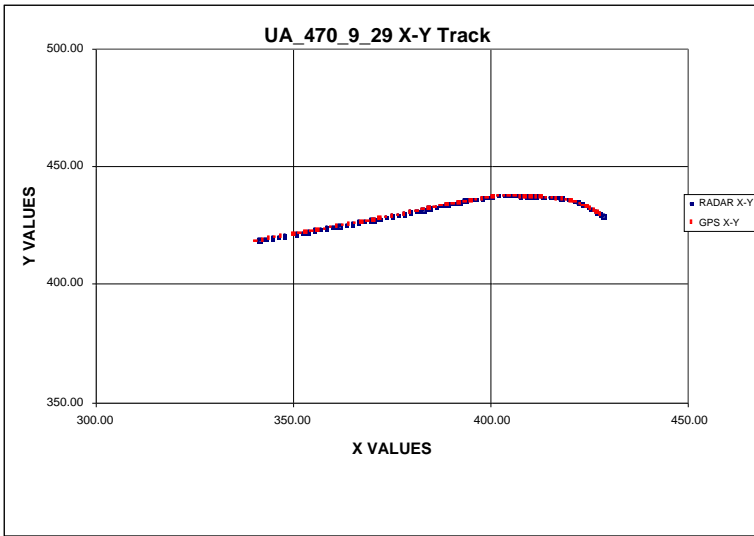


Figure A.13 Graphic Results for Case UA_470_9_29

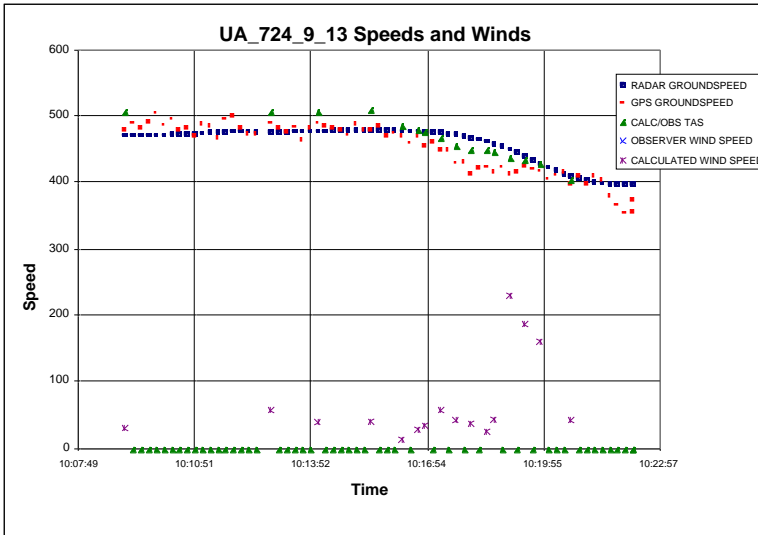
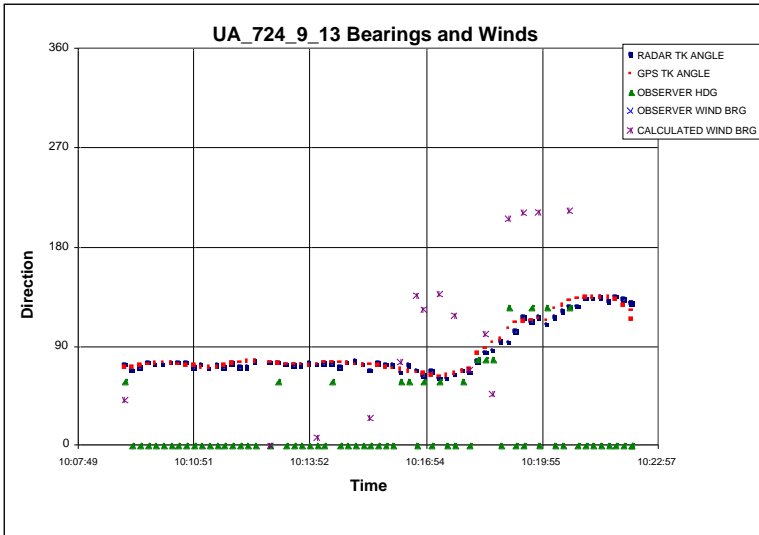
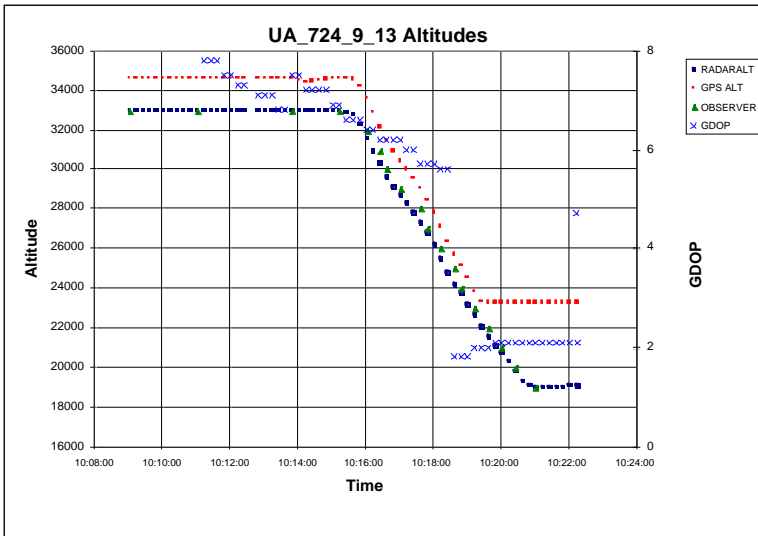
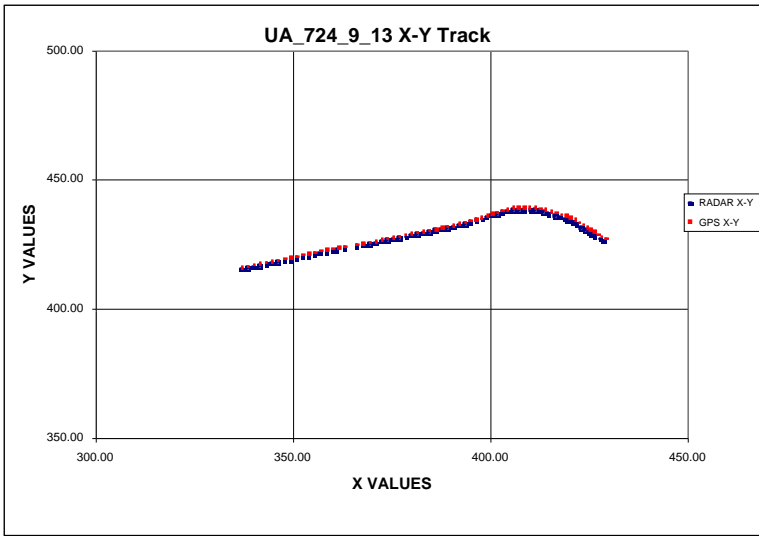


Figure A.14 Graphical Results for Case UA_724_9_13

Table A.15 Tabular Results for Case UA_724_9_28

UA_724_9_28	GPS DATA					RADAR DATA					OBSERVER DATA					C/O_TAS			CALC_WBRG			CALC_WMAG			
TOD	GPS_LAT	GPS_LON	GPS_ALT	GPS_X	GPS_Y	GPS_GS	GPS_TRK	G_SATS	GDOP	R_ALT	R_X	R_Y	R_GS	R_TRK	OBS_ALT	OBS_OAT	OBS_IAS	OBS_HDG	OBS_WBRG	OBS_WMAG	OBS_CMT	C/O_TAS	CALC_WBRG	CALC_WMAG	
10:04:05	40.09539	107.8592	33922	317.69	411.30	563	70	4	3.8	33000	318.50	411.56	534	71	330	-13	310	66							
10:04:17	40.10642	107.8228	33860	319.38	411.93	545	70	4	3.7	33000	320.31	412.25	534	70			310								
10:04:29	40.11779	107.7842	33848	321.17	412.59	558	72	4	3.7	33000	322.06	412.81	533	71											
10:04:41	40.12803	107.7447	33835	322.99	413.18	558	75	4	2.3	33000	323.75	413.31	533	73											
10:04:53	40.13640	107.7073	33858	324.72	413.65	559	76	4	2.3	33000	325.63	413.81	533	74											
10:05:05	40.14406	107.6683	33893	326.52	414.09	560	77	4	2.3	33000	327.44	414.19	533	77			320								
10:05:17	40.15102	107.6292	33907	328.32	414.48	558	78	4	2.3	33000	329.31	414.50	534	80	330			58							
10:05:29	40.15794	107.5903	33936	330.12	414.87	558	77	4	2.3	33000	331.00	414.94	535	77			-12				503	308	95		
10:05:41	40.16544	107.5490	33977	332.02	415.30	561	77	4	2.3	33000	332.88	415.31	535	78											
10:05:53	40.17257	107.5104	34022	333.80	415.70	558	77	4	2.3	33000	334.81	415.75	536	78											
10:06:05	40.17993	107.4713	34057	335.61	416.12	555	77	4	2.3	33000	336.56	416.25	538	75											
10:06:17	40.18734	107.4327	34124	337.39	416.55	555	77	4	3.5	33000	338.50	416.81	540	74											
10:06:29	40.19496	107.3933	34083	339.21	416.98	553	76	4	3.5	33000	340.25	417.25	542	75											
10:06:41	40.20306	107.3531	33952	341.06	417.45	565	75	4	3.5	33000	341.94	417.63	544	77	330										
10:06:53	40.21145	107.3149	33866	342.82	417.94	551	73	4	3.4	33000	342.75	417.88	546	74			320								
10:07:05	40.22098	107.2764	33874	344.60	418.50	560	73	4	3.4	33000	344.50	418.44	547	73			-12				503	280	65		
10:07:17	40.23087	107.2376	33967	346.38	419.07	576	72	4	2.4	33000	346.50	419.00	548	74											
10:07:29	40.24109	107.1997	34345	348.13	419.67	564	73	4	2.4	33000	348.25	419.56	549	73											
10:07:41	40.25067	107.1591	34351	350.00	420.23	564	74	4	2.4	33000	349.94	420.13	551	72											

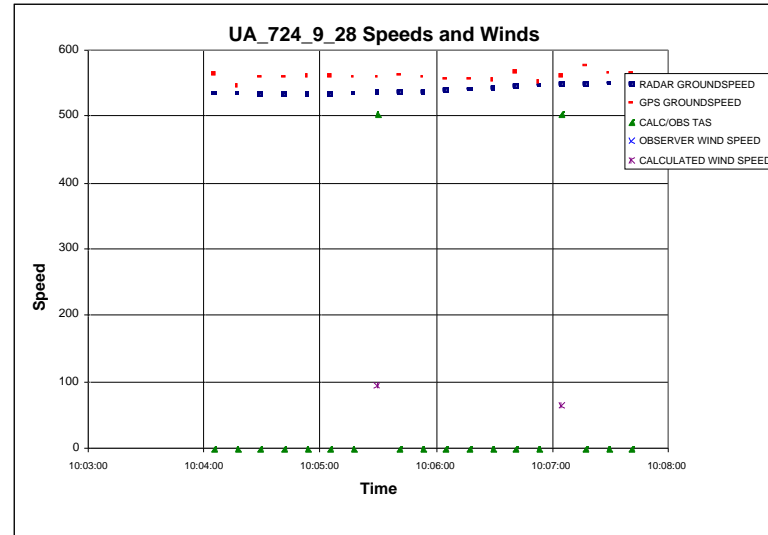
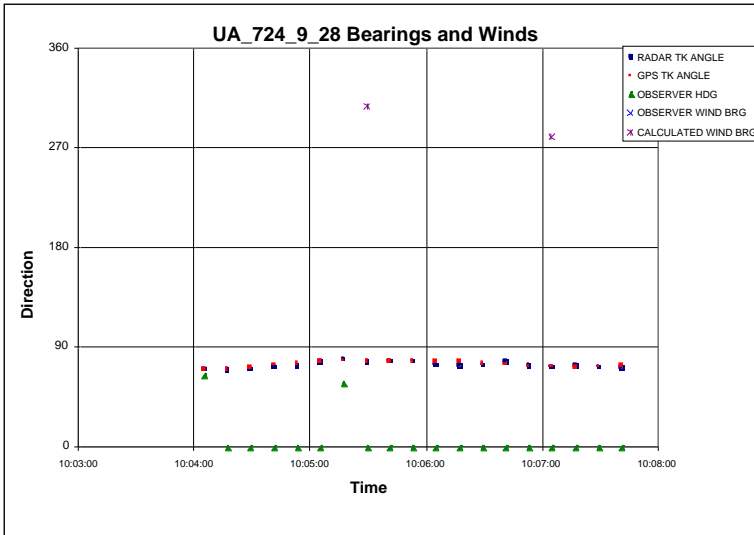
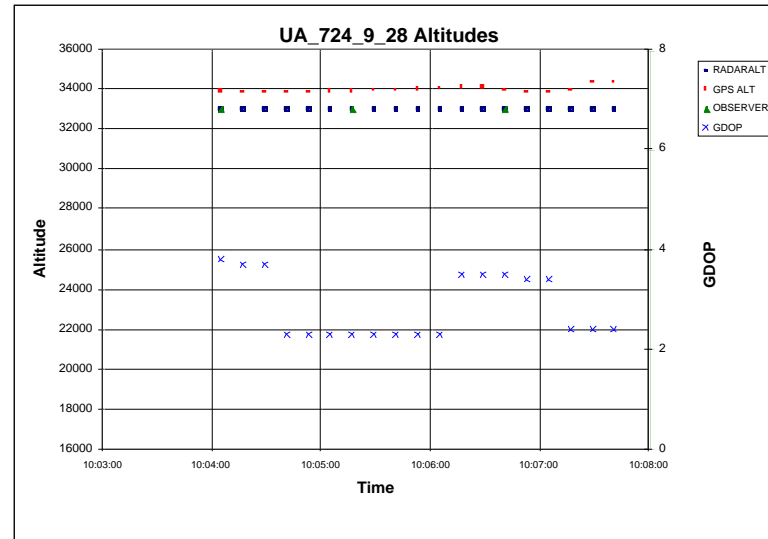
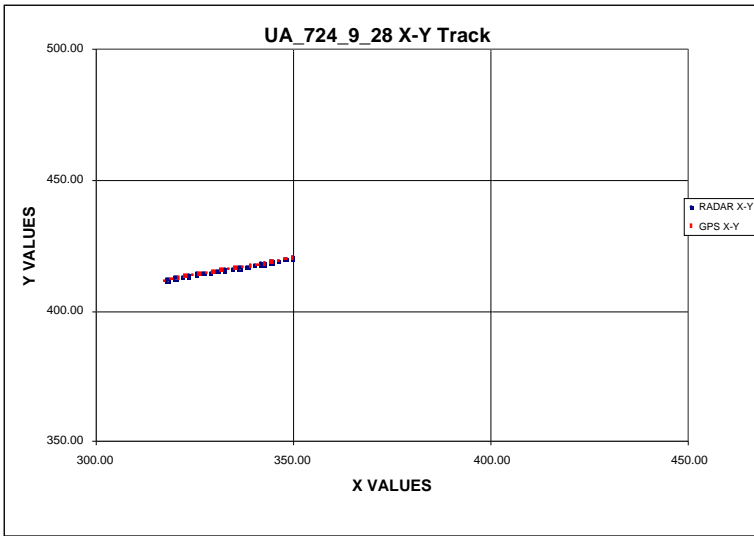


Figure A.15 Graphic Results for Case UA_724_9_28

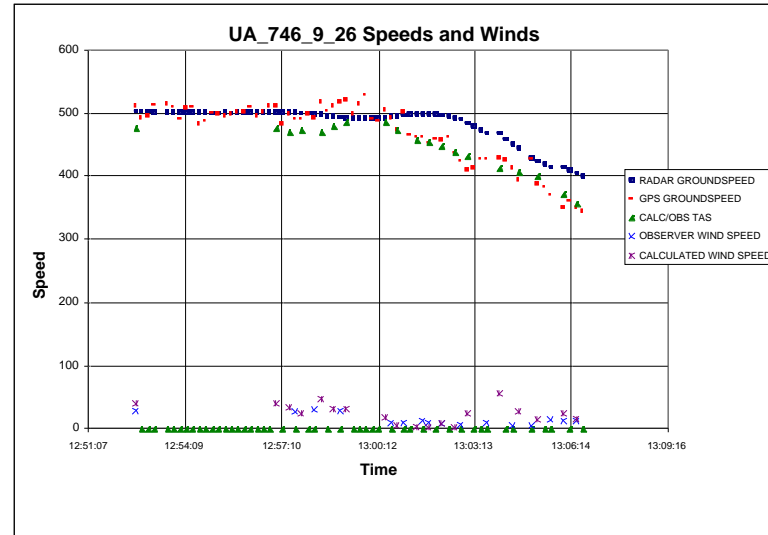
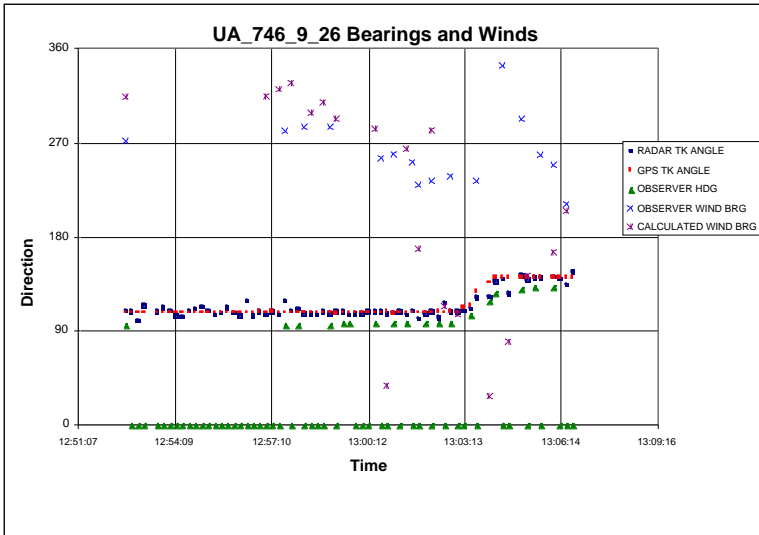
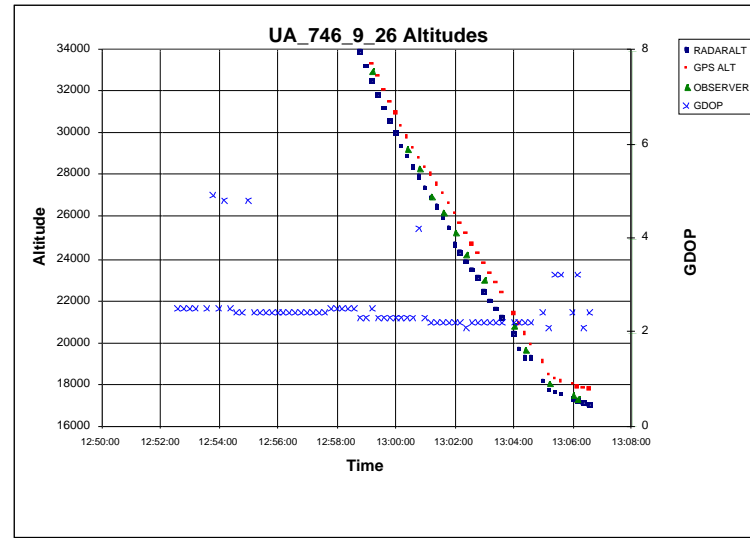
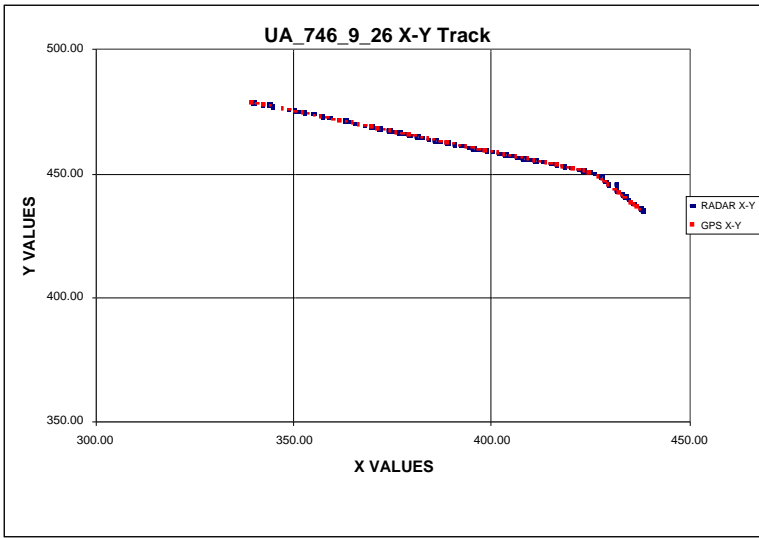


Figure A.16 Graphic Results for Case UA_746_9_26

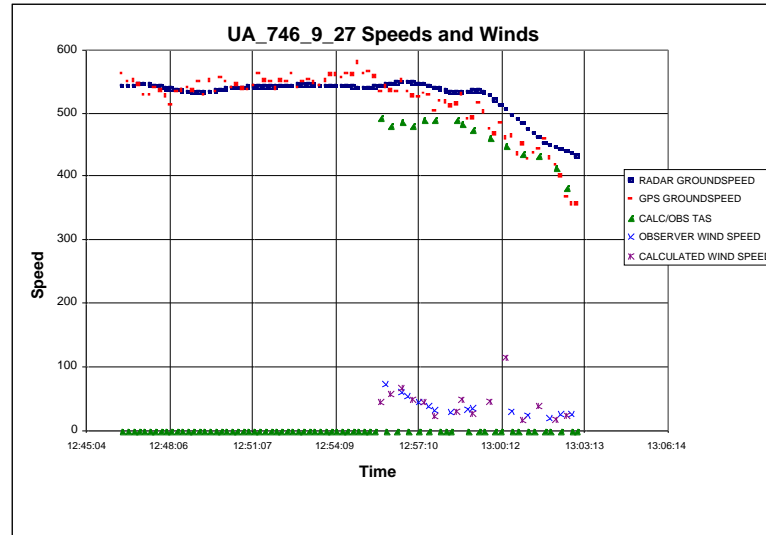
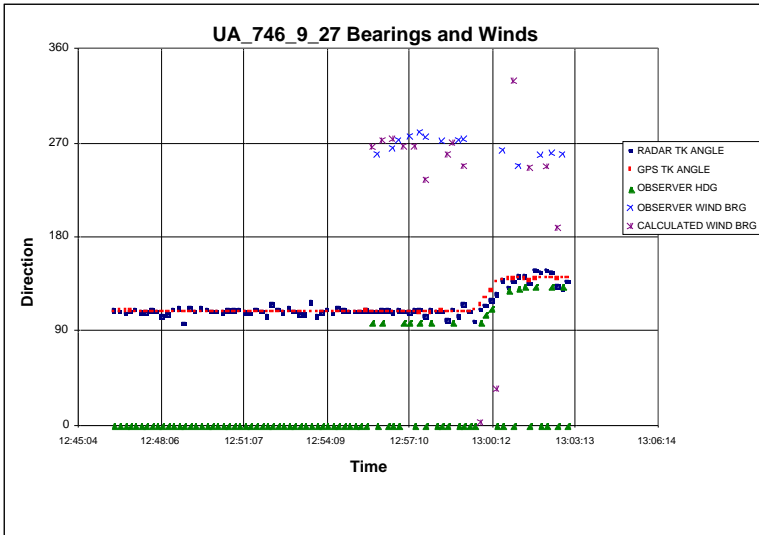
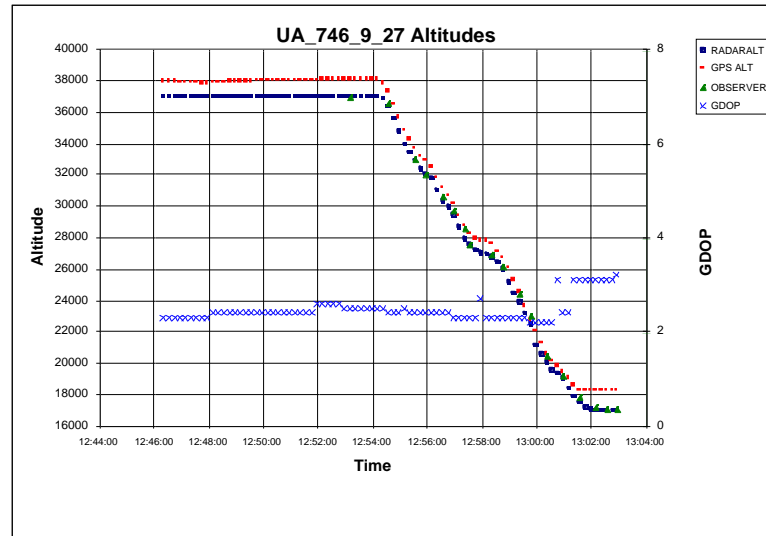
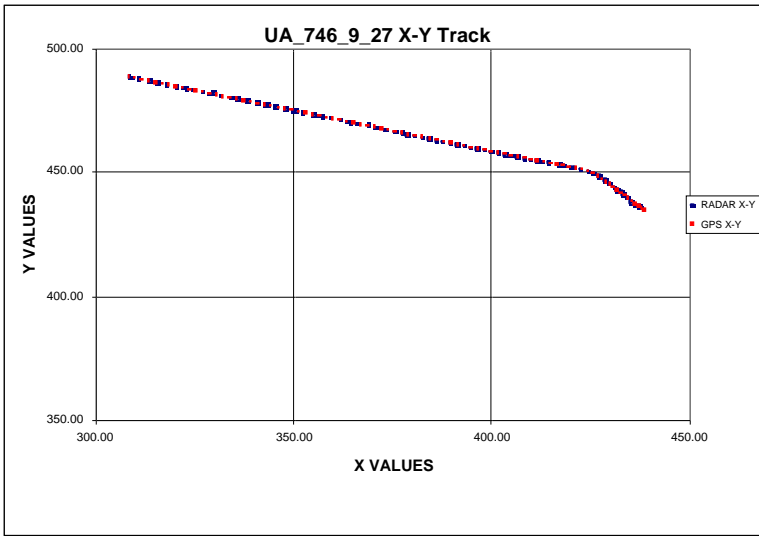


Figure A.17 Graphic Results for Case UA_746_9_27

Table A.18 (continued)

13:00:43	40.80723	105.7236	25123	415.67	453.62	422	108	4	2.8	24900	415.31	453.56	432	111	251				417	0	18
13:00:55	40.80024	105.6966	24759	416.90	453.21	421	108	4	2.8	24600	417.13	453.44	432	99	245	95	195	46			
13:01:07	40.79285	105.6678	24409	418.21	452.77	409	108	4	2.8	24400	418.19	452.94	432	110			199	42	415	39	15
13:01:19	40.78557	105.6393	24077	419.52	452.35	413	108	4	2.8	23800	420.19	452.44	431	106	238	95					
13:01:31	40.77826	105.6103	23717	420.84	451.92	426	108	4	2.8	23500	421.44	451.94	430	110					403	322	28
13:01:43	40.77073	105.5812	23325	422.18	451.49	414	109	4	2.8	23200	422.63	451.50	428	110		95	207	33			
13:01:55	40.76363	105.5546	22937	423.40	451.08	408	111	4	2.8	22900	423.25	451.19	426	115	230		215	32			
13:02:07	40.75486	105.5266	22482	424.68	450.56	435	124	4	1.9	22500	424.56	450.63	423	114		95					
13:02:19	40.74144	105.5023	22038	425.80	449.77	392	136	4	1.9	21800	426.31	449.44	420	121		119					
13:02:31	40.72470	105.4827	21751	426.70	448.78	395	142	4	2.3	21600	427.00	448.44	417	135	215		215	30			
13:02:43	40.70704	105.4657	21462	427.49	447.72	390	143	4	5.4	21500	427.94	447.56	415	134		134					
13:02:55	40.69052	105.4492	21045	428.25	446.74	383	139	4	2.3	21200	428.38	447.00	411	140	212				393	218	43
13:03:07	40.67381	105.4306	20864	429.11	445.75	373	139	4	2.3	20900	429.06	445.94	407	145			212	27	392	206	44
13:03:19	40.65773	105.4135	20526	429.90	444.79	376	140	4	2.3	20300	430.31	444.50	403	141							
13:03:31	40.64125	105.3958	20193	430.72	443.82	365	139	4	5.3	20000	431.25	443.56	399	137	201				387	188	32
13:03:43	40.62441	105.3776	19841	431.57	442.82	373	140	4	2.3	19600	432.06	442.63	396	138			212	18			
13:03:55	40.60882	105.3606	19611	432.36	441.89	370	141	4	2.4	19400	432.44	442.13	393	142							
13:04:07	40.59263	105.3435	19327	433.15	440.93	369	140	4	1.9	19100	433.13	441.06	390	145	190						
13:04:19	40.57642	105.3260	19041	433.96	439.97	363	140	4	2.4	18800	434.00	440.19	388	138			218	17			
13:04:31	40.56062	105.3092	18714	434.74	439.03	362	140	4	5.1	18000	435.06	438.75	385	142	184				377	194	24
13:04:43	40.54432	105.2919	18359	435.55	438.07	372	141	4	2.4	17700	435.88	437.81	383	140			221	18	373	201	21
13:04:55	40.52894	105.2761	18041	436.28	437.16	374	141	4	2.4	17500	436.25	436.69	381	154	176						
13:05:07	40.51333	105.2598	17709	437.04	436.23	354	140	4	2.4	17100	437.06	436.38	379	140							
13:05:19	40.49724	105.2429	17481	437.83	435.28	345	140	4	2.4	16900	437.44	435.25	378	154		282			363	210	24
13:05:23	40.49125	105.2365	17507	438.12	434.92	365	140	4	2.4	16939	437.90	434.74	377	150			219	11	367	187	31

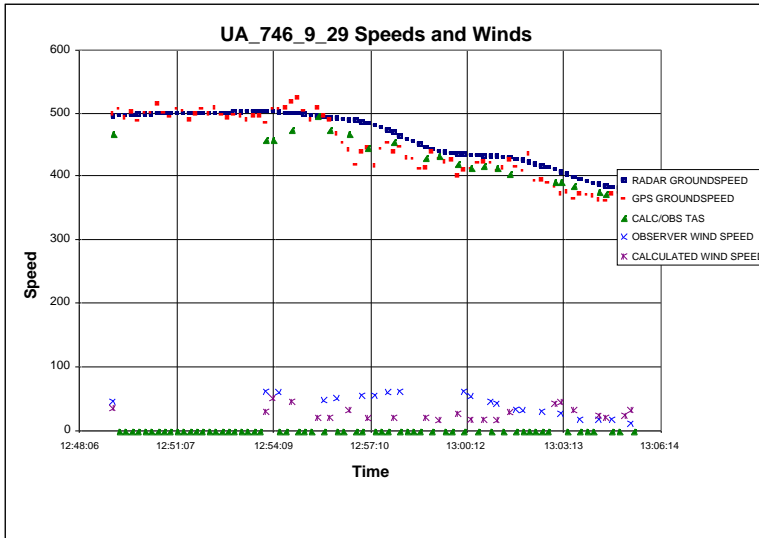
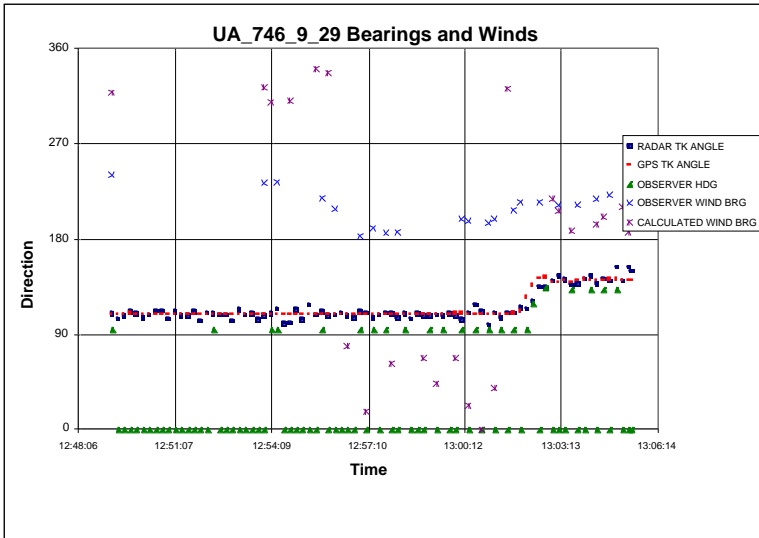
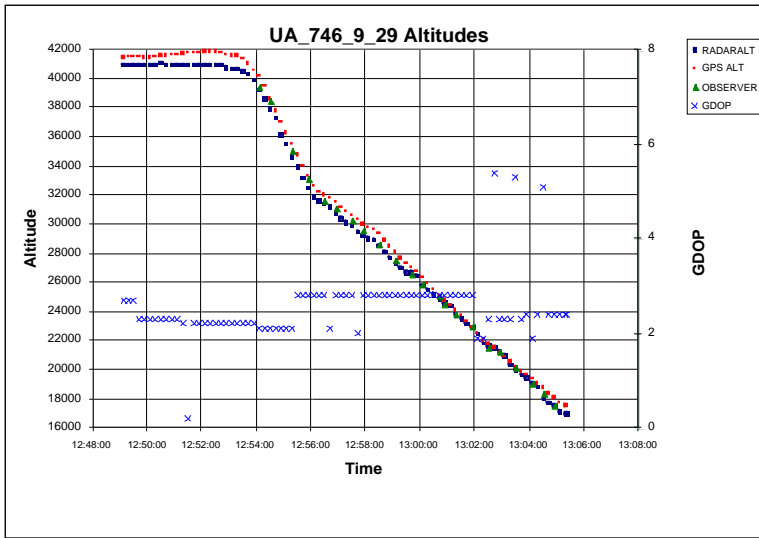
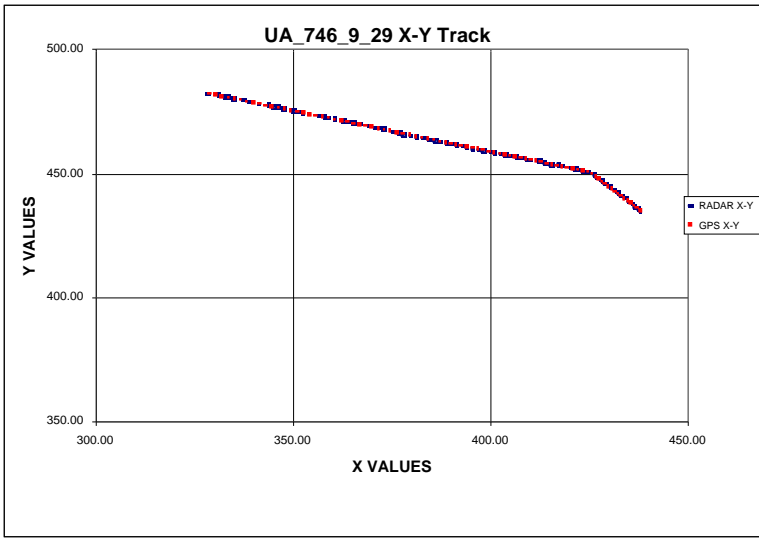


Figure A.18 Graphic Results for Case UA-746_9_29

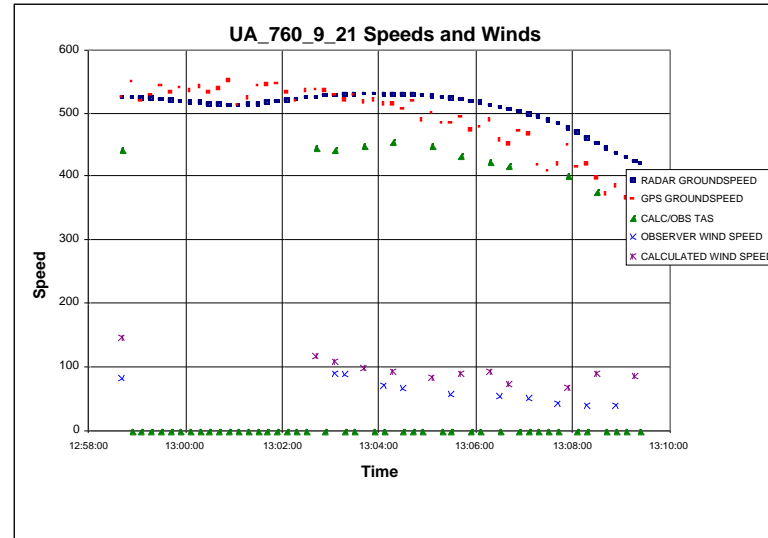
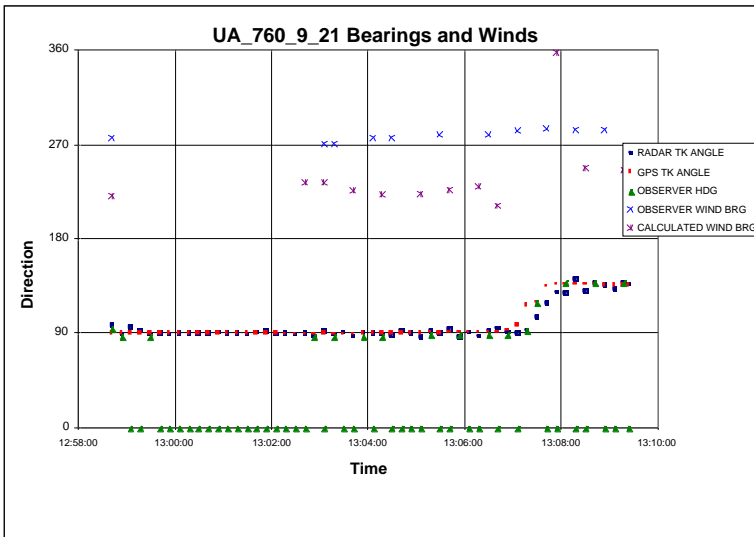
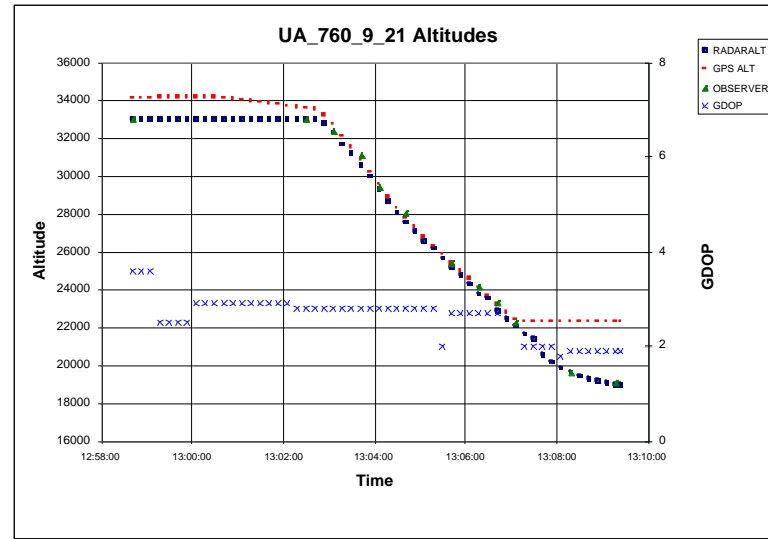
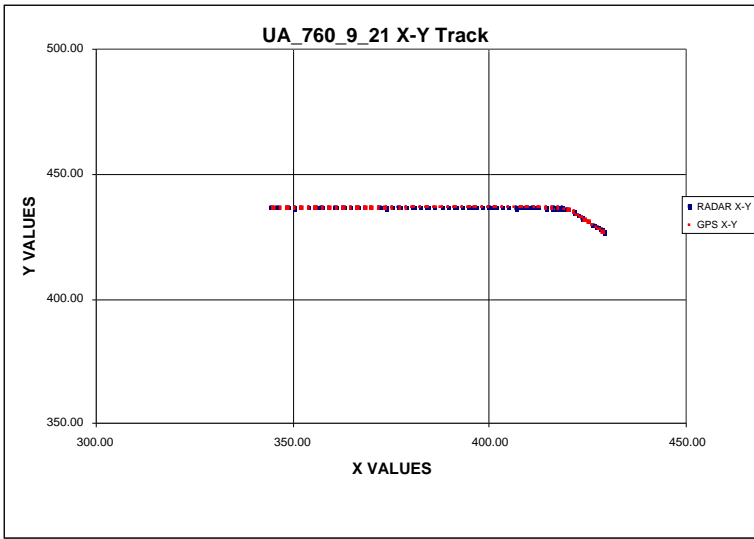


Figure A.19 Graphic Results for Case UA_760_9_21

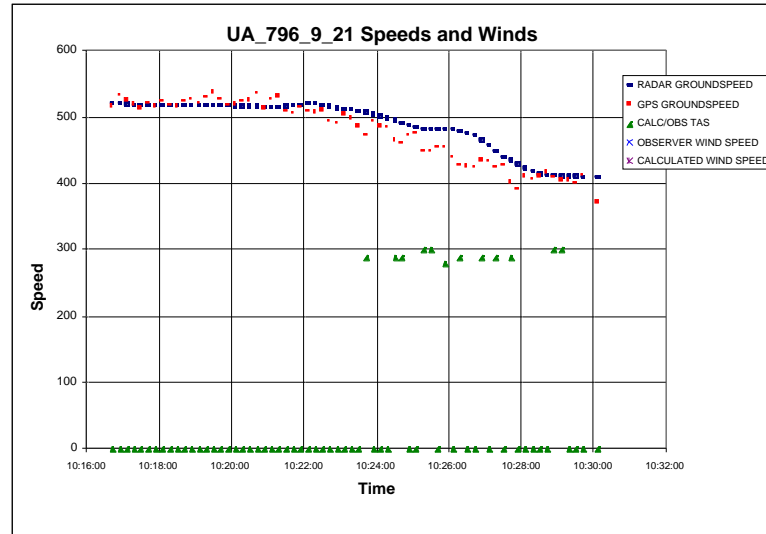
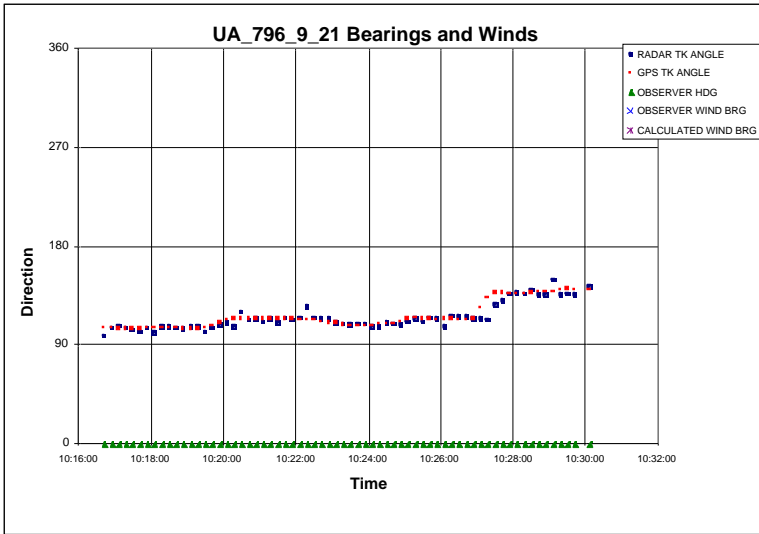
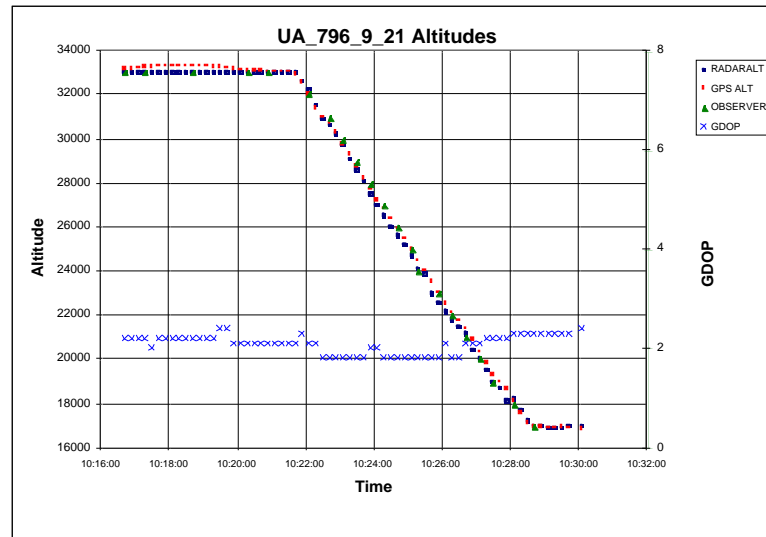
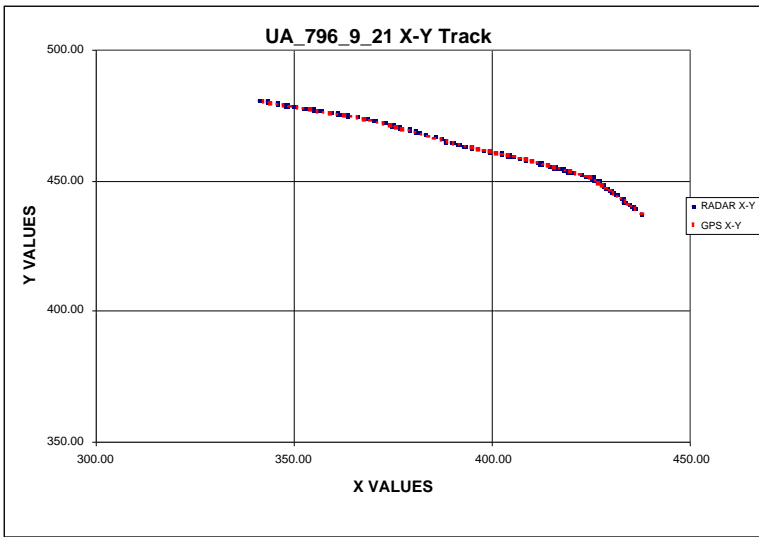


Figure A.20 Graphic Results for Case UA_796_9_21

Table A.21 (continued)

10:56:08	40.76339	105.5847	24173	422.02	451.04	423	119	4	3.1	23600	422.44	450.88	472	109				305
10:56:19	40.75173	105.5570	23422	423.29	450.36	429	127	4	2.0	23100	423.63	450.13	472	118				
10:56:31	40.73763	105.5318	22820	424.45	449.52	419	128	4	2.0	22600	424.69	449.38	471	123	230		1	
10:56:43	40.72285	105.5079	22368	425.55	448.65	417	128	4	2.0	21200	426.44	448.00	468	127	220			
10:56:55	40.70867	105.4851	21985	426.60	447.81	418	126	4	3.1	20800	427.56	447.19	465	126			4	
10:57:08	40.69440	105.4594	21081	427.78	446.97	413	129	4	2.0	20400	428.75	446.44	461	123	210			
10:57:19	40.68103	105.4371	20378	428.81	446.18	402	130	4	3.1	20000	429.31	445.88	456	132			4	120
10:57:31	40.66636	105.4148	19695	429.84	445.31	394	134	4	2.9	19700	430.19	445.00	451	134	200			
10:57:43	40.65080	105.3940	19305	430.80	444.39	398	137	4	1.9	18600	431.56	443.63	445	135			4	300
10:57:55	40.63434	105.3743	18624	431.71	443.42	398	135	4	1.9	17700	432.44	442.63	439	138	190		4	300
10:58:08	40.61776	105.3539	18122	432.66	442.43	387	133	4	1.9	17200	433.38	441.75	433	134				130
10:58:19	40.60302	105.3336	17773	433.59	441.56	391	131	4	2.9	17000	433.94	441.19	426	135				
10:58:31	40.58844	105.3122	17466	434.58	440.70	362	130	4	1.9	17000	434.94	440.44	421	129				
10:58:43	40.57514	105.2917	17396	435.53	439.91	352	130	4	2.9	17000	436.38	439.31	415	128				
10:58:55	40.56197	105.2718	17321	436.45	439.14	353	131	4	2.9	16900	437.19	438.50	410	133				
10:59:08	40.54833	105.2522	17120	437.36	438.33	339	135	4	2.9	16600	437.94	437.69	405	136				
10:59:19	40.53573	105.2357	16831	438.12	437.59	329	134	4	0.9	16300	438.88	437.00	399	129				
10:59:22	40.53230	105.2313	16717	438.33	437.38	333	134	4	1.9	16225	438.97	436.91	397	130				

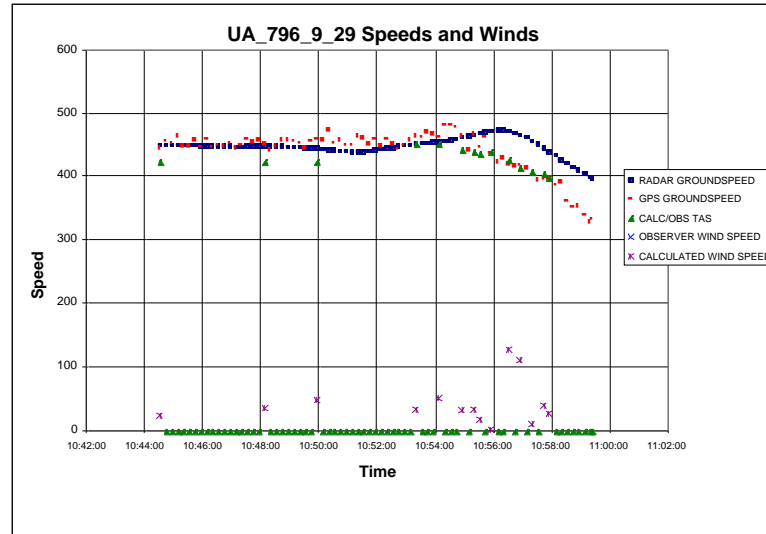
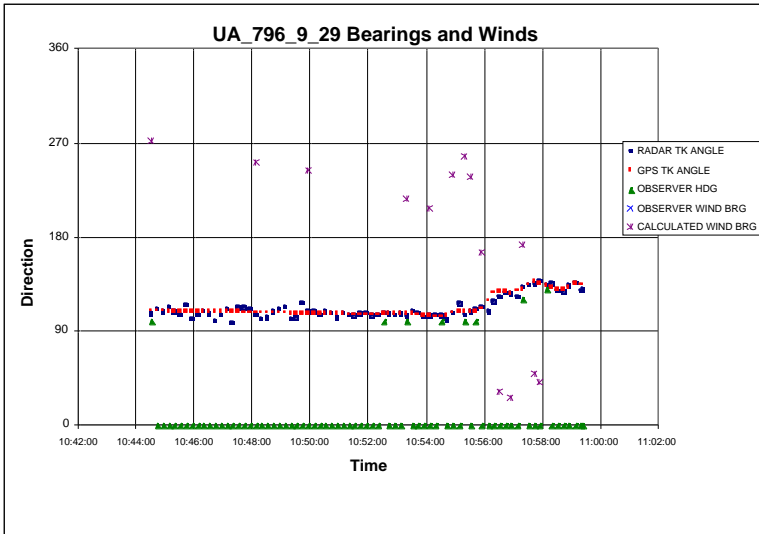
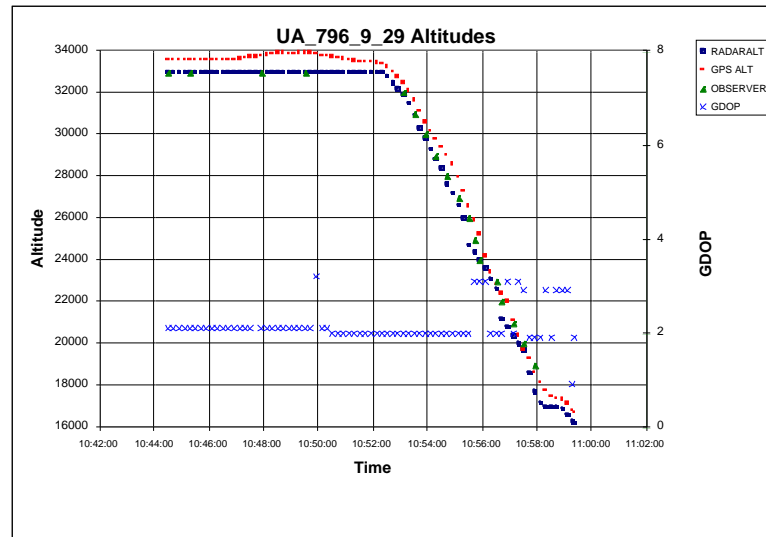
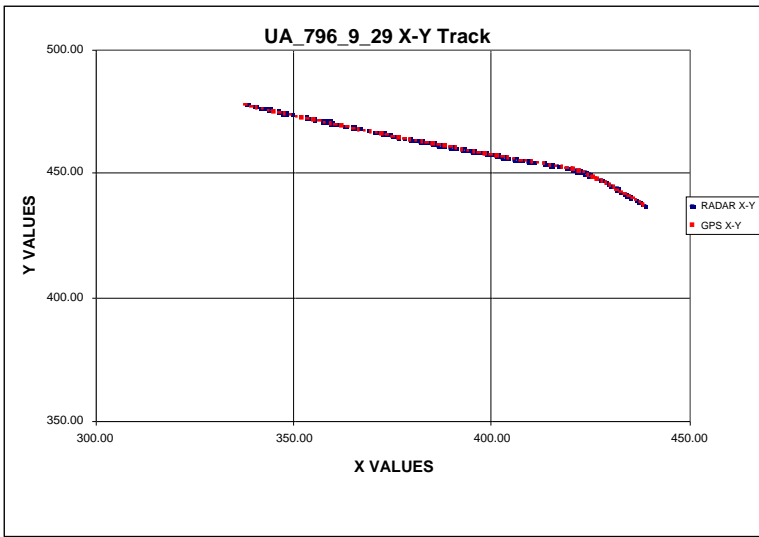


Figure A.21 Graphic Results for Case UA_796_9_29

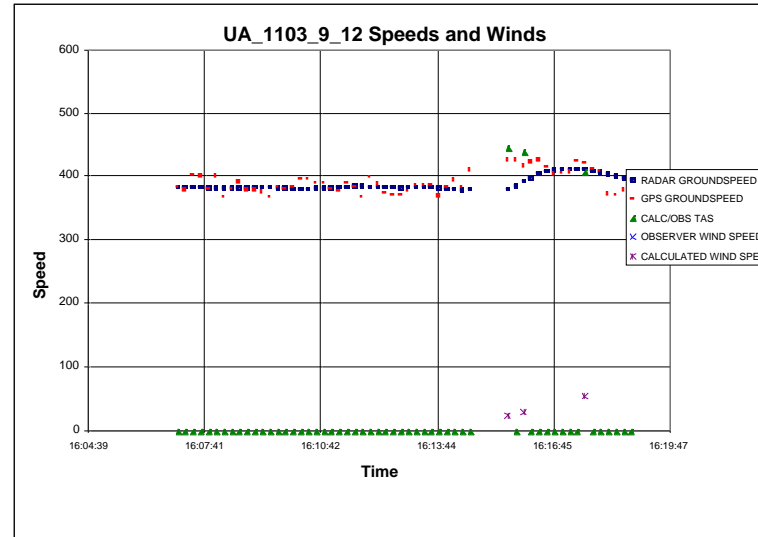
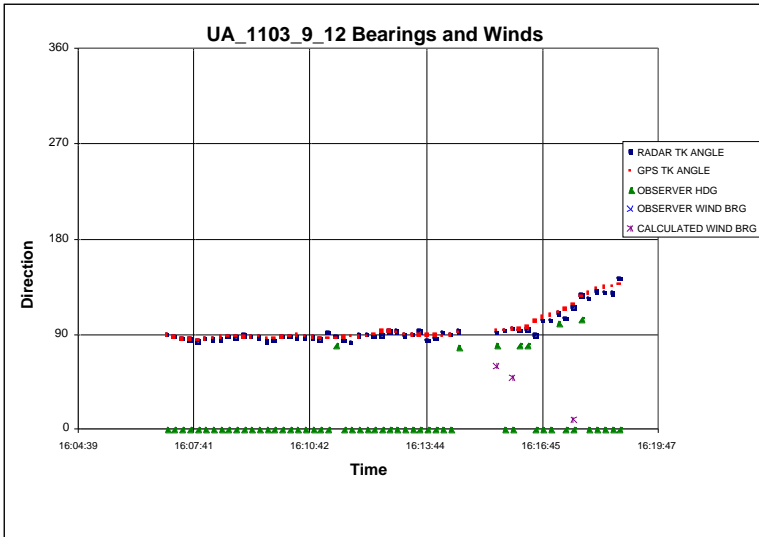
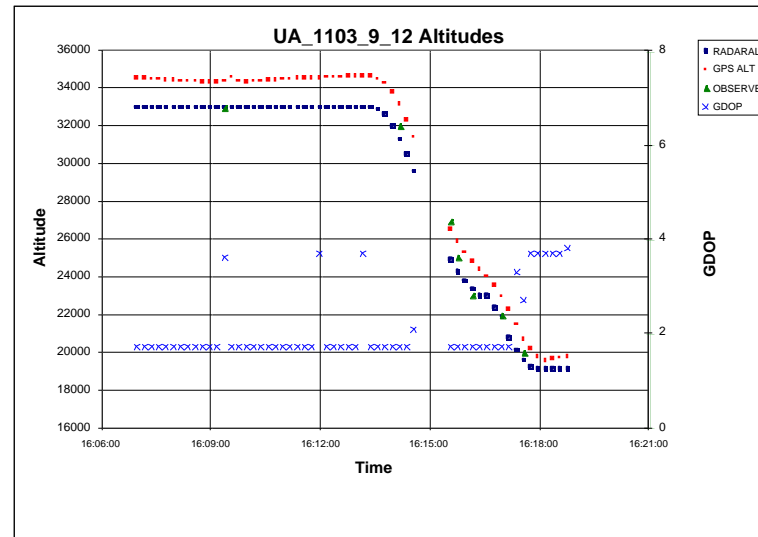
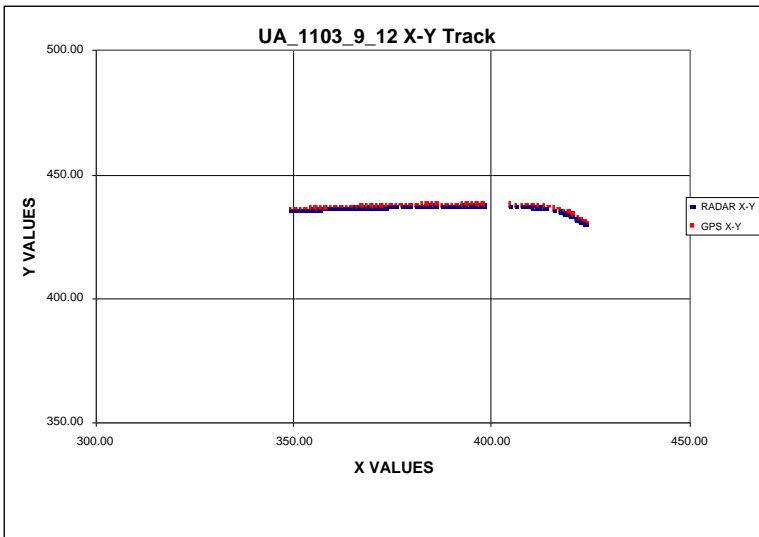


Figure A.22 Graphic Results for Case UA_1103_9_12

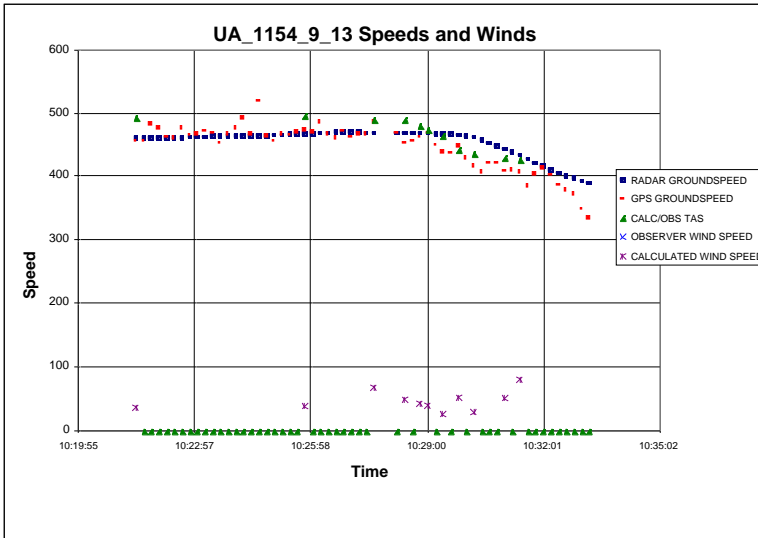
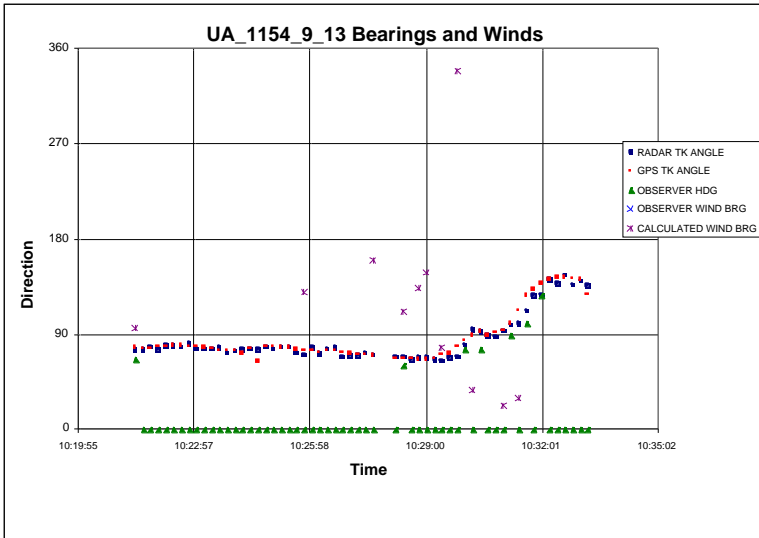
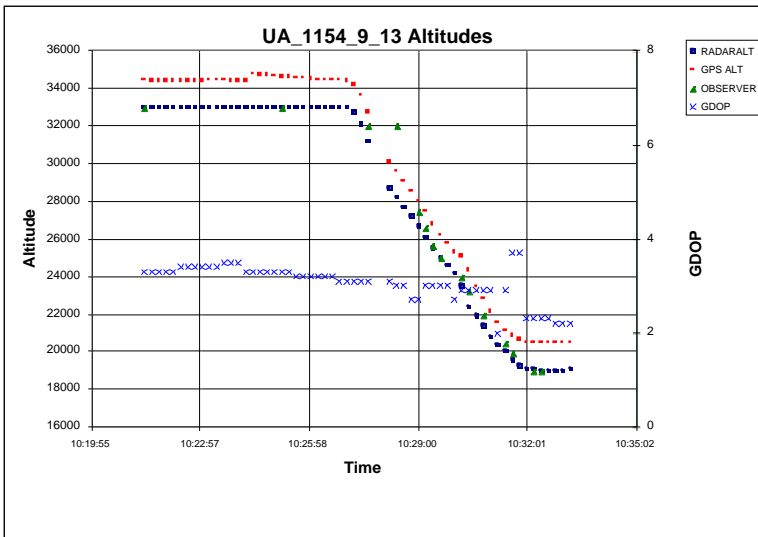
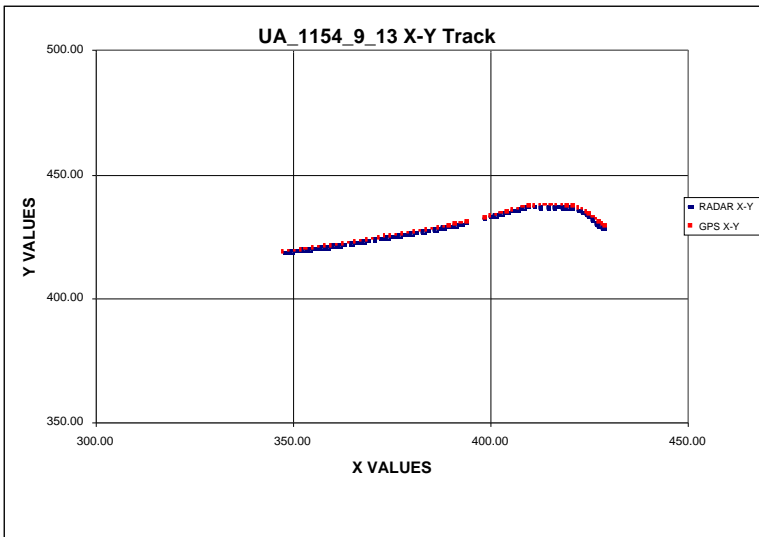


Figure A.23 Graphic Results for Case UA_1154_9_13

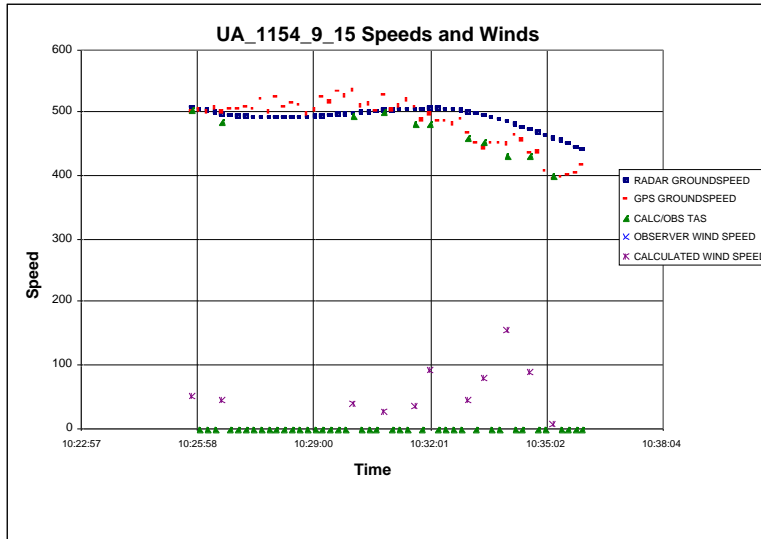
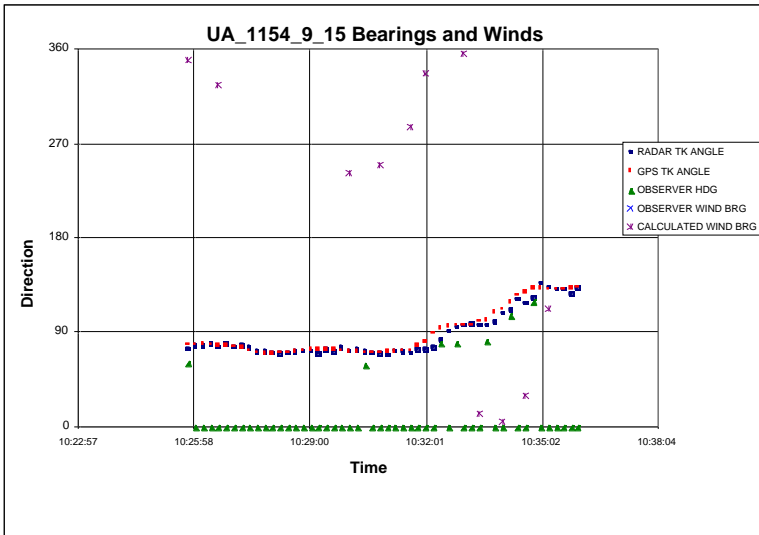
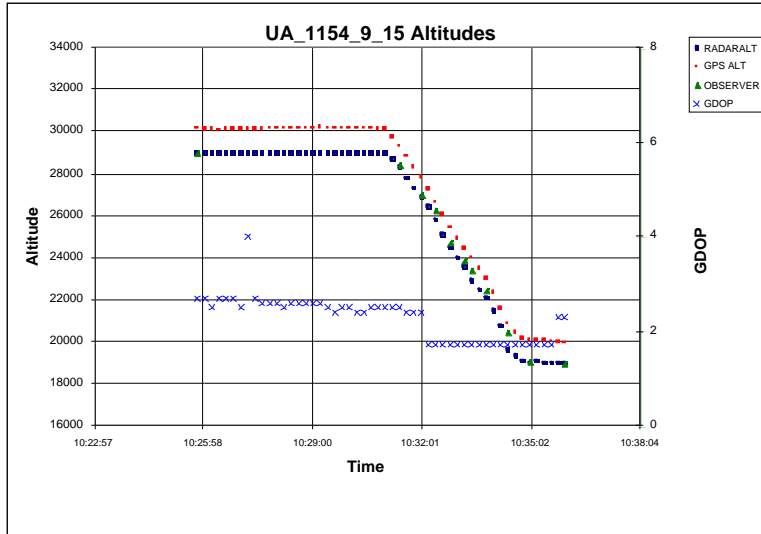
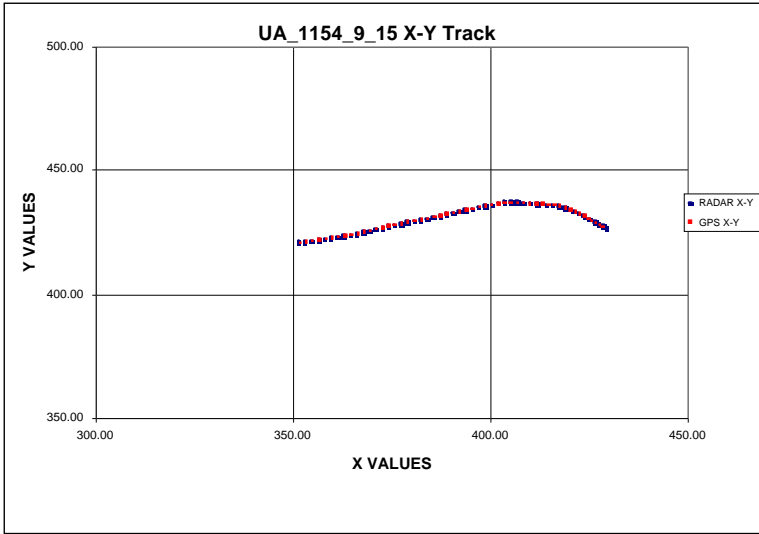


Figure A.24 Graphic Results for Case UA_1154_9_15

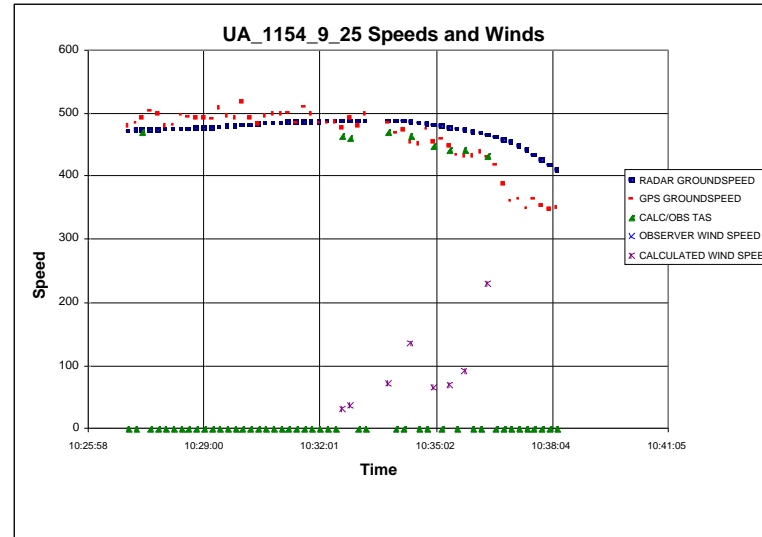
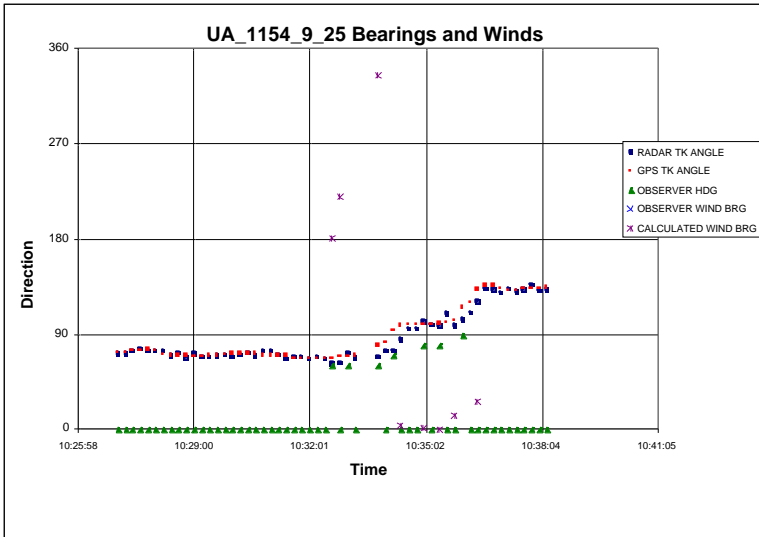
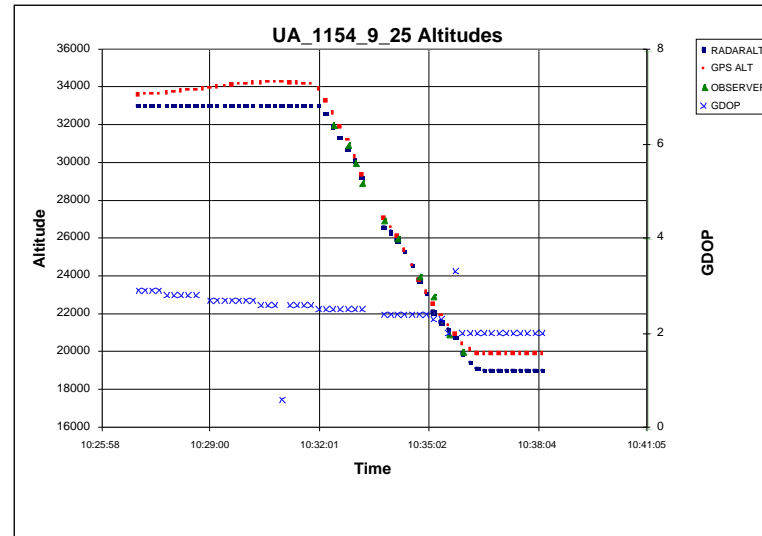
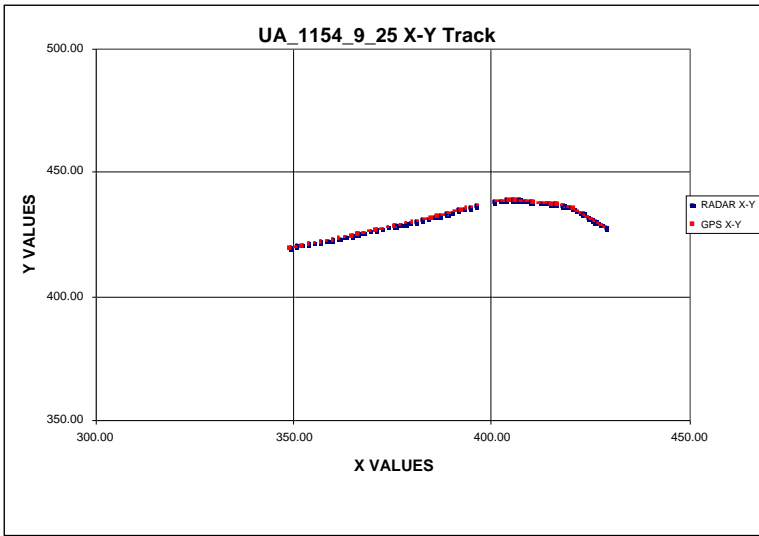


Table A.25 Graphic Results for Case UA_1154_9_25

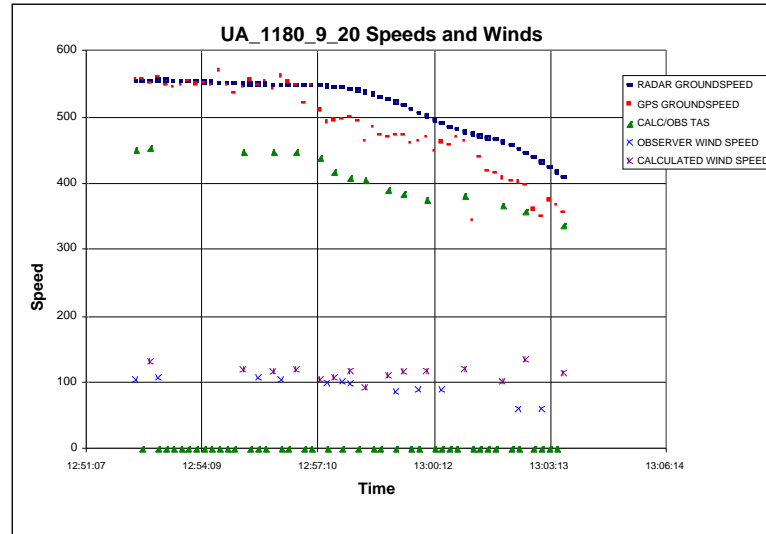
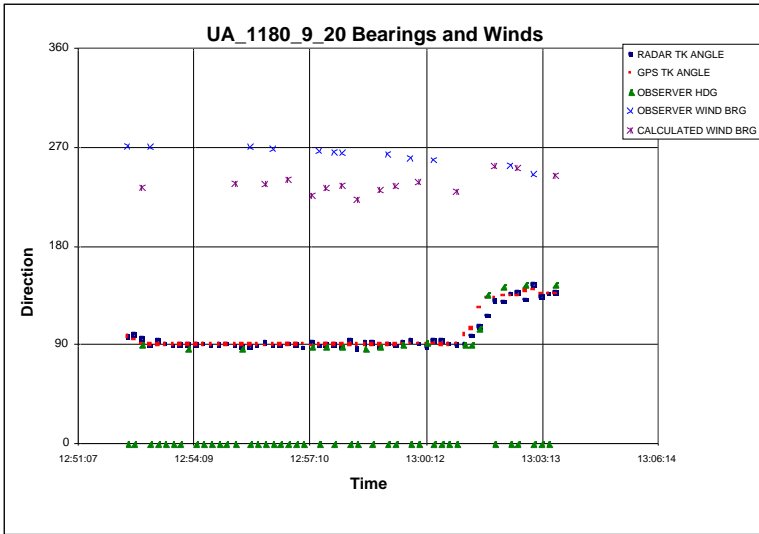
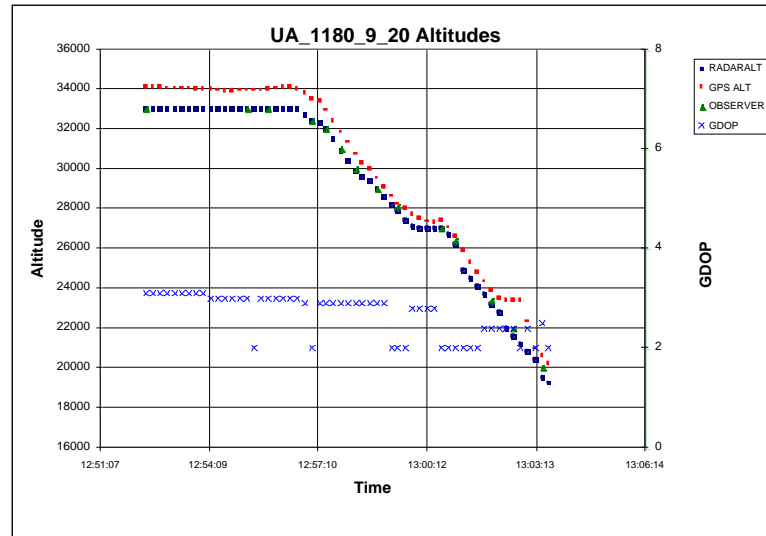
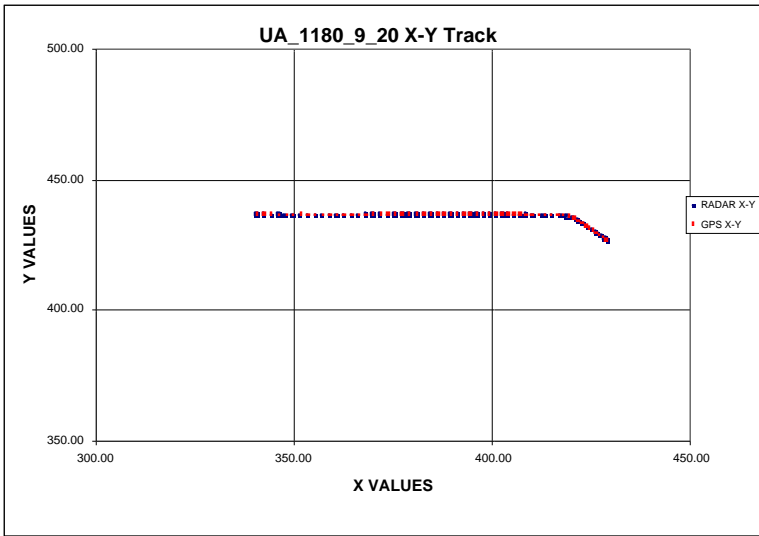


Figure A.26 Graphic Results for Case UA_1180_9_20

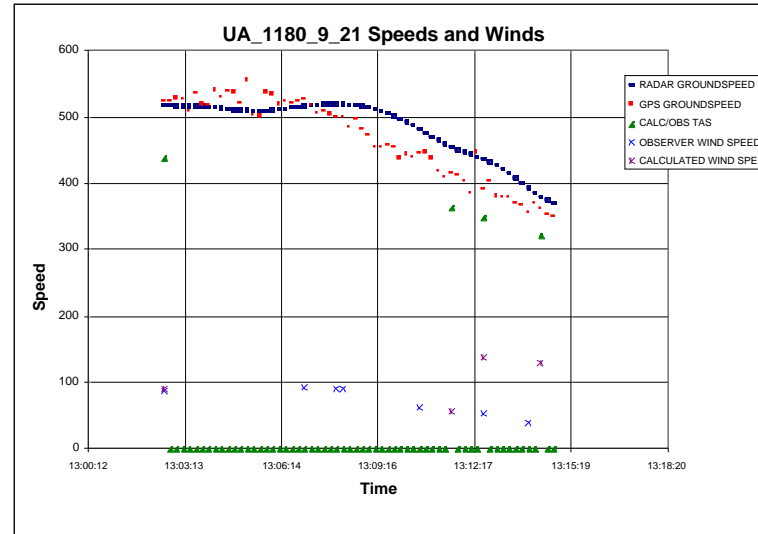
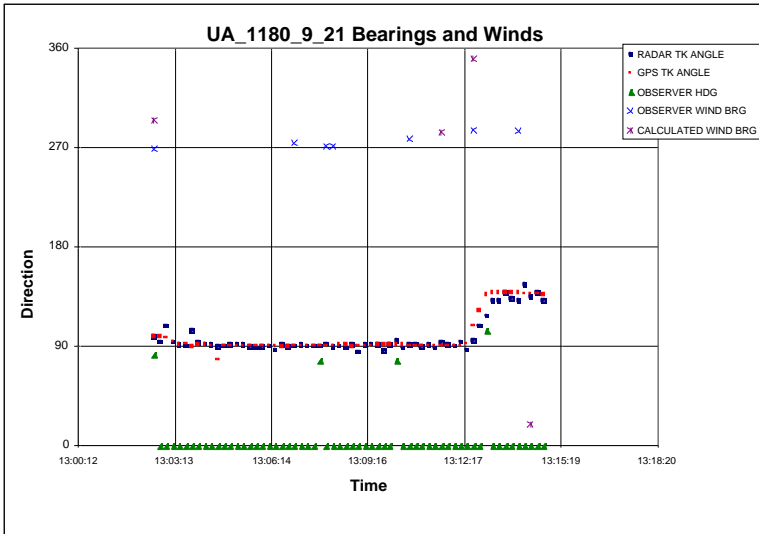
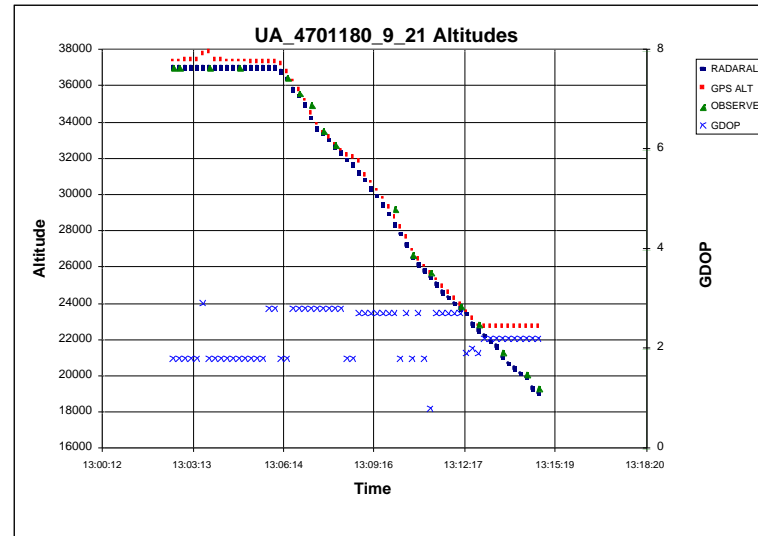
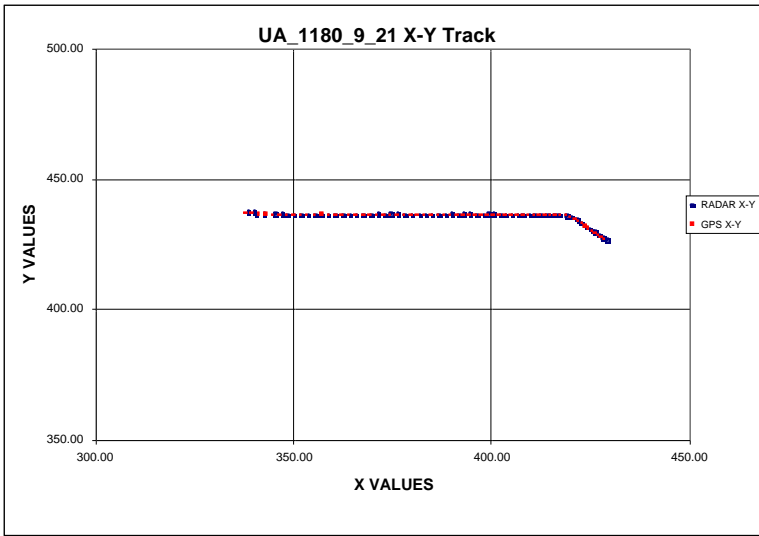


Figure A.27 Graphic Results for Case UA_1180_9_21

Table A.28 Tabular Results for Case UA_1618_9_13

UA_1618_9_13	GPS DATA						RADAR DATA						OBSERVER DATA			CALC									
TOD	GPS_LAT	GPS_LON	GPS_ALT	GPS_X	GPS_Y	GPS_GS	GPS_TRK	G_SATS	GDOP	R_ALT	R_X	R_Y	R_GS	R_TRK	OBS_ALT	OBS_OAT	OBS_IAS	OBS_HDG	OBS_WBRG	OBS_WMAG	OBS_CMT	C/O_TAS	CALC_WBRG	CALC_WMAG	
10:21:41	40.26833	106.2597	33847	391.31	421.17	414	81	4	4.7	31600	392.06	420.63	425	82											
10:21:53	40.27177	106.2299	33377	392.69	421.38	416	81	4	4.7	31100	393.38	420.81	425	82											
10:22:05	40.27517	106.2004	32885	394.04	421.59	407	81	4	4.6	31100	394.88	421.00	425	83	310										
10:22:17	40.27856	106.1710	32383	395.39	421.80	390	81	4	4.6	30600	395.38	421.00	424	88									434		
10:22:29	40.28191	106.1410	31863	396.77	422.00	411	82	4	4.5	30100	396.75	421.31	423	80											
10:22:41	40.28505	106.1121	31353	398.09	422.19	400	82	4	4.5	29700	398.00	421.50	421	81	300			69		108	26				
10:22:53	40.28815	106.0833	30849	399.41	422.39	403	82	4	4.5	29200	399.44	421.69	420	82				69							
10:23:05	40.29127	106.0546	30339	400.73	422.58	386	82	4	4.4	28700	400.75	421.94	418	80											
10:23:17	40.29436	106.0260	29818	402.05	422.77	394	82	4	4.4	28200	402.19	422.13	417	82						99	23				
10:23:29	40.29746	105.9968	29279	403.39	422.96	409	82	4	4.4	27700	403.44	422.25	415	84								417	21		16
10:23:41	40.30034	105.9685	28751	404.68	423.14	391	82	4	4.3	27200	404.75	422.44	413	82	280			69							
10:23:53	40.30326	105.9403	28214	405.97	423.33	376	81	4	0.3	26700	406.06	422.63	411	82								412	65		37
10:24:05	40.30637	105.9124	27676	407.25	423.52	379	81	4	4.2	26300	407.38	422.81	410	82	260					90	20				
10:24:17	40.30968	105.8842	27149	408.55	423.73	367	81	4	4.2	25800	408.50	423.13	408	77								406	62		19
10:24:29	40.31296	105.8564	26629	409.82	423.93	390	81	4	4.2	25300	409.81	423.31	406	80						76	16				
10:24:41	40.31628	105.8283	26104	411.11	424.14	388	81	4	4.2	24800	411.13	423.56	404	80	250			69							
10:24:53	40.31956	105.8006	25595	412.38	424.34	370	81	4	4.1	24200	412.31	423.63	402	85											
10:25:05	40.32273	105.7731	25099	413.64	424.54	388	81	4	4.1	23800	413.69	423.88	400	81						85	14				
10:25:17	40.32573	105.7460	24612	414.88	424.74	383	82	4	4.0	23300	415.56	424.13	397	82				69				395	39		16
10:25:29	40.32855	105.7191	24135	416.12	424.92	378	82	4	3.1	22800	416.88	424.31	395	82	230										
10:25:41	40.33129	105.6921	23693	417.35	425.09	372	82	4	3.1	22300	418.13	424.44	393	84								387	41		19
10:25:53	40.33401	105.6653	23263	418.58	425.27	377	82	4	3.1	21900	418.56	424.50	391	82						100	12				
10:26:05	40.33674	105.6382	22838	419.82	425.44	370	82	4	3.1	21500	419.81	424.69	388	82	210			69							
10:26:17	40.33945	105.6115	22416	421.05	425.61	369	82	4	3.1	20700	421.69	424.94	385	82								382	40		16
10:26:29	40.34223	105.5849	21953	422.27	425.79	373	82	4	3.1	20400	422.88	425.19	383	79				69		91	12				
10:26:41	40.34496	105.5586	21487	423.47	425.97	361	82	4	3.1	20000	424.13	425.31	380	83	200										
10:26:53	40.34772	105.5322	21029	424.68	426.15	362	82	4	3.1	19600	424.69	425.44	378	79								378	44		19
10:27:05	40.35056	105.5057	20583	425.89	426.33	353	84	4	3.1	19300	425.94	425.50	375	85											
10:27:17	40.35319	105.4801	20337	427.07	426.50	351	93	4	3.1	19200	427.00	425.75	373	79	190					78	10				
10:27:28	40.35388	105.4568	20158	428.14	426.56	343	108	4	3.0	19020	428.52	425.41	369	92								360	9		169

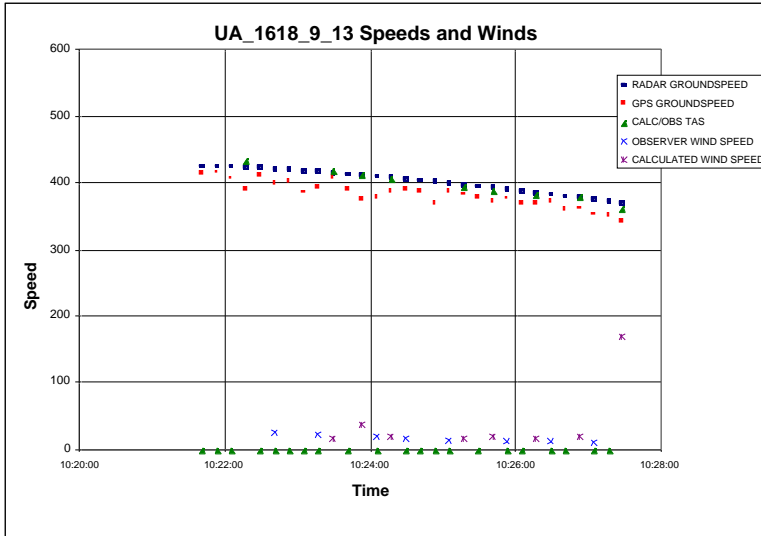
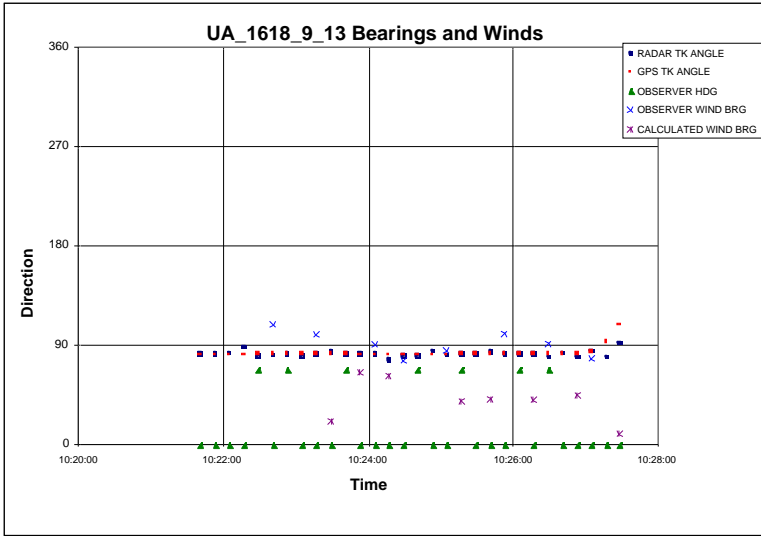
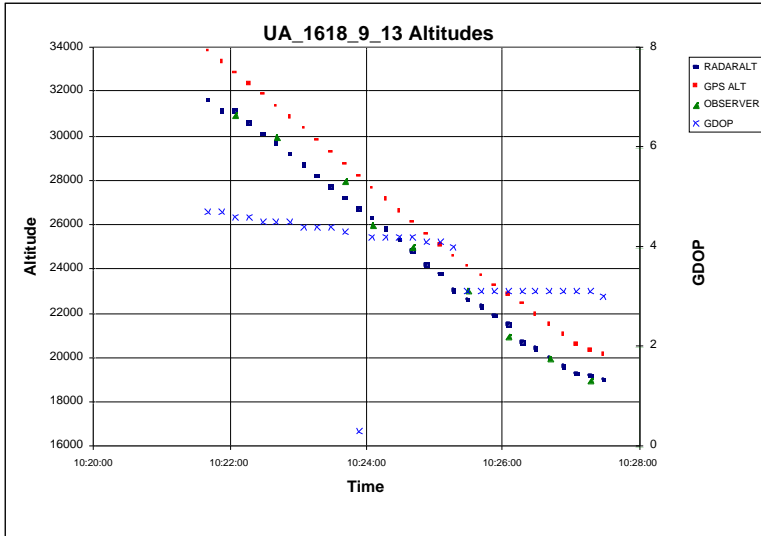
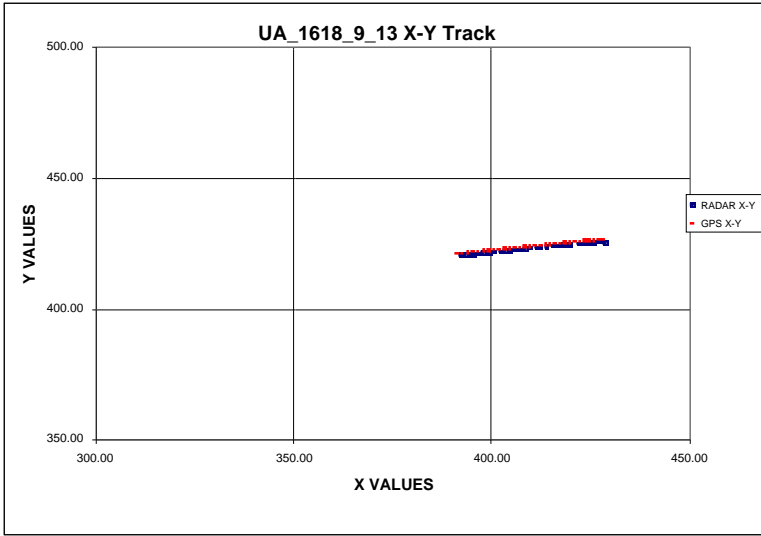


Figure A.28 Graphic Results for Case UA_1618_9_13

Table A.29 Tabular Results for Case UA_1618_9_15

UA_1618_9_15	GPS DATA				GPS DATA				RADAR DATA				OBSERVER DATA				DATA										
TOD	GPS_LAT	GPS_LON	GPS_ALT	GPS_X	GPS_Y	GPS_GS	GPS_TRK	G_SATS	GDOP	R_ALT	R_X	R_Y	R_GS	R_TRK	OBS_ALT	OBS_OAT	OBS_IAS	OBS_HDG	OBS_WBRG	OBS_WMAG	OBS_CMT	C/O_TAS	CALC_WBRG	CALC_WMAG			
10:15:35	40.25430	106.9488	34135	359.67	420.38	499	85	4	1.9	33000	359.63	420.50	479	85	330			273	72	248		31	448	279	52		
10:15:47	40.25697	106.9135	34166	361.29	420.53	506	85	3	2.1	33000	361.13	420.63	479	85	330			271					445	276	62		
10:15:59	40.25967	106.8775	34164	362.94	420.69	502	85	4	1.9	33000	362.81	420.75	479	86													
10:16:11	40.26248	106.8415	34205	364.59	420.85	494	85	3	2.2	33000	364.63	420.94	480	85													
10:16:23	40.26518	106.8054	34184	366.26	421.00	479	86	3	2.2	33000	366.13	421.06	480	85													
10:16:35	40.26754	106.7688	34178	367.94	421.14	487	85	4	4.2	33000	367.94	421.25	480	84													
10:16:47	40.26977	106.7335	34209	369.56	421.27	482	85	3	4.3	33000	369.56	421.38	481	85													
10:16:59	40.27213	106.6981	34207	371.18	421.40	503	85	4	1.9	33000	371.19	421.56	482	84													
10:17:11	40.27461	106.6615	34214	372.86	421.54	504	85	4	1.9	33000	372.88	421.63	483	87													
10:17:23	40.27712	106.6254	34233	374.52	421.70	486	85	3	4.2	33000	374.56	421.88	484	83	330				73								
10:17:35	40.27956	106.5893	34225	376.18	421.84	496	85	4	1.9	33000	376.13	421.94	485	86													
10:17:47	40.28196	106.5545	34225	377.78	421.98	488	85	4	2.0	33000	377.69	422.13	486	84					275		237		36	451	280	38	
10:17:59	40.28442	106.5184	34234	379.43	422.13	494	85	4	2.0	33000	379.38	422.31	488	84													
10:18:11	40.28688	106.4834	34225	381.04	422.27	483	85	3	4.1	33000	381.00	422.38	488	87													
10:18:23	40.28944	106.4475	34114	382.69	422.43	500	85	3	4.1	32800	382.63	422.56	489	84													
10:18:35	40.29218	106.4118	33666	384.33	422.59	494	85	4	3.8	32400	384.19	422.69	489	85	327												
10:18:47	40.29468	106.3761	33065	385.97	422.74	493	85	4	3.8	31800	386.00	422.81	490	86													
10:18:59	40.29724	106.3406	32401	387.60	422.90	492	85	4	3.8	31100	387.56	423.00	490	84	315												
10:19:11	40.29989	106.3048	31716	389.24	423.06	485	85	4	3.0	30400	389.25	423.13	490	85				285					455	274	30		
10:19:23	40.30255	106.2690	31205	390.89	423.22	487	85	4	3.0	29800	390.81	423.25	490	85	300												
10:19:35	40.30484	106.2344	30680	392.47	423.36	481	84	4	3.0	29300	392.44	423.44	490	84					292		245		30	454	271	27	
10:19:47	40.30740	106.1994	30147	394.08	423.52	469	84	4	3.0	28800	394.19	423.63	490	84													
10:19:59	40.30993	106.1647	29631	395.67	423.68	484	84	4	3.0	28300	395.88	423.75	491	85													
10:20:11	40.31246	106.1299	29110	397.27	423.84	462	84	4	3.0	27800	397.13	424.13	491	77	285								445	276	16		
10:20:23	40.31491	106.0953	28588	398.86	423.99	460	85	4	3.0	27300	398.88	424.06	491	87													
10:20:35	40.31701	106.0625	28114	400.36	424.12	454	85	4	3.0	26800	400.44	424.19	491	86													
10:20:47	40.31895	106.0291	27595	401.90	424.25	449	85	4	3.0	26300	401.94	424.31	490	85						265							
10:20:59	40.32080	105.9966	27088	403.38	424.36	433	85	4	3.0	25800	403.50	424.50	489	84					293		278		21	432	348	11	
10:21:11	40.32272	105.9625	26583	404.95	424.49	440	85	4	2.9	25300	404.88	424.56	488	86													
10:21:23	40.32460	105.9302	26100	406.44	424.61	438	85	4	2.9	24900	406.44	424.56	486	89													
10:21:35	40.32642	105.8994	25624	407.84	424.73	432	85	4	2.9	24400	407.75	424.75	483	84	240												
10:21:47	40.32830	105.8687	25147	409.25	424.85	427	85	4	2.9	23900	409.31	424.88	479	85													
10:21:59	40.33023	105.8370	24657	410.70	424.97	415	85	4	2.9	23500	410.63	425.00	475	85	230						73		302	18			
10:22:11	40.33212	105.8064	24200	412.11	425.10	423	85	4	1.8	23000	412.44	425.06	472	87	230												
10:22:23	40.33389	105.7771	23750	413.45	425.21	408	85	4	1.8	22300	414.38	425.13	467	88													
10:22:35	40.33566	105.7468	23224	414.84	425.33	412	84	4	2.9	21900	415.75	425.25	462	86													
10:22:47	40.33789	105.7168	22862	416.22	425.48	406	85	4	2.8	21500	417.13	425.44	457	83	220						73						
10:22:59	40.33985	105.6876	22442	417.55	425.60	396	85	4	2.8	21200	417.75	425.44	452	88													
10:23:11	40.34176	105.6581	21994	418.91	425.73	402	85	4	2.8	20800	419.06	425.63	447	84	210						285		319	19	392	307	5
10:23:23	40.34358	105.6295	21562	420.22	425.86	381	85	4	1.8	20500	420.38	425.69	441	86													
10:23:35	40.34535	105.6017	21160	421.50	425.97	412	85	4	1.8	19800	422.38	425.88	436	85													
10:23:47	40.34715	105.5733	20826	422.80	426.09	387	84	4	1.8	19600	423.63	426.06	430	83	200												
10:23:59	40.34892	105.5455	20654	424.07	426.21	375	84	4	1.8	19500	425.00	426.00	425	90													
10:24:11	40.35072	105.5180	20522	425.33	426.34	357	85	4	1.8	19300	425.56	426.19	419	77	195												
10:24:23	40.35209	105.4920	20352	426.52	426.43	362	86	4	1.8	19200	426.69	426.25	414	84										333	292	32	
10:24:35	40.35321	105.4674	20210	427.65	426.51	348	97	4	1.8	18900	428.06	425.94	406	97													
10:24:38	40.35309	105.4605	20160	427.96	426.51	348	101	4	1.8	18799	428.44	425.95	404	95													

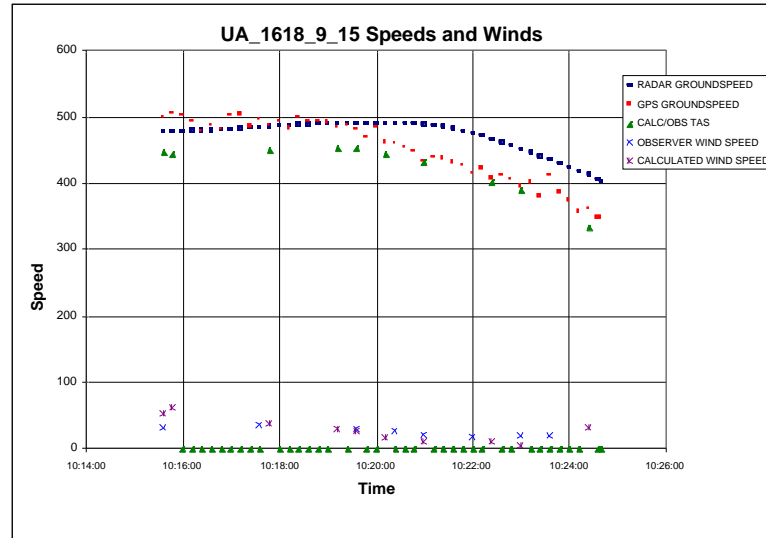
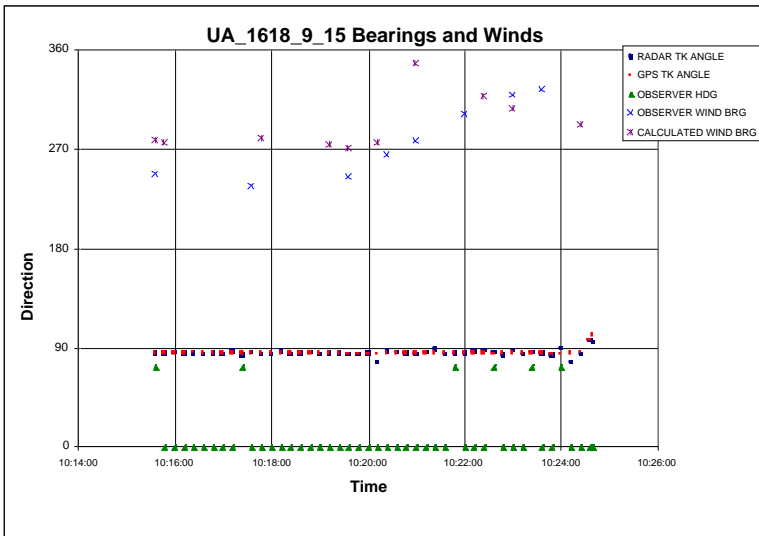
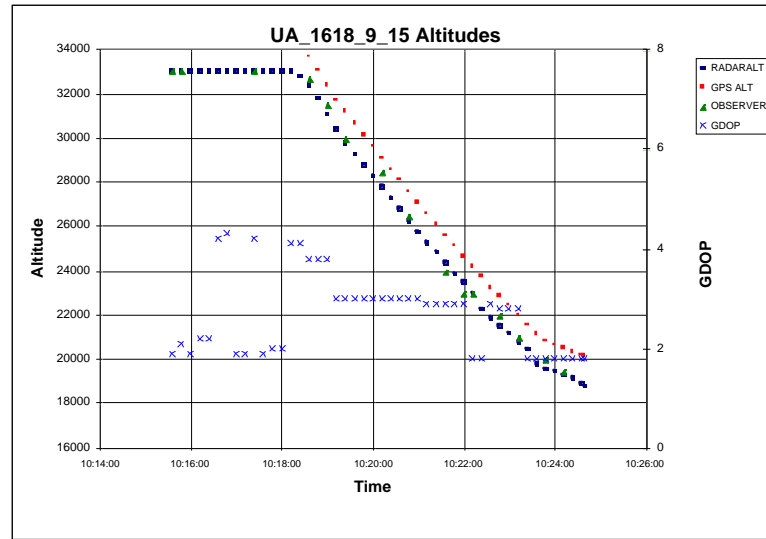
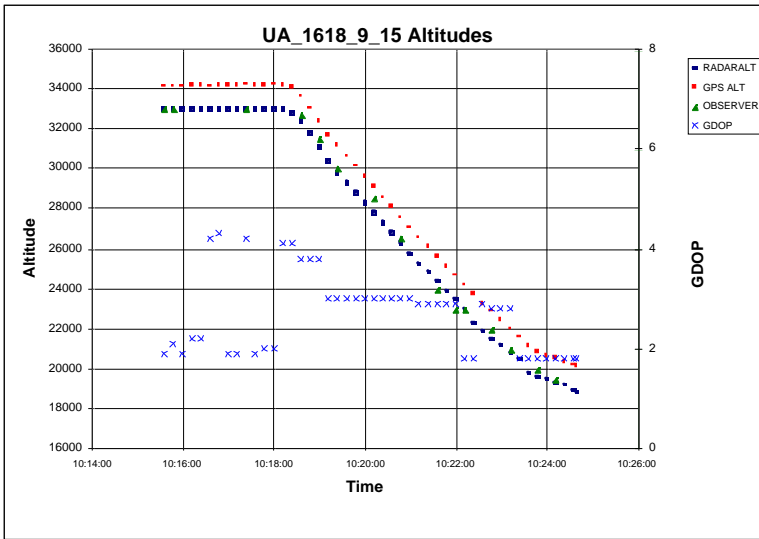


Figure A.29 Graphic Results for Case UA_1618_9_15

Table A.30 Tabular Results for Case UA_1790_9_19

UA_1790_9_19	GPS DATA						RADAR DATA						OBSERVER DATA				OBSERVER DATA								
TOD	GPS_LAT	GPS_LON	GPS_ALT	GPS_X	GPS_Y	GPS_GS	GPS_TRK	G_SATS	GDOP	R_ALT	R_X	R_Y	R_GS	R_TRK	OBS_ALT	OBS_OAT	OBS_IAS	OBS_HDG	OBS_WBRG	OBS_WMAG	OBS_CMT	C/O_TAS	CALC_WBRG	CALC_WMAG	
10:41:52	40.38046	106.6084	33912	375.31	427.89	516	76	4	2.2	33000	375.25	427.94	500	76	330	-16	298	59		gnd spd 508		483	311	63	
10:42:04	40.38737	106.5717	33903	376.99	428.30	513	76	4	2.2	33000	376.94	428.44	501	74							ekr +65	484	313	59	
10:42:16	40.39421	106.5359	33901	378.64	428.71	522	76	4	2.2	33000	378.56	428.88	501	75											
10:42:27	40.40111	106.5008	33864	380.25	429.12	509	75	4	2.3	33000	380.25	429.25	501	77											
10:42:40	40.40848	106.4651	33797	381.88	429.56	518	71	4	3.6	33000	381.94	429.75	501	74											
10:42:51	40.41666	106.4301	33997	383.49	430.05	500	73	4	2.3	33000	383.56	430.19	501	75											
10:43:04	40.42520	106.3933	34020	385.18	430.57	519	71	4	2.3	33000	385.19	430.69	502	73											
10:43:15	40.43376	106.3590	33781	386.74	431.08	533	72	4	2.3	33000	386.75	431.25	502	71											
10:43:28	40.44262	106.3230	33350	388.39	431.62	512	71	4	2.3	32700	388.38	431.75	502	72											
10:43:39	40.45163	106.2883	32770	389.98	432.16	509	71	4	2.3	32100	390.13	432.31	503	72											
10:43:52	40.46087	106.2528	32127	391.61	432.72	522	71	4	2.3	31600	391.69	433.00	503	68											
10:44:03	40.47013	106.2176	31287	393.22	433.28	517	71	4	2.4	30700	393.31	433.63	504	69											
10:44:52	40.50715	106.0725	27562	399.85	435.52	526	72	4	2.4	27100	399.75	435.75	504	71	275			340	58						
10:45:04	40.51561	106.0372	26855	401.47	436.04	525	72	4	2.4	26300	401.44	436.19	504	74	266							504	301	32	
10:45:15	40.52429	106.0020	26180	403.07	436.56	511	71	4	2.4	25700	403.06	436.81	505	70								500	305	20	
10:45:27	40.53361	105.9665	25511	404.69	437.13	507	70	4	2.4	25000	404.81	437.31	506	73											
10:45:39	40.54362	105.9321	24820	406.27	437.74	501	77	4	2.5	24200	406.44	437.81	506	73	250			340							
10:45:51	40.55090	105.8969	24193	407.87	438.18	489	83	4	2.5	23600	408.00	438.31	506	72					80						
10:46:03	40.55417	105.8614	23576	409.49	438.40	493	85	4	2.5	23000	409.56	438.56	507	78	235			340					487	178	66
10:46:15	40.55674	105.8249	22930	411.16	438.56	497	90	4	2.5	22400	411.06	438.69	506	83	230			340					475	196	56
10:46:27	40.55679	105.7898	22280	412.77	438.57	480	92	4	2.5	21100	413.94	438.38	506	92	220					80					
10:46:40	40.55545	105.7526	21513	414.47	438.51	472	99	4	2.6	20600	415.50	438.25	505	94					340						
10:46:51	40.55055	105.7191	20917	416.00	438.23	463	110	3	2.2	20100	417.19	438.00	503	97	210										95
10:47:03	40.54193	105.6867	20491	417.49	437.72	457	114	3	2.2	19800	417.81	437.44	501	111					345						100
10:47:15	40.53123	105.6551	20163	418.94	437.09	449	121	3	2.2	19500	419.13	436.81	498	114	199								455	30	77
10:47:27	40.51735	105.6270	20134	420.24	436.28	445	127	3	2.2	19200	420.44	436.06	495	118	195			334							
10:47:40	40.50198	105.6012	20134	421.43	435.36	449	130	3	2.2	19000	422.06	434.56	489	128											
10:47:52	40.48545	105.5759	20133	422.59	434.39	456	131	3	2.1	19000	423.44	433.81	484	122	190										
10:48:04	40.46893	105.5511	20133	423.74	433.41	445	130	3	2.1	18900	424.50	432.63	478	133	190										
10:48:16	40.45248	105.5263	20133	424.88	432.43	436	130	3	2.1	18900	425.06	432.13	473	132											
10:48:28	40.43631	105.5021	20133	426.01	431.47	419	130	3	2.1	18900	426.25	431.25	468	128											
10:48:40	40.42106	105.4788	20134	427.08	430.57	405	129	3	2.1	18900	427.69	429.88	462	132											
10:48:52	40.40677	105.4565	20134	428.11	429.73	394	129	3	2.1	18900	428.69	429.13	456	128											
10:49:04	40.39314	105.4348	20134	429.12	428.92	376	128	3	2.1	19000	429.94	428.38	450	123											
10:49:16	40.38010	105.4136	20134	430.10	428.15	363	129	3	2.1	19000	430.19	428.06	443	136											
10:49:18	40.37717	105.4089	20134	430.32	427.98	370	129	3	2.1	19000	430.42	427.87	442	135											

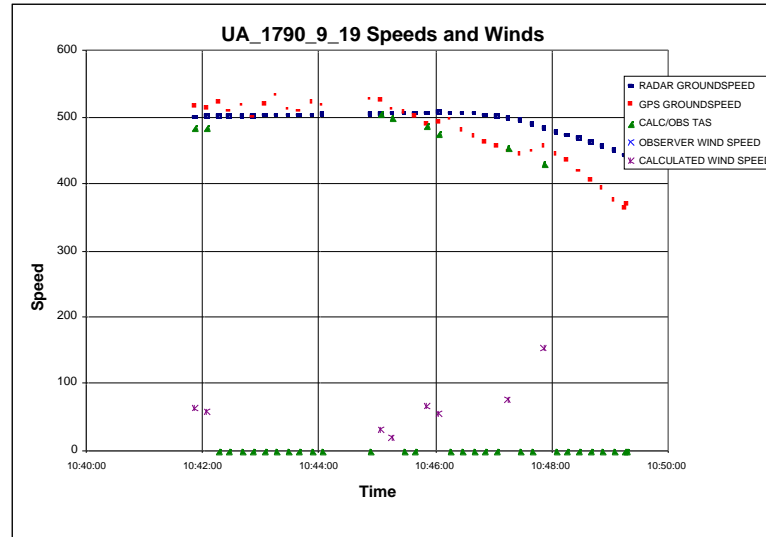
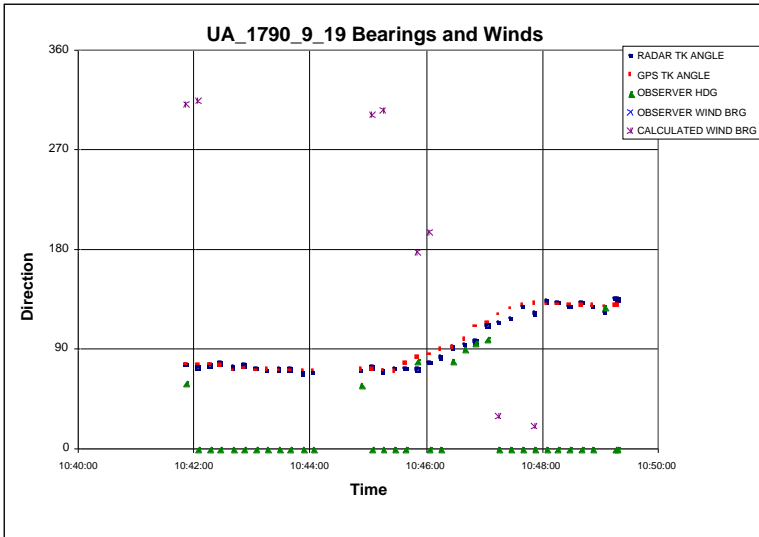
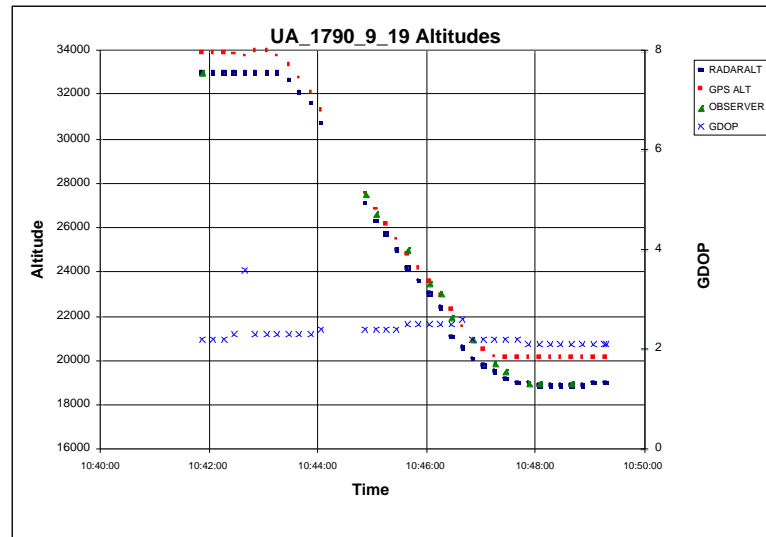
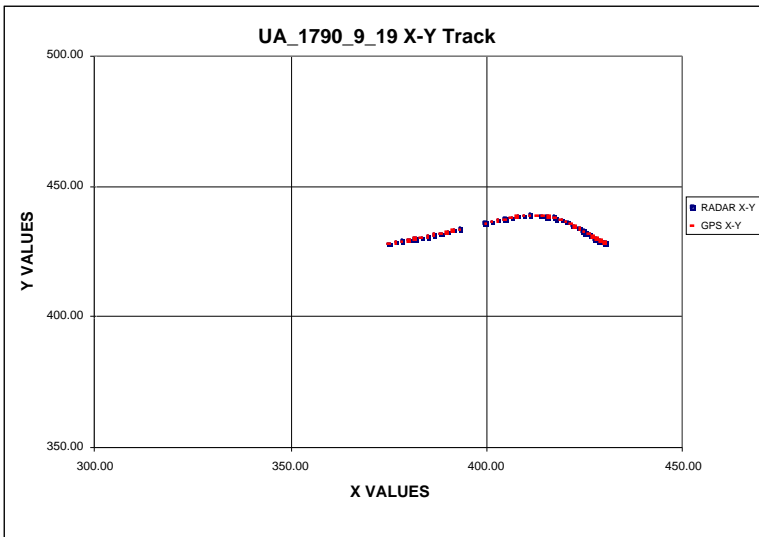


Figure A.30 Graphic Results for Case UA-1790_9_19

Table A.31 Tabular Results for Case UA_1790_9_27

UA_1790_9_27	GPS DATA										RADAR DATA			OBSERVER DATA			CALC DATA							
TOD	GPS_LAT	GPS_LON	GPS_ALT	GPS_X	GPS_Y	GPS_GS	GPS_TRK	G_SATS	GDOP	R_ALT	R_X	R_Y	R_GS	R_TRK	OBS_ALT	OBS_OAT	OBS_IAS	OBS_HDG	OBS_WBRG	OBS_WMAG	OBS_CMT	C/O_TAS	CALC_WBRG	CALC_WMAG
11:03:03	40.21502	106.3813	32732	385.73	417.97	567	81	4	1.5	31700	386.06	417.94	558	85	330									
11:03:15	40.21973	106.3398	32379	387.64	418.25	566	80	4	2.9	31400	387.94	418.31	559	80										
11:03:27	40.22485	106.2993	32029	389.50	418.56	554	80	4	3.0	31000	389.81	418.63	561	81										
11:03:39	40.23030	106.2584	31648	391.38	418.89	561	79	4	1.5	30600	391.50	418.88	561	81										
11:03:51	40.23624	106.2169	31224	393.29	419.26	556	78	4	2.8	30200	393.25	419.25	560	79										
11:04:03	40.24254	106.1773	30680	395.11	419.64	558	78	4	2.4	29600	395.06	419.63	558	78								485		
11:04:15	40.24876	106.1390	29932	396.87	420.02	552	79	4	2.4	28800	396.81	420.00	556	78	290									
11:04:27	40.25464	106.0992	29157	398.69	420.38	546	79	4	2.9	28100	398.75	420.44	554	78				68						
11:04:39	40.26031	106.0602	28653	400.48	420.72	567	81	4	1.4	27600	400.50	420.75	553	79										
11:04:51	40.26520	106.0195	28212	402.35	421.02	535	81	4	2.4	27200	402.38	421.00	552	81								520	315	26
11:05:03	40.26966	105.9814	27684	404.10	421.30	533	82	4	2.4	26700	404.19	421.25	552	82	270			68						
11:05:15	40.27362	105.9428	26890	405.87	421.55	534	83	4	2.4	25800	405.81	421.63	551	78										
11:05:51	40.28330	105.8261	24186	411.22	422.16	521	84	4	2.4	23200	411.38	422.06	551	83	230			68				495	322	53
11:06:03	40.28580	105.7897	23422	412.89	422.33	534	84	4	2.4	22600	413.31	422.31	549	83								501	317	58
11:06:15	40.28849	105.7523	22572	414.61	422.50	519	83	4	2.4	21900	415.13	422.63	548	81	220							488	311	48
11:06:27	40.29171	105.7139	21808	416.37	422.71	504	83	4	2.4	21300	415.81	422.63	545	87										
11:06:39	40.29482	105.6767	21056	418.08	422.91	525	83	4	2.4	20700	417.56	422.81	543	85	210							486	305	54
11:06:51	40.29828	105.6386	20426	419.83	423.13	495	81	4	3.2	19500	420.00	423.06	539	84				72						
11:07:03	40.30186	105.6039	20005	421.42	423.36	466	83	4	2.4	19200	421.81	423.38	534	81	190									
11:07:15	40.30529	105.5698	19769	422.98	423.58	458	83	4	2.4	19000	423.44	423.63	529	81										
11:07:27	40.30850	105.5364	19652	424.51	423.79	403	93	4	2.4	18900	424.06	423.69	522	83								429	17	79
11:07:39	40.30622	105.5060	19678	425.91	423.67	389	102	4	2.4	19000	425.69	423.75	516	86								405	9	134
11:07:51	40.30095	105.4780	19748	427.20	423.37	390	110	4	2.4	19000	426.94	423.56	508	95										
11:08:03	40.29371	105.4537	19741	428.32	422.95	382	112	4	2.5	19000	428.56	422.75	490	109				130						
11:08:13	40.28670	105.4323	19654	429.31	422.54	376	113	4	2.5	18914	429.63	422.48	474	106	190									

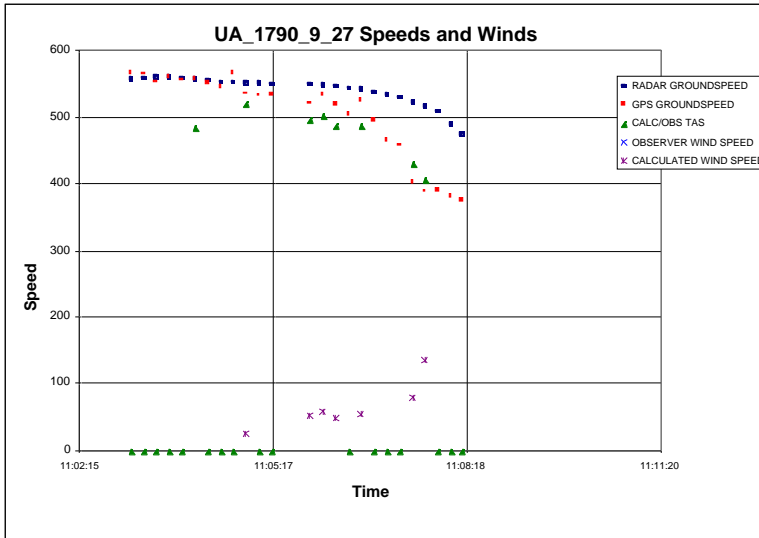
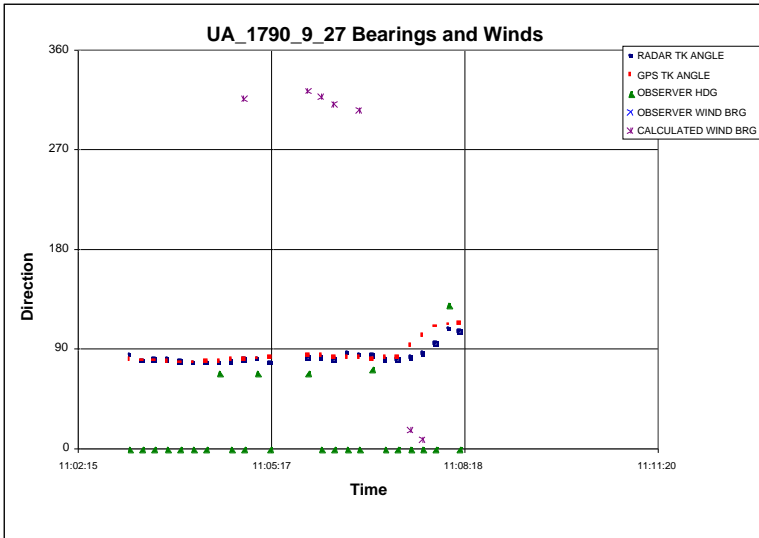
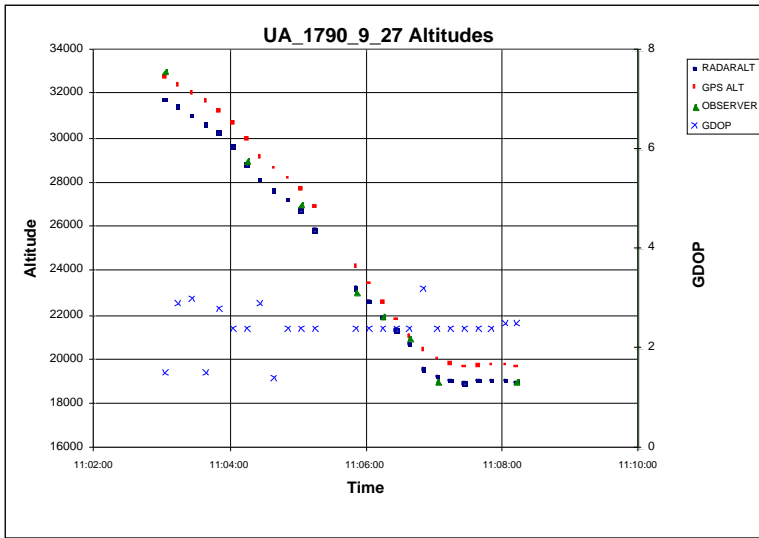
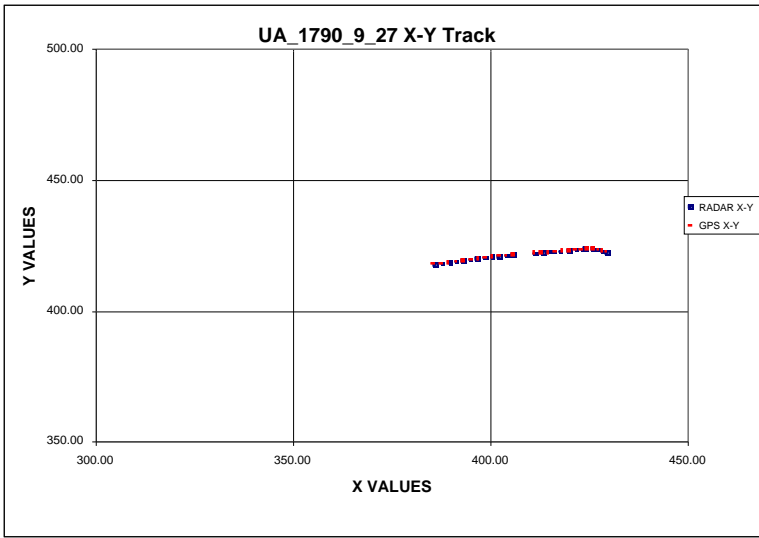


Figure A.31 Graphic Results for Case UA_1790_9_27